# Supporting Information

# Catalytic Enantioselective Addition of Indoles to Activated *N*-Benzyl Pyridinium Salts: Nucleophilic Dearomatization of Pyridines with Unusual C-4 Regioselectivity

*Giulio Bertuzzi, Alessandro Sinisi, Lorenzo Caruana,* Andrea Mazzanti, Mariafrancesca Fochi* and Luca Bernardi**

Department of Industrial Chemistry "Toso Montanari" and INSTM RU Bologna
Alma Mater Studiorum – University of Bologna
V. Risorgimento 4, 40136 Bologna (Italy)
E-mail: lorenzo.caruana2@unibo.it; mariafrancesca.fochi@unibo.it; luca.bernardi2@unibo.it

## Table of contents

## General methods and materials

**General Methods.** $^{1}H$ and $^{13}C$ NMR spectra were recorded on a Varian Inova 300, Mercury 400 or Inova 600 spectrometer. Chemical shifts (δ) are reported in ppm relative to residual solvents signals for $^{1}H$ and $^{13}C$ NMR. $^{13}C$ NMR were acquired with $^{1}H$ broad-band decoupled mode. Chromatographic purifications were performed using 70-230 mesh silica. Mass spectra were recorded on a micromass LCT spectrometer using electrospray (ESI) ionization techniques. Two additional representative HRMS(ESI) spectra were recorded for products **4ga** and **6**. Optical rotations were measured on a Perkin Elmer 241 Polarimeter provided with a sodium lamp and are reported as follows: $[\alpha]_{\lambda}^{T\,(^{\circ}C)}$ (c = g/100 mL, solvent). The enantiomeric excess of the products (*ee*) were determined by chiral stationary phase HPLC (Daicel Chiralpak AD-H, AS or Chiralcel OD columns), using an UV detector operating at 254 nm. The absolute configuration of compounds **4** in the reactions catalysed by **3a** was tentatively assigned to be S, in analogy with the S absolute configuration of compound **4gd** determined by anomalous diffraction X-ray analysis (see page S12). The structural assignment of compounds **4** and **5**, and the determination of their ratios in the catalytic reactions, is outlined in the dedicated section (see page S5).

**Materials**. Analytical grade solvents and commercially available reagents were used as received, unless otherwise stated. Pyridinium salts **1a-j** were synthesized as reported below from commercially available 3-nitropyridine or 3-cyanopyridine and the respective benzyl bromides (4-methoxybenzyl bromide was prepared according to a literature procedure[1]). 1,8-Bis(dimethylamino)naphthalene (proton sponge PS) was obtained from Sigma-Aldrich and used as received. Catalyst **3a** was prepared following literature procedures.[2]

**Preparation of the racemic products**.

In a test tube equipped with a magnetic stirring bar, pyridinium salts **1a-k** (0.05 mmol), indoles **2a-f** (0.065 mmol), quinuclidine (5.6 mg, 0.05 mmol) and *N*,*N*′−bis[3,5−bis(trifluoromethyl)phenyl]−thiourea (Schreiner's thiourea) (2.5 mg, 0.005 mmol) were stirred in toluene (0.250 mL) at room temperature for 2 hours. DCM was then added and the resulting solution was passed through a short plug of silica and washed with $Et_2O$ (4x). Evaporation of the solvents afforded the crude product, which was purified by column chromatography on silica gel (*n*-hexane/EtOAc). Products **4** were thus obtained as red solids in nearly quantitative yields.

Racemic **6** and **7** were synthesized by employing racemic **4ga** in the respective reactions.

## Synthesis of *N*-alkyl pyridinium salts (1a-k).

**General procedure**. In a round bottom flask equipped with a magnetic stirring bar and a reflux condenser, 3-nitropyridine or 3-cyanopyridine (2 mmol) and the benzyl bromide (3 mmol) were dissolved in acetonitrile (4 mL) and the resulting mixture was heated to reflux for 18h.

Hereafter, the mixture was cooled to 0 °C and $Et_2O$ was added dropwise with stirring until a precipitate was formed. The solid was then filtered and washed repeatedly with cold $Et_2O$ to afford the desired pyridinium salt.

**_N_-Benzyl-3-nitropyridinium bromide (1a)**

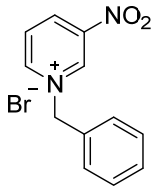

Obtained as a dark yellow powder in 50% yield from 3-nitropyridine and benzyl bromide. $^1$H NMR (300 MHz, DMSO-*d*6) δ = 10.39 (s, 1H), 9.53 (d, J = 6.1 Hz, 1H), 9.40 (d, J = 8.5 Hz, 1H), 8.46 (dd, $J_1$ = 8.6 Hz, $J_2$ = 6.2 Hz, 1H), 7.68-7.60 (m, 2H), 7.54-7.47 (m, 3H), 6.08 (s, 2H) ppm.

**_N_-(4-Bromobenzyl)-3-nitropyridinium bromide (1b)**

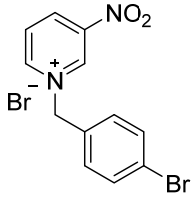

Obtained as a light yellow powder in 82% yield from 3-nitropyridine and 4-bromobenzyl bromide. $^1$H NMR (300 MHz, DMSO-*d*6) δ = 10.36 (s, 1H), 9.51 (dt, $J_1$ = 6.1 Hz, $J_2$ = 1.1 Hz, 1H), 9.39 (ddd, $J_1$ = 8.5 Hz, $J_2$ = 2.3 Hz, $J_3$ = 1.1 Hz, 1H), 8.45 (dd, $J_1$ = 8.6, $J_2$ = 6.3 Hz, 1H), 7.74-7.70 (m, 2H), 7.63-7.58 (m, 2H), 6.04 (s, 2H) ppm.

**_N_-(3,5-Bis(trifluoromethyl)benzyl)-3-nitropyridinium bromide (1c)**

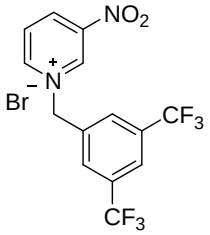

Obtained as a light yellow powder in 36% yield from 3-nitropyridine and 3,5-bis (trifluoromethyl)benzyl bromide. $^1$H NMR (300 MHz, DMSO-*d*6) δ = 10.41 (s, 1H), 9.56 (dt, $J_1$ = 6.2 Hz, $J_2$ = 1.2 Hz, 1H), 9.39 (ddd, $J_1$ = 8.6 Hz, $J_2$ = 2.3 Hz, $J_3$ = 1.1 Hz, 1H), 8.47-8.41 (m, 3H), 8.25 (s, 1H), 6.16 (s, 2H) ppm.

**_N_-(2-Naphthalen-2-ylmethyl)-3-nitropyridinium bromide (1d)**

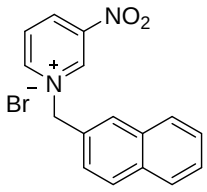

Obtained as a dark yellow powder in 82% yield from 3-nitropyridine and 2-(bromomethyl)naphthalene. $^1$H NMR (300 MHz, DMSO-*d*6) δ = 10.41 (s, 1H), 9.55 (dt, $J_1$ = 6.2 Hz, $J_2$ = 1.1 Hz, 1H), 9.37 (ddd, $J_1$ = 8.6 Hz, $J_2$ = 2.2 Hz, $J_3$ = 1.1 Hz, 1H), 8.42 (dd, $J_1$ = 8.7, $J_2$ = 6.3 Hz, 1H), 8.14 (s, 1H), 8.02 (d, J = 8.5 Hz, 1H), 7.98-7.91 (m, 2H), 7.68 (dd, $J_1$ = 8.5 Hz, $J_2$ = 1.8 Hz, 1H), 7.63-7.57 (m, 2H), 6.21 (s, 2H) ppm.

***N*-([1,1'-Biphenyl]-4-ylmethyl)-3-nitropyridinium bromide (1e)**

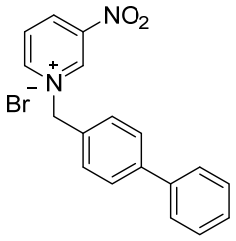

Obtained as an off-white powder in quantitative yield from 3-nitropyridine and 4-(bromomethyl)-1,1'-biphenyl. $^1$H NMR (300 MHz, DMSO-*d*6) δ = 10.42 (s, 1H), 9.57 (dt, $J_1$ = 6.2 Hz, $J_2$ = 1.1 Hz, 1H), 9.40 (ddd, $J_1$ = 8.6 Hz, $J_2$ = 2.2 Hz, $J_3$ = 1.1 Hz, 1H), 8.43 (dd, $J_1$ = 8.6, $J_2$ = 6.2 Hz, 1H), 7.82-7.69 (m, 6H), 7.59-7.40 (m, 3H), 6.11 (s, 2H) ppm.

***N*-(4-Methoxybenzyl)-3-nitropyridinium bromide (1f)**

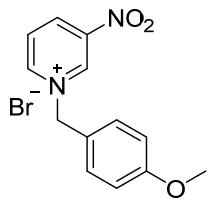

Obtained as a dark yellow powder in 72% yield from 3-nitropyridine and 4-methoxybenzyl bromide. $^1$H NMR (300 MHz, DMSO-*d*6) δ = 10.29 (s, 1H), 9.45 (dt, $J_1$ = 6.2 Hz, $J_2$ = 1.0 Hz, 1H), 9.33 (ddd, $J_1$ = 8.6 Hz, $J_2$ = 2.4 Hz, $J_3$ = 1.2 Hz, 1H), 8.39 (dd, $J_1$ = 8.6, $J_2$ = 6.1 Hz, 1H), 7.63-7.57 (m, 2H), 7.05-7.00 (m, 2H), 5.95 (s, 2H), 3.83 (s, 3H) ppm.

***N*-(4-Methoxybenzyl)-3-nitropyridinium chloride (1'f)**

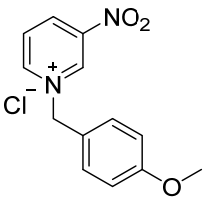

Obtained as a grey solid in 34% yield from 3-nitropyridine and 4-methoxybenzyl chloride. $^1$H NMR (300 MHz, DMSO-*d*6) δ = 10.35 (s, 1H), 9.53 (dt, $J_1$ = 6.3 Hz, $J_2$ = 1.0 Hz, 1H), 9.36 (ddd, $J_1$ = 8.6 Hz, $J_2$ = 2.3 Hz, $J_3$ = 1.2 Hz, 1H), 8.43 (dd, $J_1$ = 8.6, $J_2$ = 6.1 Hz, 1H), 7.66-7.62 (m, 2H), 7.07-7.03 (m, 2H), 6.00 (s, 2H), 3.80 (s, 3H) ppm.

***N*-(4-*tert*-Butylbenzyl)-3-nitropyridinium bromide (1g)**

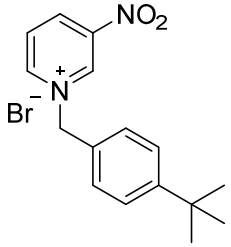

Obtained as a bright yellow powder in 86% yield from 3-nitropyridine and 4-*tert*-butylbenzyl bromide. $^1$H NMR (300 MHz, DMSO-*d*6) δ = 10.39 (s, 1H), 9.55 (dt, $J_1$ = 6.1 Hz, $J_2$ = 1.2 Hz, 1H), 9.38 (ddd, $J_1$ = 8.6 Hz, $J_2$ = 2.2 Hz, $J_3$ = 1.1 Hz, 1H), 8.45 (dd, $J_1$ = 8.6, $J_2$ = 6.0 Hz, 1H), 7.62-7.58 (m, 2H), 7.54-7.49 (m, 2H), 6.04 (s, 2H), 1.30 (s, 9H) ppm.

***N*-(4-*iso*-Propylbenzyl)-3-nitropyridinium bromide (1h)**

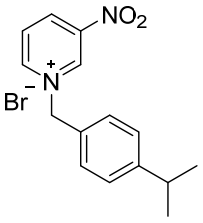

Obtained as yellow crystals in 79% yield from 3-nitropyridine and 4-*iso*-propylbenzyl bromide. $^1$H NMR (300 MHz, DMSO-*d*6) δ = 10.37 (s, 1H), 9.53 (dt, $J_1$ = 6.1 Hz, $J_2$ = 1.2 Hz, 1H), 9.38 (ddd, $J_1$ = 8.6 Hz, $J_2$ = 2.2 Hz, $J_3$ = 1.1 Hz, 1H), 8.45 (dd, $J_1$ = 8.7, $J_2$ = 6.2 Hz, 1H), 7.60-7.56 (m, 2H), 7.39-7.35 (m, 2H), 6.03 (s, 2H), 2.94 (sept, J = 6.9 Hz, 1H), 1.22 (d, J = 6.8 Hz, 6H) ppm.

***N*-(3,5-Bis(*tert*-butyl)benzyl)-3-nitropyridinium bromide (1i)**

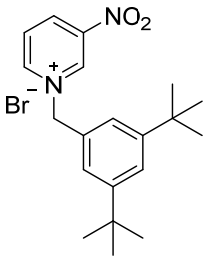

Obtained as an off-white solid in 42% yield from 3-nitropyridine and 3,5-di-*tert*-butylbenzyl bromide. $^1$H NMR (300 MHz, DMSO-*d*6) δ = 10.40 (s, 1H), 9.55 (d, J = 6.2 Hz, 1H), 9.38 (ddd, $J_1$ = 8.6 Hz, $J_2$ = 2.2 Hz, $J_3$ = 1.0 Hz, 1H), 8.46 (dd, $J_1$ = 8.5, $J_2$ = 6.2 Hz, 1H), 7.55-7.52 (m, 2H), 7.51-7.49 (m, 1H), 6.00 (s, 2H), 1.32 (s, 18H) ppm.

***N*-(4-*tert*-Butylbenzyl)-3-cyanopyridinium bromide (1j)**

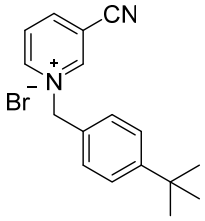

Obtained as a white powder from 3-cyanopyridine and 4-*tert*-butylbenzyl bromide. $^1$H NMR (300 MHz, DMSO-*d*6) δ = 10.02 (s, 1H), 9.45 (dt, $J_1$ = 6.3 Hz, $J_2$ = 1.3 Hz, 1H), 9.15 (dt, $J_1$ = 8.3 Hz, $J_2$ = 1.4 Hz, 1H), 8.39 (dd, $J_1$ = 8.1, $J_2$ = 6.4 Hz, 1H), 7.59-7.55 (m, 2H), 7.53-7.49 (m, 2H), 5.88 (s, 2H), 1.31 (s, 9H) ppm.

## Preparation, characterization and structural assignment of isomers 4aa and 5aa.

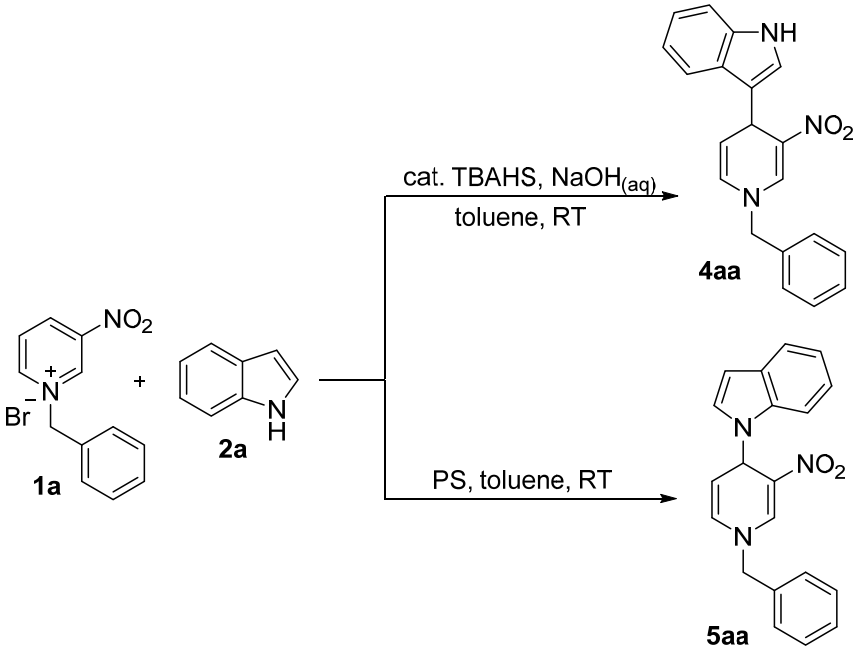


**Scheme S1.** Preparation of isomers **4aa** and **5aa.**

Isomer **4aa** was obtained adapting a literature procedure,[3] which is known to give selectively the addition of indoles to the C-4 position of the pyridinium ring, as follows. In a test tube equipped with a magnetic stirring bar, substrate **1a** (15 mg, 0.05 mmol), indole **2a** (7.6 mg, 0.065 mmol), toluene (1.3 mL), NaOH (1.3 mL of a 50% w/w solution) and tetrabutylammonium hydrogensulfate (1.7 mg, 0.005 mmol) were vigorously stirred for 18 hours. DCM was then added and the organic layer was passed through a short plug of silica, and the plug flushed with $Et_2O$ (4x). Evaporation of the solvents afforded the crude product, which was purified by column chromatography on silica gel (*n*-hexane/EtOAc 2:1). Product **4aa** was thus obtained as a bright yellow solid in 50% yield. $^1$H NMR ($CDCl_3$, 400 MHz) δ = 8.09 (d, J = 1.5 Hz, 1H), 8.05 (bs, 1H), 7.51-7.41 (m, 4H), 7.36 (d, J = 7.8 Hz, 1H), 7.34-7.31 (m, 2H), 7.14 (t, J = 7.6 Hz, 1H), 7.04 (d, J = 2.3 Hz, 1H), 6.98 (t, J = 7.4 Hz, 1H), 6.01 (dt, $J_1$ = 7.7 Hz, $J_2$ = 1.4 Hz, 1H), 5.31 (dd, $J_1$ = 7.7 Hz, $J_2$ = 4.9 Hz, 1H), 5.24 (d, J =4.9 Hz, 1H), 4.61 (s, 2H) ppm.

The structure of the isomer of interest (C-4) was later confirmed by means of X-ray diffraction analysis on a single crystal of product **4gd** and extended for analogy to all other similar structures. A further strong confirmation of this assignment was the presence of a peak between 30 and 40 ppm in the $^{13}$C NMR spectra of all products **4** isolated (*vide infra*), indicating that the $sp^3$ carbon atom of the dihydropyridine ring does not bear a N atom.[3]

Isomer **5aa**, the major side-product of the dearomatization process, was selectively prepared with an alternative procedure, as follows. In a test tube equipped with a magnetic stirring bar, product **1a** (15 mg, 0.05 mmol), indole **2a** (7.6 mg, 0.065 mmol) and PS (10.4 mg, 0.05 mmol) were vigorously stirred in toluene (0.125 mL) for 18 hours. DCM was then added and the organic layer was passed through a short plug of

silica, and the plug flushed with $Et_2O$ (4x). Evaporation of the solvents afforded the crude product, which was purified by column chromatography on silica gel (*n*-hexane/EtOAc 2:1). Product **5aa** was thus obtained as a light yellow solid in 70% yield. $^1$H NMR ($CDCl_3$, 600 MHz) δ = 8.26 (d, J = 1.4 Hz, 1H), 7.58-7.56 (m, 1H), 7.49-7.43 (m, 3H), 7.35-7.33 (m, 2H), 7.21-7.18 (m, 1H), 7.08-7.04 (m, 3H), 6.50 (d, J = 4.9 Hz, 1H), 6.46 (dd, $J_1$ = 3.3 Hz, $J_2$ = 0.9 Hz, 1H), 6.37 (dt, $J_1$ = 7.8 Hz, $J_2$ = 1.4 Hz, 1H), 5.42 (dd, $J_1$ = 7.7 Hz, $J_2$ = 5.0 Hz, 1H), 4.75 (s, 2H) ppm.

Product **5aa**, which $^1$H NMR spectrum is reported in Figure S1, was preliminary identified as an N-alkylation adduct of indole **2a** on the pyridinium ring, for the absence of the characteristic signal of the indole N-H in the $^1$H NMR spectrum (bs at about 8 ppm, present for **4aa**). Moreover, an additional signal in the vinylic region (6.46 ppm, dd), not belonging to the dihydropyridine, indicated the presence of a proton at the 3-position of the indole ring, absent for **4aa** (analogous to the signal of free indole **2a** at 6.51 ppm).

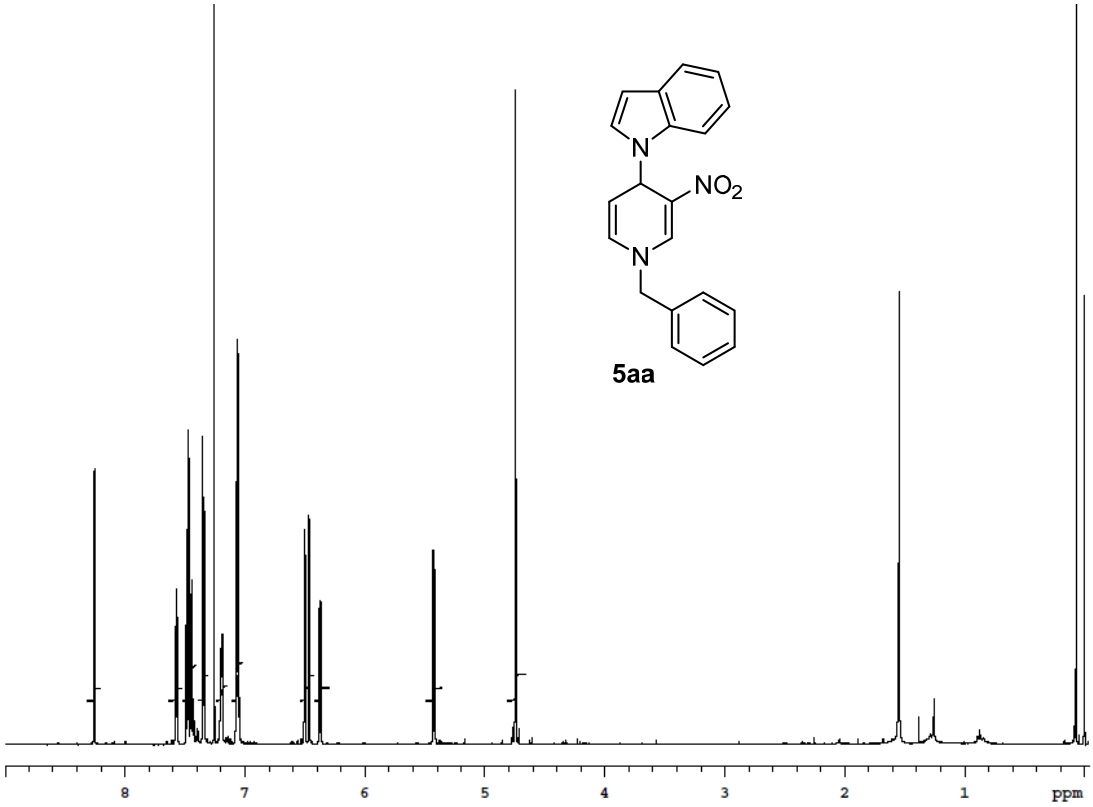


**Figure S1.** $^1$H NMR spectrum of **5aa** in $CDCl_3$ (600 MHz).

The presence of the signal at 8.26 ppm (doublet with a very small J constant of 1.1 Hz), deshielded by the conjugation with the nitro-group, rules out addition at the more hindered C-2 of the pyridinium ring. Between the two remaining conceivable regioisomers, the structure of adduct **5aa** was confirmed by means of DPFGSE-NOE NMR spectroscopy, as follows (Figures S2-S4).

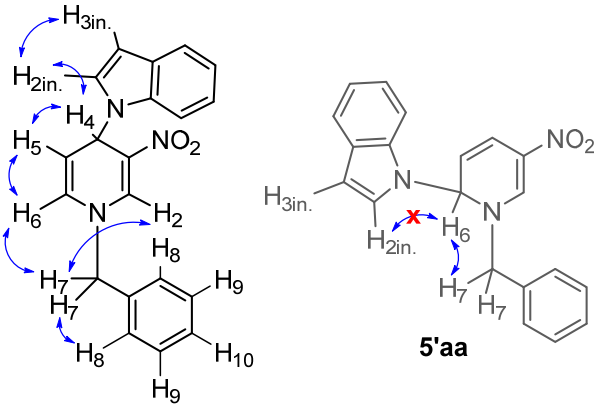


**Figure S2.** Product **5aa** and possible regioisomer **5'aa**. Blue arrows indicates DPFGSE-NOE spatial correlations

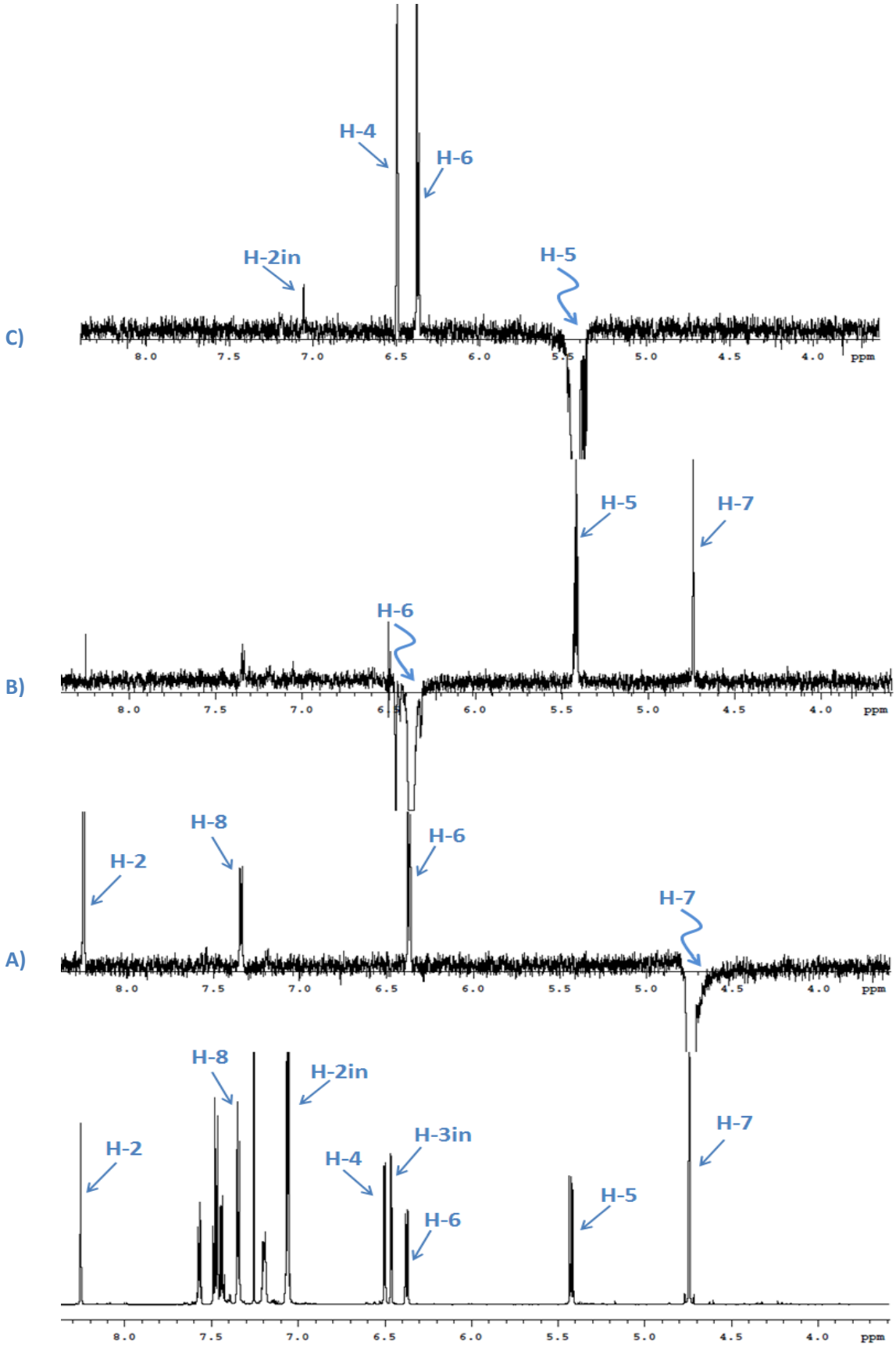


**Figure S3.** NOE spectra of product **5aa**.

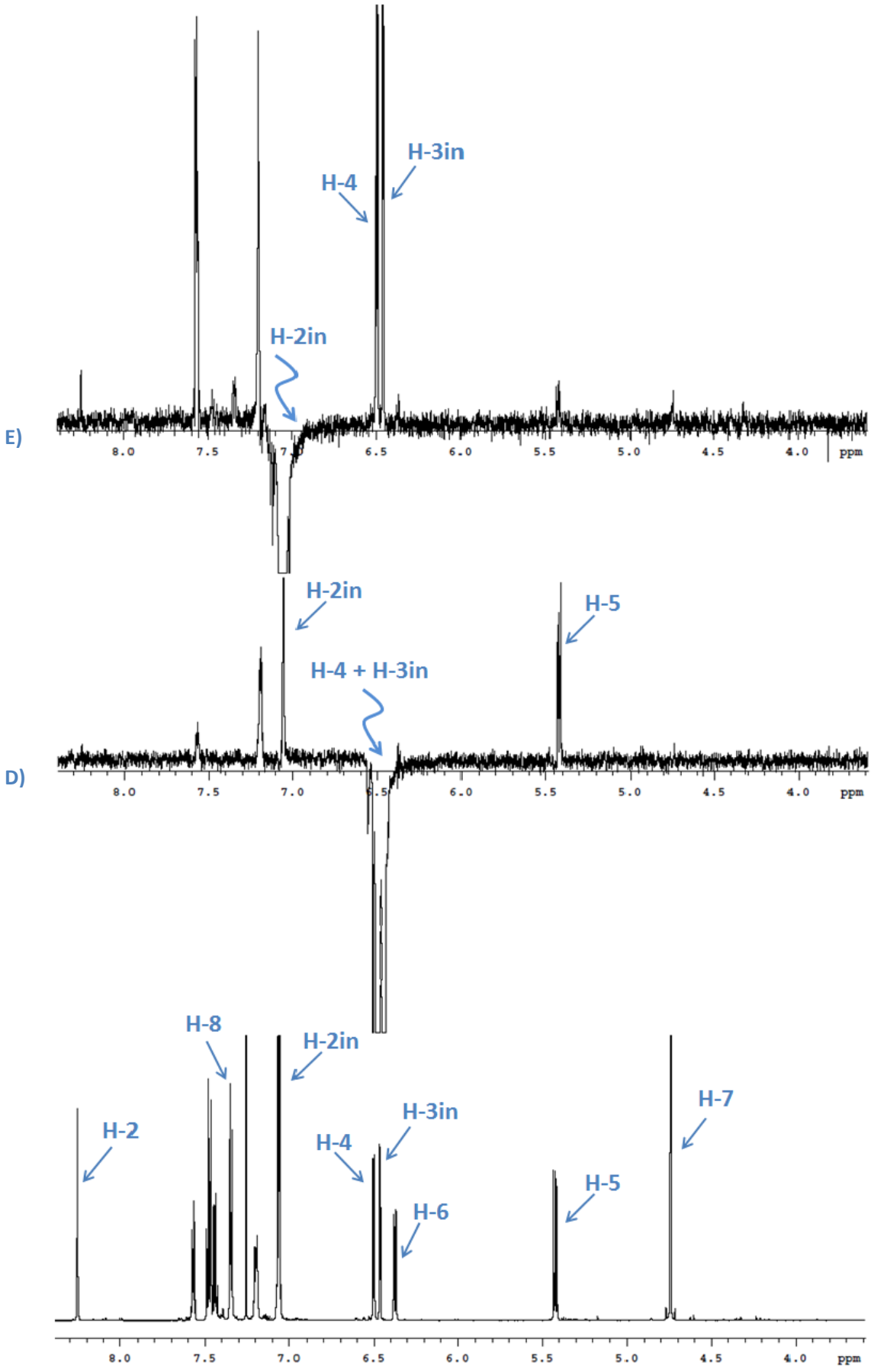


**Figure S4.** DPFGSE-NOE spectra of product **5aa**.

The signal at 8.26 ppm was assigned to H-2 due to the chemical shift and multiplicity (doublet with a coupling constant of 1.1 Hz, conjugation with the nitro-group).

The signal at 4.75 ppm was assigned to H-7 due to the multiplicity (AB system with small spread between the two diastereotopic hydrogens) and its integral value. Saturation of H-7 (Figure S3, A) resulted in the enhancement of signals at 8.26 ppm (H-2), 7.34 ppm (assigned to H-8 and acting as control signal) and at 6.37 ppm, which was assigned to H-6.

Saturation of the signal at 6.37 ppm (H-6) showed enhancement (Figure S3, B) of signals at 4.75 ppm (H-7) and at 5.42 ppm, which was assigned to H-5.

Saturation of the signal at 5.42 ppm (H-5) showed enhancement (Figure S3, C) of signals at 6.37 ppm (H-6) and 6.50 ppm, which was assigned to H-4. The signal at 6.46 ppm was therefore attributed to H-3in for exclusion (proton at the C-3 position of the indole ring is usually more shielded than the other ones). Moreover, a small enhancement of a signal at 7.05 ppm was observed (later assigned to H-2in).

Saturation of the signal at 6.50 ppm (H-4) alone was not possible, due to its close proximity with the signal at 6.46 ppm (H-3in). However, the simultaneous saturation (Figure S4, D) showed NOE enhancement of the signal at 7.05 ppm, clearly indicating H-2in belonging to this multiplet, generated by the overlap of three different signals. This is not useful for the regiochemistry assignment, since enhancement of H-2in may be due only to saturation of the H-3in signal, but allowed to identify the position of the H-2in signal in the spectrum.

Saturation of the multiplet at 7.05 ppm (containing H-2in) showed enhancement (Figure S4, E) of signals at 6.46 ppm (H-3in) and 6.50 ppm (H-4), clearly showing the regiochemistry of product **5aa**.[4]

Structure **5'aa**, on the other hand, would have showed enhancement of the H-2in upon saturation of H-6 (the proton near the H-7 protons of the benzyl moiety), which was not observed. Moreover, gHSQC experiment (Figure S5) showed H-4 correlating with a carbon signal at 48.4 ppm (C-4), perfectly in agreement with an $sp^3$ carbon deshielded by the N-atom, while H-6 correlates with a carbon signal at 128.7 ppm (C-6), typical of a vinylic carbon. This is consistent with structure **5aa**, while **5'aa** would have shown H-6 correlating with a signal at about 70 ppm ($sp^3$ deshielded by two nitrogen atoms) and H-4 with a signal in the vinylic region.

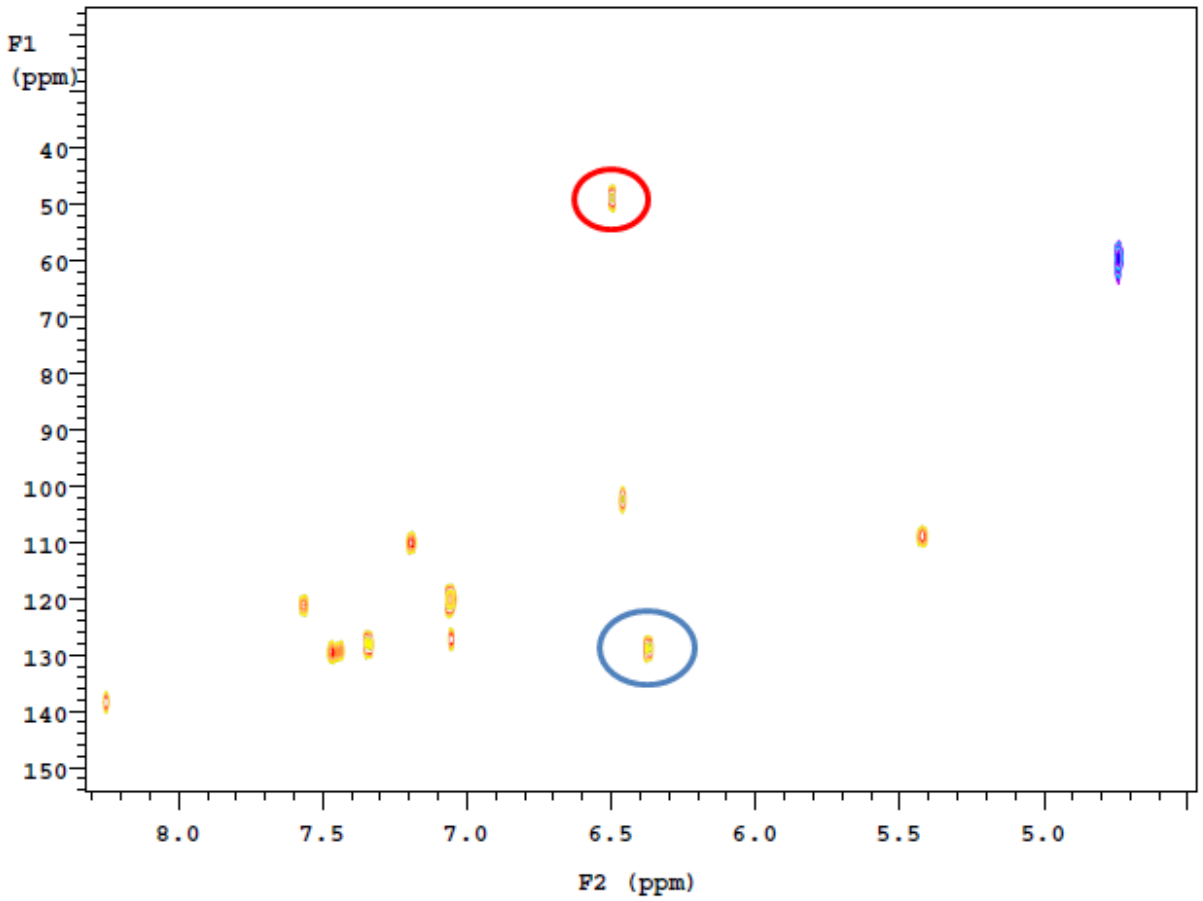


**Figure S5.** gHSQC spectrum (in red: correlation H-4 – C-4; in blue: correlation H-6 – C-6).

A diagnostic signal of isomer **4aa** is the proton at 6.0 ppm (doublet of triplets) while the analogous signal for product **5aa** is found at 6.4 ppm. Therefore, during the whole optimization process the isomeric ratio **4aa**/**5aa** was determined by the integration of these two signals in the $^{1}$H NMR spectrum of the crude products (*vide infra*).

## Crystal data for compound 4gd

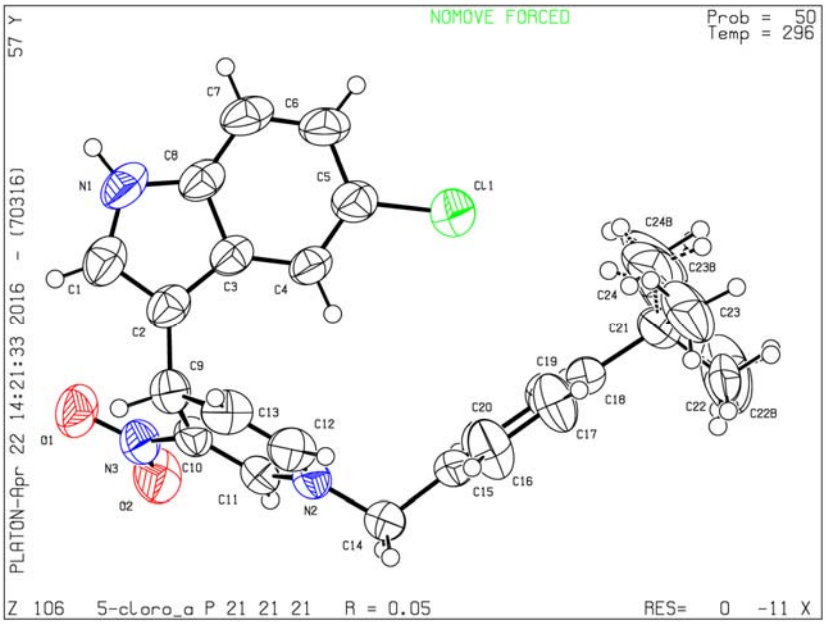


Molecular formula: $C_{24}H_{24}N_3O_2Cl$; $M_r$ = 421.91, orthorhombic, space group $P2_12_12_1$ (19), $a$ = 10.4050(4), $b$ = 14.2652(6), $c$ = 14.6935(6) Å; $V$ = 2180.95(15) Å$^3$, T = 296(2) K, $Z$ = 4, $\rho_c$ = 1.285 g cm$^{-3}$, $F(000)$ = 888, graphite-monochromated $Mo_{K\alpha}$ radiation ($\lambda$ = 0.71073 Å), $\mu(Mo_{K\alpha})$ = 0.200 mm$^{-1}$, yellow brick (0.40 × 0.30 × 0.015 mm$^3$), empirical absorption correction with SADABS (transmission factors: 0.924 – 0.997), 2400 frames, exposure time 20 s, $1.99 \leq \theta \leq 26.00$, $-12 \leq h \leq 12$, $-17 \leq k \leq 17$, $-18 \leq l \leq 18$, 20389 reflections collected, 4133 independent reflections ($R_{int}$ = 0.0223), solution by intrinsic phasing method and subsequent Fourier syntheses, full-matrix least-squares on $F_o^2$ (SHELXL-2014/7), hydrogen atoms refined with a riding model, data / restraints / parameters = 4133/ 3/ 309, $S(F^2)$ = 0.964, $R(F)$ = 0.0639 and $wR(F^2)$ = 0.1719 on all data, $R(F)$ = 0.0466 and $wR(F^2)$ = 0.1365 for 3259 reflections with $I > 2\sigma(I)$, weighting scheme $w = 1/[\sigma^2(F_o^2) + (0.1053P)^2 + 0.7766P]$ where $P = (F_o^2 + 2F_c^2)/3$, largest difference peak and hole 0.415 and –0.394 e Å$^{-3}$. Flack parameter: 0.034(18) for *S* configuration at C9. The *t*-butyl group was found to be disordered over two positions and it was accordingly modelled with separate parts (53:47 optimized ratio). Crystallographic data have been deposited with the Cambridge Crystallographic Data Centre as supplementary publication no. CCDC-1476006. Copies of the data can be obtained free of charge on application to CCDC, 12 Union Road, Cambridge CB21EZ, UK (fax: (+44) 1223-336-033; e-mail: deposit@ccdc.cam.ac.uk).

## First attempts of catalytic enantioselective dearomatization of pyridinium salts 1 with indoles 2. Representative results:

1) **Inverted phase transfer catalysis approach**

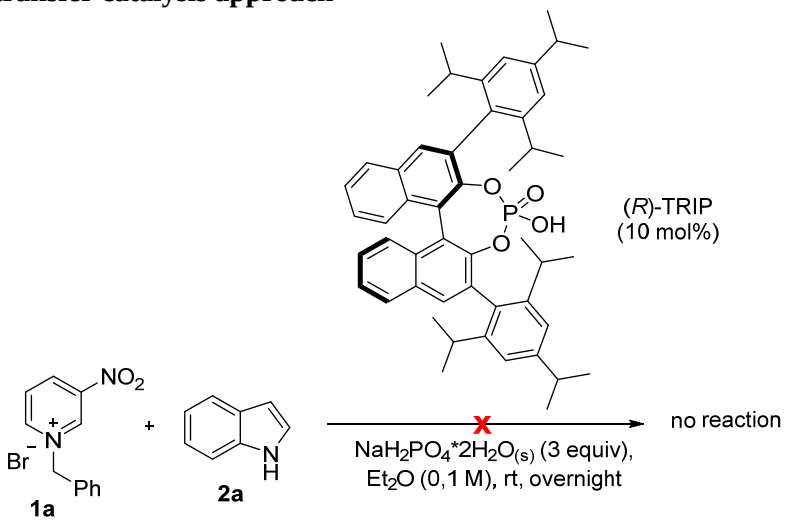


**Scheme S2.** Reaction conditions: **1a** (0.05 mmol), **2a** (0.065 mmol), (*R*)-TRIP (10 mol%), $NaH_2PO_4$*$2H_2O$ (0.15 mmol), $Et_2O$ (500 μL), RT, 18-24 h.

Exploiting the low solubility of pyridinium salts **1** in common organic solvents, an inverted phase-transfer catalytic approach was first attempted (for a representative result, see Scheme S2). No reaction was observed.

**2) Anion binding catalysis approach**

a) With Jacobsen-type thiourea **3p** (Figure S6), without base no reaction was observed (Table S1, entry 1).

b) Since it was clear that a stoichiometric amount of base is needed for the dearomatization to occur, we performed the same reaction with two different bases. A strong base-dependent selectivity was observed since aqueous $NaHCO_3$ furnished only product **5aa,** while solid $Na_2CO_3$ rendered **4aa** as the sole product (compare entry 2 and 3 in Table S1). However, in both cases the products were found to be racemic, underlying that the reactions were promoted by the base alone.

c) To discard completely this type of activation we also performed three attempts with non-basic thioureas **3p-r** (Figure S6), with the optimal base for the reaction development (PS). The results obtained (Table S1) were generally worse than the ones observed with the bifunctional catalysts reported in Figure S7 and Table S3.

**Table S1**[a]

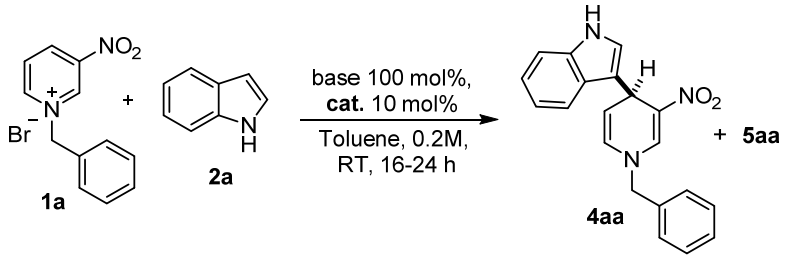


| Entry | Catalyst | Base | Conversion[b,c] (%) | **4aa**/**5aa**[b] | ee **4aa**/**5aa**[d] (%) |
|---|---|---|---|---|---|
| 1 | **3p** | None | < 5% | - | - |
| 2 | **3p** | $NaHCO_{3\,(aq)}$ (5% wt.) | 80 | < 5:95 | -/rac |
| 3 | **3p** | $Na_2CO_{3\,(s)}$ | 70 | > 95:5 | rac/- |
| 4 | **3p** | PS | 64 | 20:80 | 28/rac |
| 5 | **3q** | PS | 50 | 20:80 | rac/24 |
| 6 | **3r** | PS | 60 | 10:90 | rac/8 |

[a] Reaction conditions: **1a** (0.05 mmol), **2a** (0.065 mmol), catalyst **3** (10 mol%), base (0.05 mmol), toluene (250 µL), RT, 18-24 h. [b] Determined on the crude mixture by $^1$H NMR. [c] Overall conversion in products **4aa** and **5aa**. [d] Determined by chiral stationary phase HPLC.

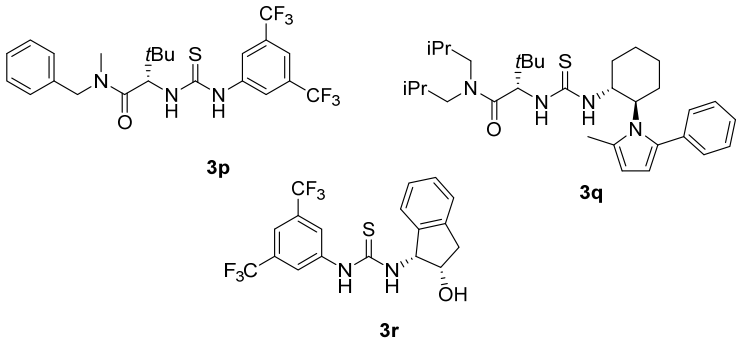


**Figure S6.** Catalysts screened in Table S1

# Additional optimization results in the reaction between pyridinium salts 1 and indole 2a catalysed by basic catalysts 3.

## 1) Screening of auxiliary bases in the reaction: representative results

**Table S2**[a]

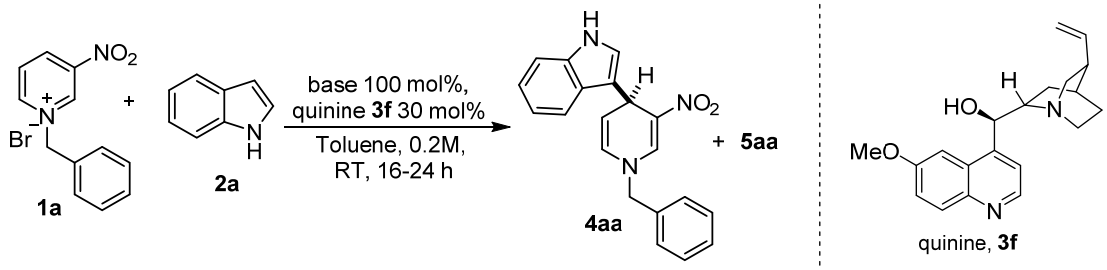


| Entry | Base | Conversion[b,c] (%) | **4aa**/**5aa**[b] | ee[d] (%) |
|---|---|---|---|---|
| 1 | None | 30 | >95:5 | 25 |
| 2 | Pyridine | 75 | >95:5 | rac |
| 3 | $Et_3N$ | 60 | 65:35 | 10 |
| 4 | Quinuclidine | 80 | >95:5 | rac |
| 5 | NaOAc | 40 | 85:15 | rac |
| 6 | Proton Sponge (PS) | 47 | 35:65 | 25 |

[a] Reaction conditions: **1a** (0.05 mmol), **2a** (0.065 mmol), cat. **3f** (30 mol%), base (0.05 mmol), toluene (250 µL), RT, 16-24h. [b] Determined on the crude mixture by $^1$H NMR. [c] Overall conversion in products **4aa** and **5aa**. [d] Of product **4aa**, determined by chiral stationary phase HPLC.

Preliminary experiments showed that a catalyst bearing a tertiary amine basic moiety (quinine **3f**), was able to promote the reaction, rendering the C-4 addition product **4aa** with low yet promising enantioselectivity (entry 1). It was obvious already from this first experiment that a stoichiometric amount of an auxiliary base was required in order to neutralize the HBr formed and achieve catalyst turnover. We therefore carried out reactions with different base candidates and quinine **3f** as a preliminary catalyst. Both strong (entries 3,4) and weak (entry 2) organic bases, along with inorganic ones (entry 5) showed satisfactory conversions but very low *ee* values for adduct **4aa**, accompanied by variable amounts of **5aa**, resulting from indole *N*-alkylation, obtained as a racemate in all cases. These results suggested that these reactions were promoted by the auxiliary bases, rather than by the catalyst. Only an attempt performed with proton sponge (1,8-dimethylamino naphthalene, PS), rendered the same enantioselectivity obtained with quinine **3f** alone (compare entries 1 and 6). Although this positive result was accompanied by the formation of larger amounts of racemic **5aa**, we chose this base to perform a subsequent catalyst screening, postponing this selectivity problem to later optimization.

## 2) Catalyst screening: representative results

**Table S3**[a]

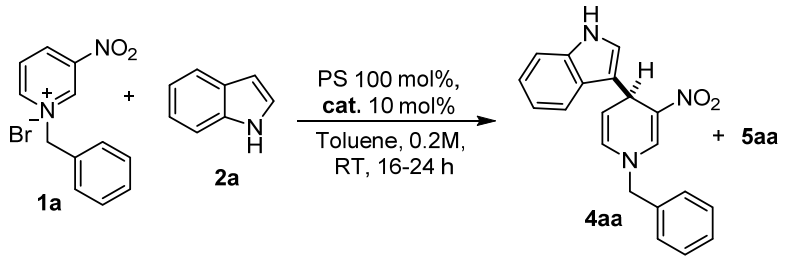


| Entry | Catalyst | Conversion[b,c] (%) | **4aa**/**5aa**[b] | ee[d] (%) |
|---|---|---|---|---|
| **1** | **3a** | **60** | **65:45** | **68** |
| 2 | **3b** | 64 | 40:60 | 40 |
| 3 | **3c** | 50 | 50:50 | 33 |
| 4 | **3d** | 49 | 35:65 | 30 |
| 5 | **3e** | 55 | 50:50 | 50 |
| 6 | **3f** | 47 | 35:65 | 25 |
| 7 | **3g** | 49 | 63:37 | 22 |
| 8 | **3h** | 50 | 75:25 | rac |
| 9 | **3i** | 51 | 69:31 | 10 |
| 10 | **3j** | 50 | 52:48 | 25 |
| 11 | **3k** | 51 | 48:52 | 13 |
| 12 | **3l** | 40 | 75:25 | 8 |
| 13 | **3m** | 45 | 62:38 | 18 |
| 14 | **3n** | 50 | 80:20 | 10 |
| 15 | **3o** | 56 | 25:75 | rac |

[a] Reaction conditions: **1a** (0.05 mmol), **2a** (0.065 mmol), cat **3** (10 mol%), PS (0.05 mmol), toluene (250 µL), RT, 16-24h. [b] Determined on the crude mixture by $^1$H NMR. [c] Overall conversion in products **4aa** and **5aa**. [d] Of product **4aa**, determined by chiral stationary phase HPLC.

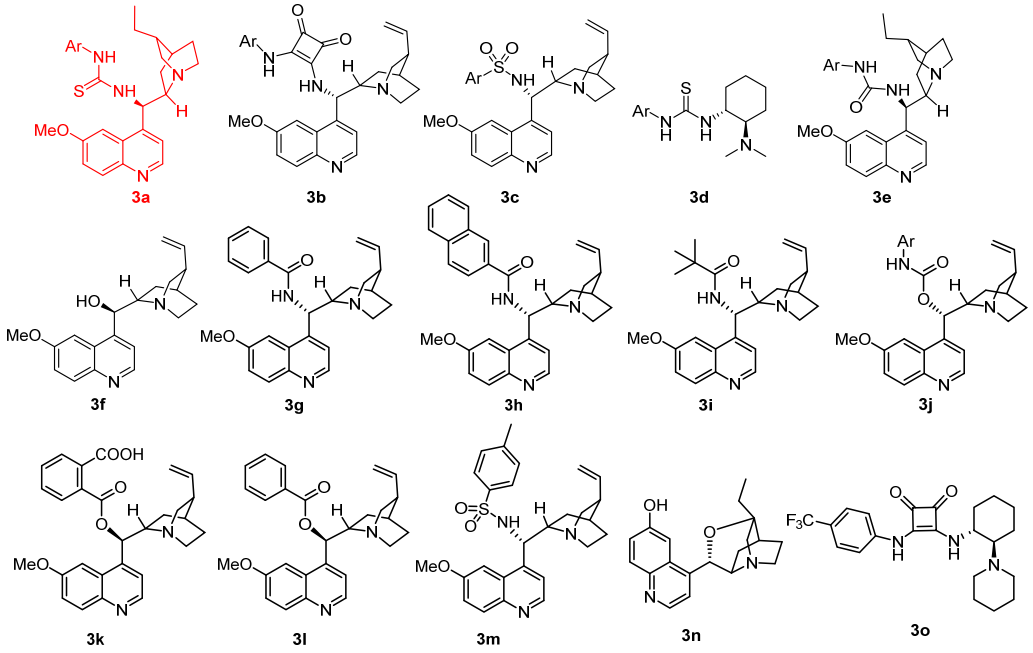


**Figure S7.** Catalysts screened in Table S3; Ar = $(CF_3)_2C_6H_3$.

Among others, bifunctional catalysts bearing a basic functionality along with H-bond donor moieties, such as squaramide (**3b**, entry 2), sulphonamide (**3c**, entry 3), urea (**3e**, entry **5**) and thiourea (**3d** and **3a** entries 4 and 1) performed better than quinine **3f** (entry 6) in terms of enantioselectivity of **4aa**, with the most promising result obtained with catalyst **3a**. The **4**/**5** selectivity of these reactions remained rather poor, with isomer **5aa** always produced in racemic form. As shown in Table S3, entries 7-15, the other cinchona alkaloid derivatives (**3g-n**) and cyclohexyldiamine **3o** tested (Figure S7) were found to be able to promote the reaction between **1a** and **2a**, but afforded lower enantioselectivities than catalyst **3a** (entry 1).

### 3) Preliminary solvent screening at RT with substrate 1a:

**Table S4**[a]

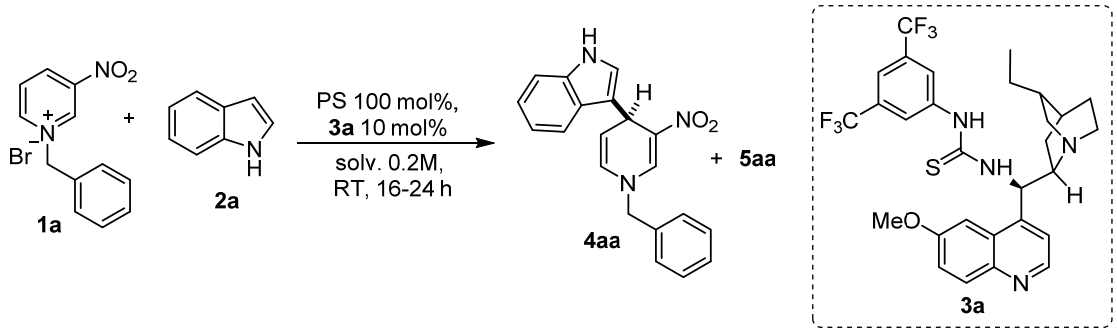


| Entry | Solvent | Conversion[b,c] (%) | **4aa**/**5aa**[b] | ee[d] (%) |
|---|---|---|---|---|
| 1 | Dichloromethane | 67 | 70:30 | 6 |
| 2 | Chloroform | 57 | 67:33 | 35 |
| 3 | Dichloroethane | 66 | 75:25 | 10 |
| 4 | Acetonitrile | 62 | 70:30 | 6 |
| 5 | Ethyl Acetate | 57 | 65:35 | 50 |
| 6 | Tetrahydrofuran | 54 | 55:45 | 14 |
| 7 | Diethyl ether | 45 | 65:35 | 66 |
| 8 | MCPE | 55 | 52:48 | 61 |
| **9** | **Toluene** | **60** | **55:45** | **68** |
| 10 | Toluene[e] | 85 | 70:30 | 60 |
| 11 | Toluene[f] | 84 | 70:30 | 55 |

[a] Reaction conditions: **1a** (0.05 mmol), **2a** (0.065 mmol), cat **3a** (10 mol%), PS (0.05 mmol), solvent (250 µL), RT, 16-24h. [b] Determined on the crude mixture by $^1$H NMR. [c] Overall conversion in products **4aa** and **5aa**. [d] Of product **4aa**, determined by chiral stationary phase HPLC. [e] 20 mg of 3 Å molecular sieves were added to the reaction mixture. [f] 20 mg of 4 Å molecular sieves were added to the reaction mixture.

Different solvents were initially tested (Table S4, entries 1-9): toluene was selected for further optimization. The use of molecular sieves of different pore sizes (Table S4, entries 10 and 11) increased the **4**/**5** ratio in favour of the C-4 addition product but furnished lower enantiomeric excesses.

**4) Solvent screening of aromatic solvents at -20 °C, with substrate 1g:**

**Table S5**[a]

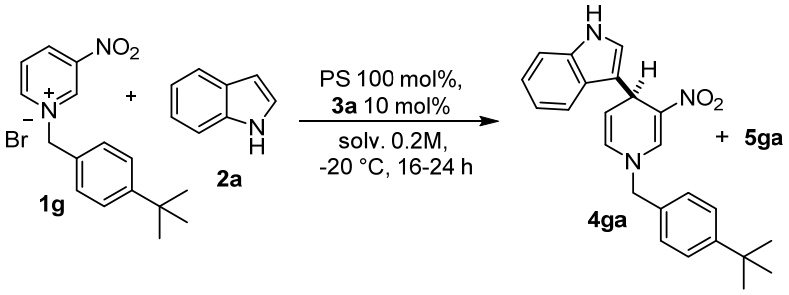


| Entry | Solvent | Conversion[b,c] (%) | **4ga**/**5ga**[b] | ee[d] (%) |
|---|---|---|---|---|
| 1 | Benzotrifluoride | 92 | 57:43 | 79 |
| 2 | Fluorobenzene | 76 | 60:40 | 87 |
| 3 | Chlorobenzene | 84 | 71:29 | 88 |
| 4 | Xylenes | 82 | 67:33 | 87 |
| **5** | **Toluene** | **88** | **71:29** | **87** |

[a] Reaction conditions: **1g** (0.05 mmol), **2a** (0.065 mmol), cat **3a** (10 mol%), PS (0.05 mmol), solvent (250 µL), RT, 16-24h. [b] Determined on the crude mixture by $^1$H NMR. [c] Overall conversion in products **4aa** and **5aa**. [d] Of product **4aa**, determined by chiral stationary phase HPLC.

Having established that lowering the reaction temperature and placing a *t*-Bu group on the 4-position of the benzyl ring gave better enantioselectivities (see main text), several aromatic solvents were tested in the dearomatization of substrate **1g** with indole **2a** under these newly found conditions (Table S5); toluene was confirmed as the optimal (Table S5, entry 5).

## Control experiments and mechanistic insights

We initially believed the reaction to proceed by simple halide-extraction performed by the thioureidic portion of catalyst **3a**; in other words, coordination of the bromide counterion by the two N-H bonds would render the substrate soluble in the reaction medium, and at the same increase its reactivity.[5] This reasoning was preliminary supported by the complete insolubility of substrate **1g** in toluene.

In order to support this initial hypothesis with experimental $^1$H NMR data, we mixed product **1g** and catalyst **3a** in toluene-*d*8. Whereas pyridinium salt alone did not give signals, due to its insolubility, in the presence of the catalyst a new species soluble in toluene appeared (Figures S8-S9). However, the resulting spectrum appeared much more complicated than expected, showing anomalous signals in the vinylic region. We therefore suspected that activation of the pyridinium ion by the catalyst was beyond the initially hypothesised halide coordination – solid phase extraction. A nucleophilic attack of the quinuclidinic nitrogen of the catalyst on the electrophilic pyridinium cation **1g** was thus considered.

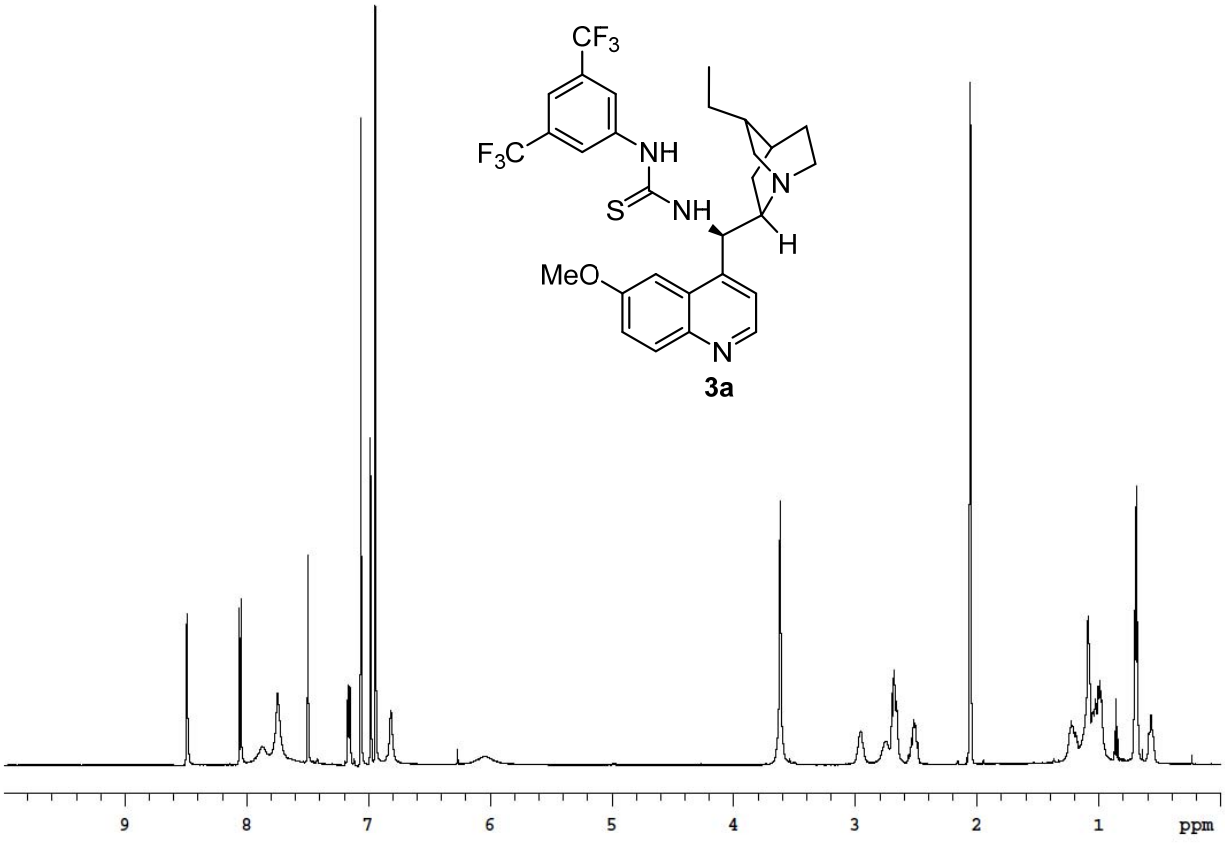


**Figure S8.** $^1$H NMR spectrum of catalyst **3a** in toluene-*d*8

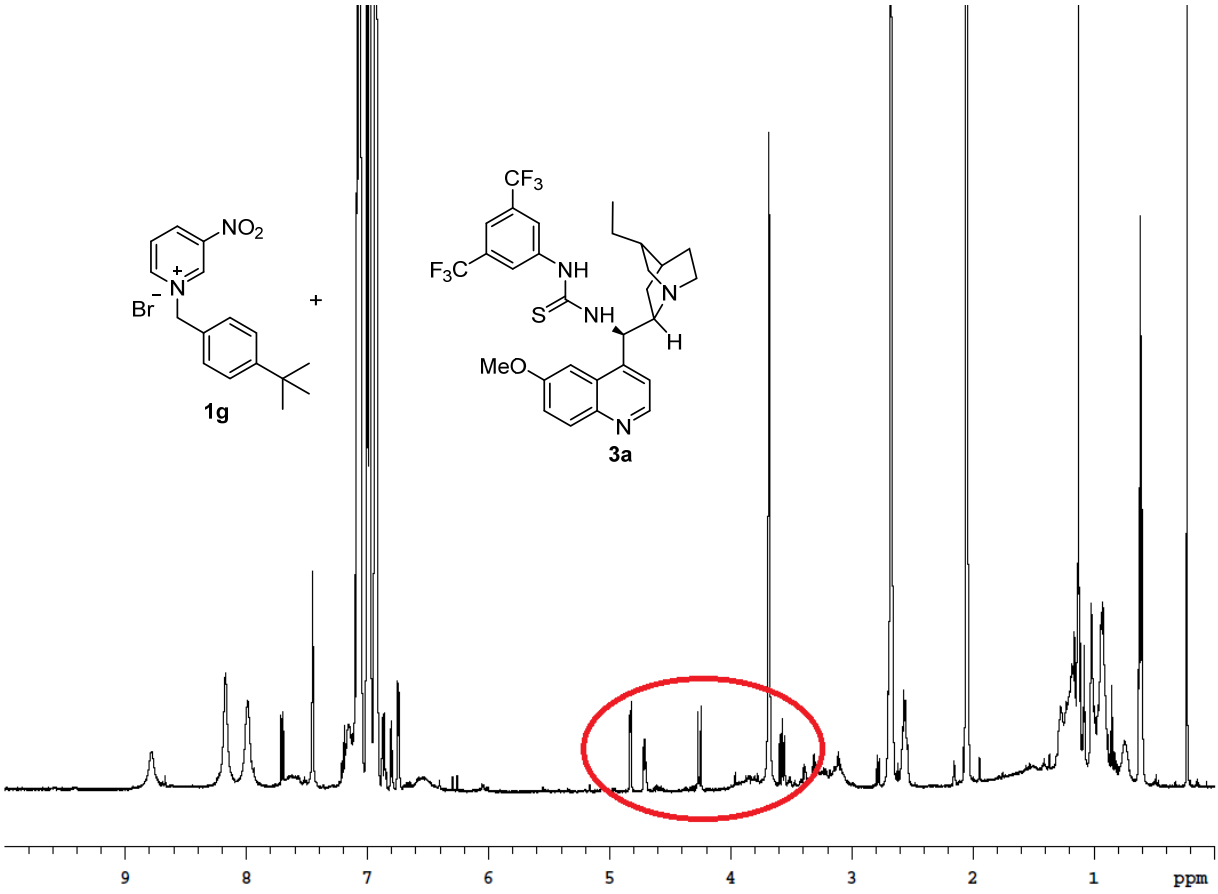


**Figure S9.** $^{1}$H NMR spectrum resulting from mixing equimolar amounts of catalyst **3a** and pyridinium salt **1g** in toluene-*d*8

Therefore, we decided to repeat the experiment by mixing equimolar amounts pyridinium **1g** and quinuclidine in toluene-*d*8, in order to obtain a simpler spectrum, after having verified that quinuclidine behaved similarly to catalyst **3a** in the reaction between **1g** and **2a** (complete regioselectivity towards C-4 addition product **4ga**). This showed clearly the typical pattern of a dihydropyridine along with the signals of quinuclidine (Figure S10), shifted from the original position (quinuclidine alone in toluene-*d*8, spectrum not shown).

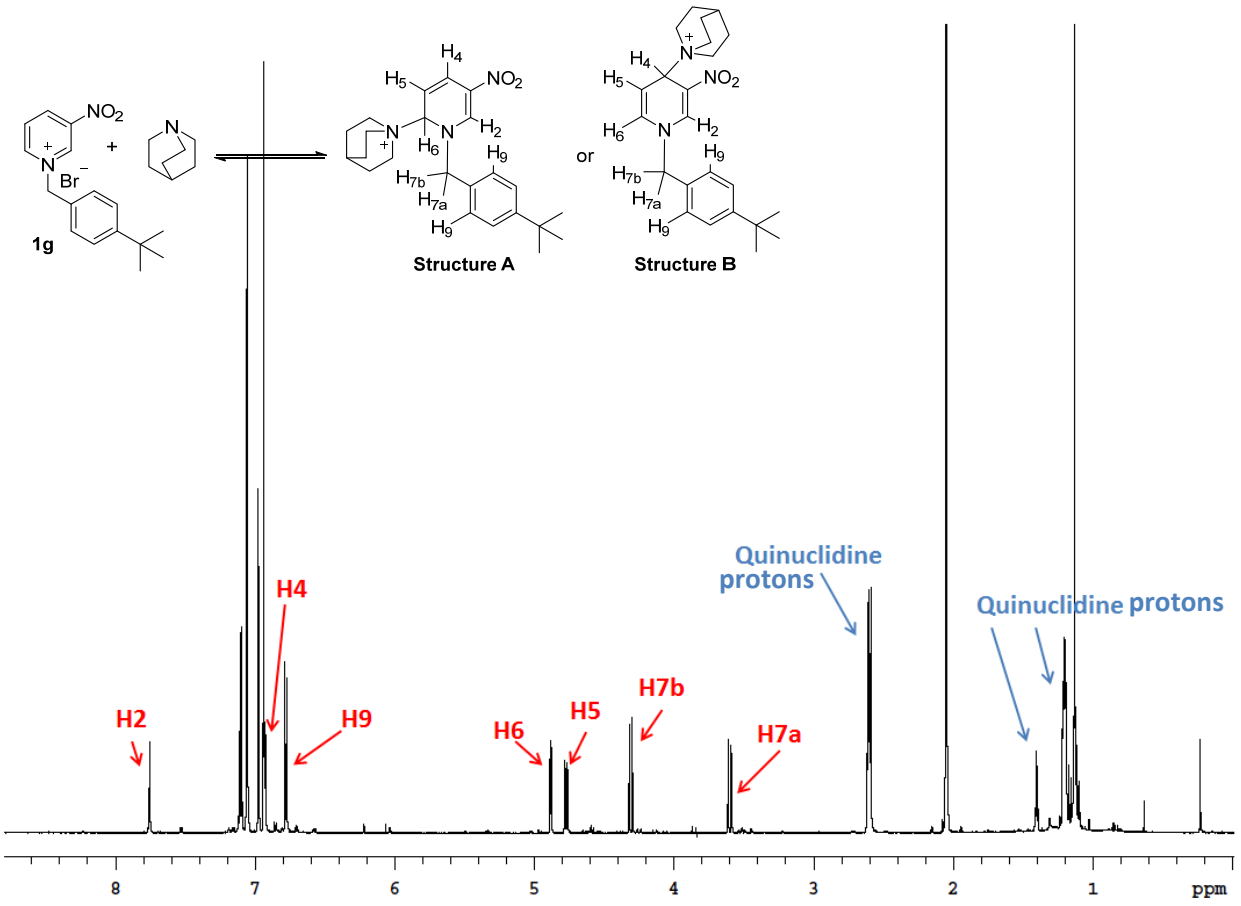


**Figure S10.** $^{1}$H NMR spectrum resulting from mixing equimolar amounts of quinuclidine and pyridinium salt **1g** in toluene-*d*8 (dihydropyridine intermediate)

This proved the hypothesis that the catalyst, which also bears a quinuclidine ring, besides possibly coordinating the bromide anion, also binds the substrate **1** by nucleophilic addition. This would lead to the formation of an intermediate dihydropyridine, subsequently captured by the nucleophile (indole). We then moved to characterize the regiochemistry of this intermediate (i.e. structure A vs structure B, Figure S10 and S11).

We initially tried to see correlations between protons of the quinuclidine and the dihydropyridine, either by DPFGSE-NOE or gHMBC experiments. This proved to be unsuccessful, probably due to a rapid interconversion between the dearomatized (structures A or B) and the aromatic (**1g**) forms.

Nevertheless, a complete characterization and signal assignment of the dihydropyridinic portion was performed by $^{1}$H NMR, DPFGSE-NOE and gHSQC NMR experiments (Figures S12-S13).

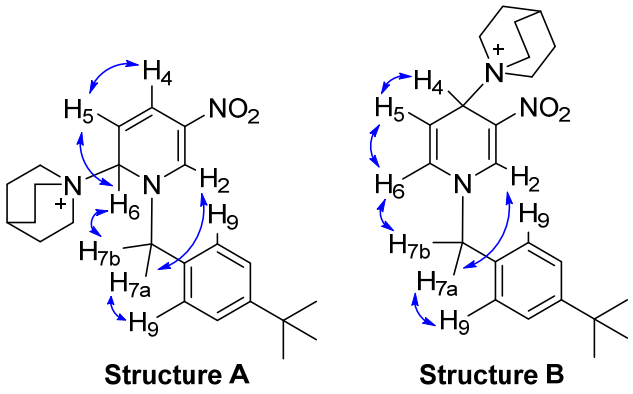


**Figure S11.** Blue arrows indicates NOE spatial correlations in structures A or B

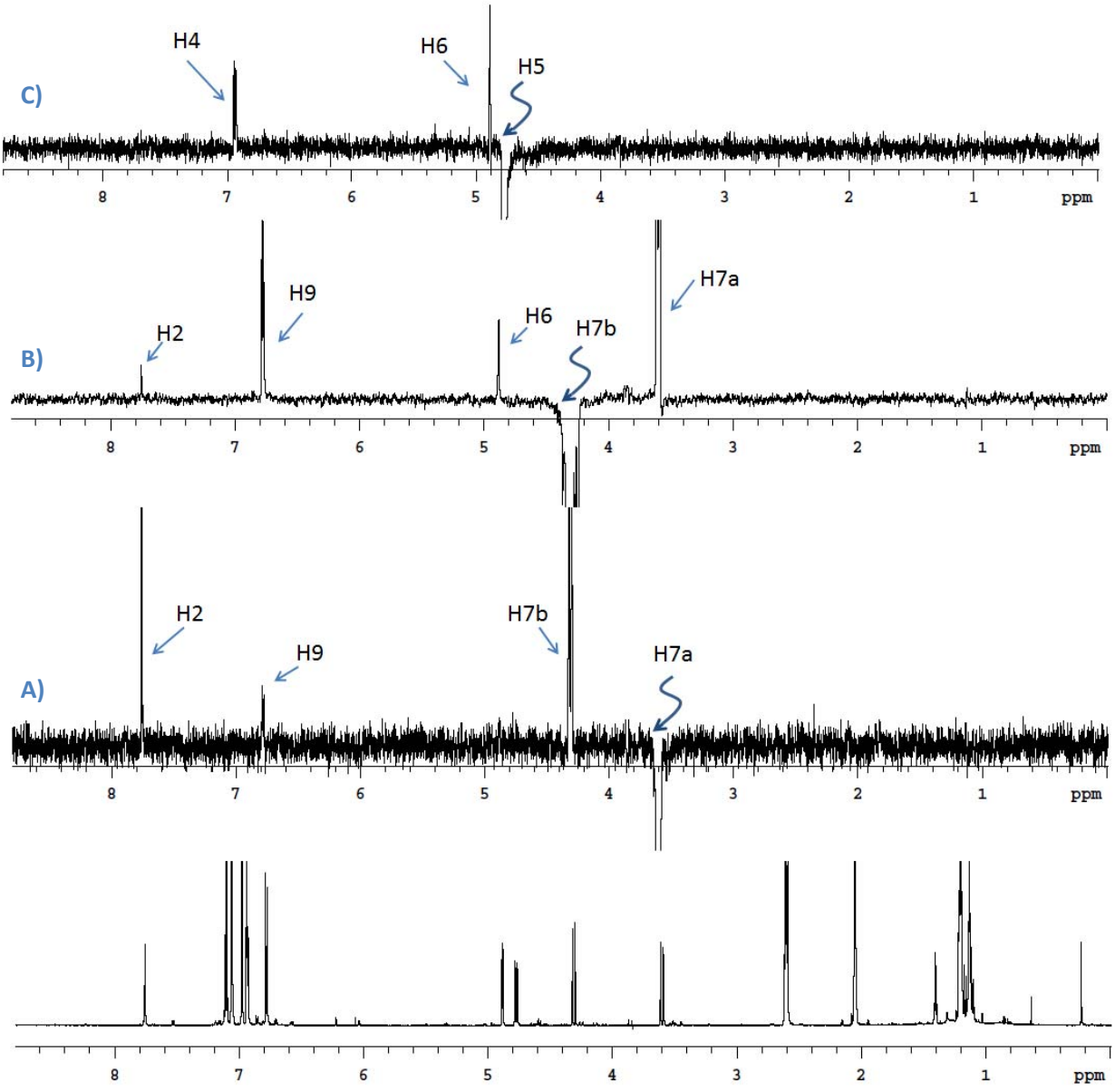


**Figure S12.** DPFGSE-NOE spectra

The signal at 7.75 ppm was assigned at H-2 due to the chemical shift and multiplicity (singlet, conjugation with the nitro-group).

Saturation of signals at 3.60 (Figure S12, A) and 4.31 ppm (Figure S12, B) (doublets) resulted in the enhancement of the signal at 6.78 ppm (H-9), along with a mutual one. In addition, the gHSQC spectrum showed correlation of these two protons with the same carbon ($CH_2$). They were therefore assigned at the two diastereotopic benzylic protons H-7a and H-7b. Moreover, saturation of the signal at 4.31 ppm (H-7b) showed enhancement (Figure S12, B) of the signal at 4.88 ppm (d) which was assigned to H-6. Saturation of signal at 3.60 ppm (H-7a) resulted also in the enhancement (Figure S12, A) of H-2 signal at 7.75 ppm, confirming the previous assignment.

The signal at 4.77 ppm was assigned to H-5 by multiplicity (dd) and its saturation showed enhancement (Figure S12, C) of the signal corresponding to H-6 and revealed the signal at 6.94 ppm, corresponding to H-4, overlapped with the residual solvent signal in the $^1$H NMR spectrum.

These patterns are consistent with both structures A and B.

$^{13}$C chemical shifts corresponding to C-7 (56.35 ppm), C-6 (77.2 ppm), C-5 (112.2 ppm), C-4 (119.9 ppm), C-2 (141.3 ppm) and C-9 (128.1 ppm) were assigned by gHSQC experiment along with the previous assignments of the $^1$H NMR signals (Figure S13).

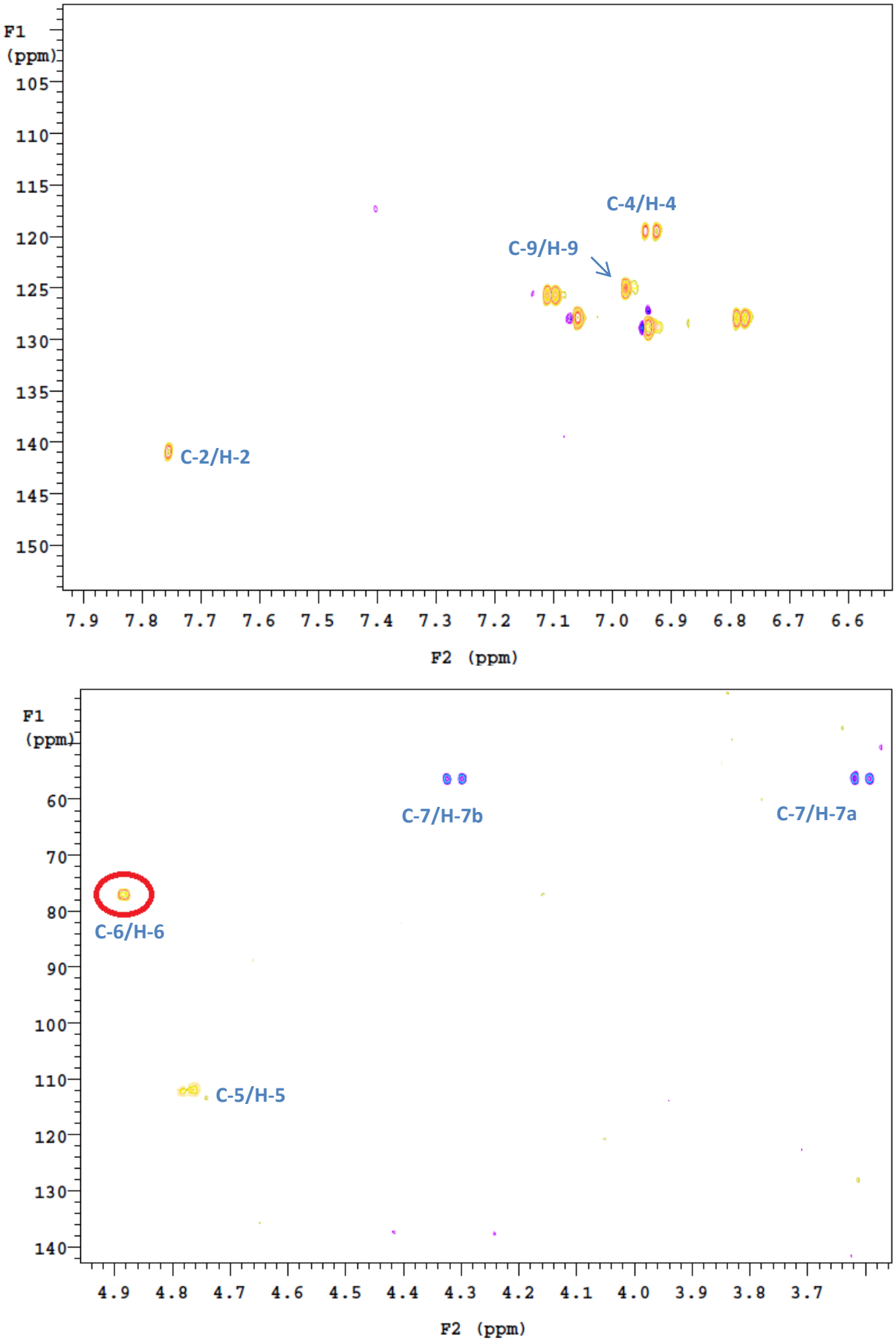


**Figure S13.** gHSQC spectra. Aromatic region top, vinylic region bottom

In particular, we focused on the chemical shift of C-6 at 77.2 ppm, which contrasts with the other CH carbons of the dihydropyridine ring. This led us to consider that this may be the $sp^3$-hybridized carbon. To support this hypothesis we found that a previously reported product,[6] bearing a C-H moiety between a cationic and a neutral nitrogen atom showed analogous $^{13}C$ and $^{1}H$ NMR chemical shifts. We therefore propose **structure A** to be correct, resulting from the addition of quinuclidine to the more reactive C6 of the pyridinium ring (Figure S10).

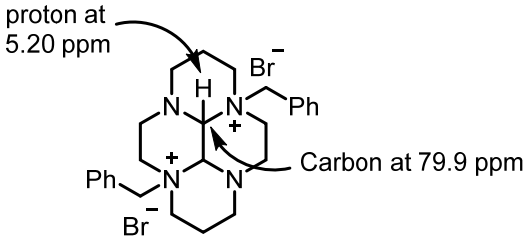


**Figure S14.** Product reported in literature

Since a coordination of the thiourea portion of the catalyst to the bromide can be envisioned, we performed an additional experiment adding an achiral thiourea (*N*,*N*′-bis[3,5-bis(trifluoromethyl)phenyl]thiourea, Schreiner's thiourea) to this dihydropyridine-quinuclidinium intermediate. We observed a substantial shift (1.4 ppm) in the signals of the thiourea (compared to the spectrum of thiourea alone in toluene-*d*8), suggesting a strong coordination of the bromide anion (Figures S15-S16).

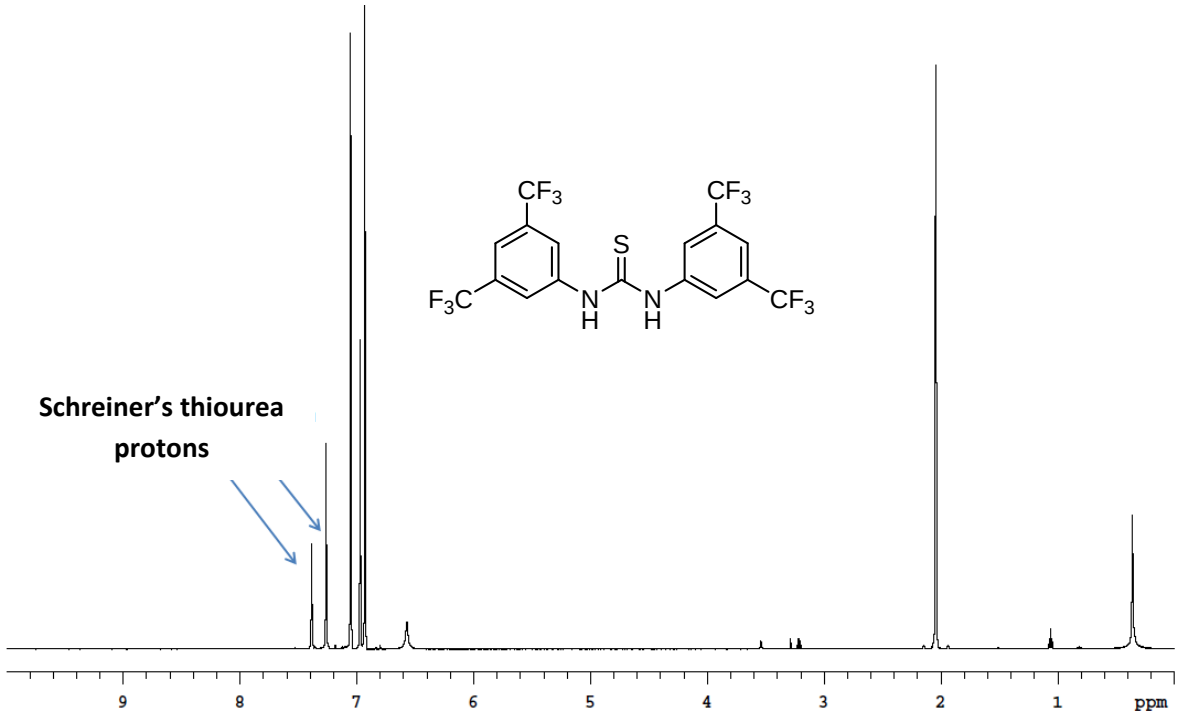


**Figure S15.** $^{1}$H NMR spectrum of Schreiner's thiourea in toluene-*d*8

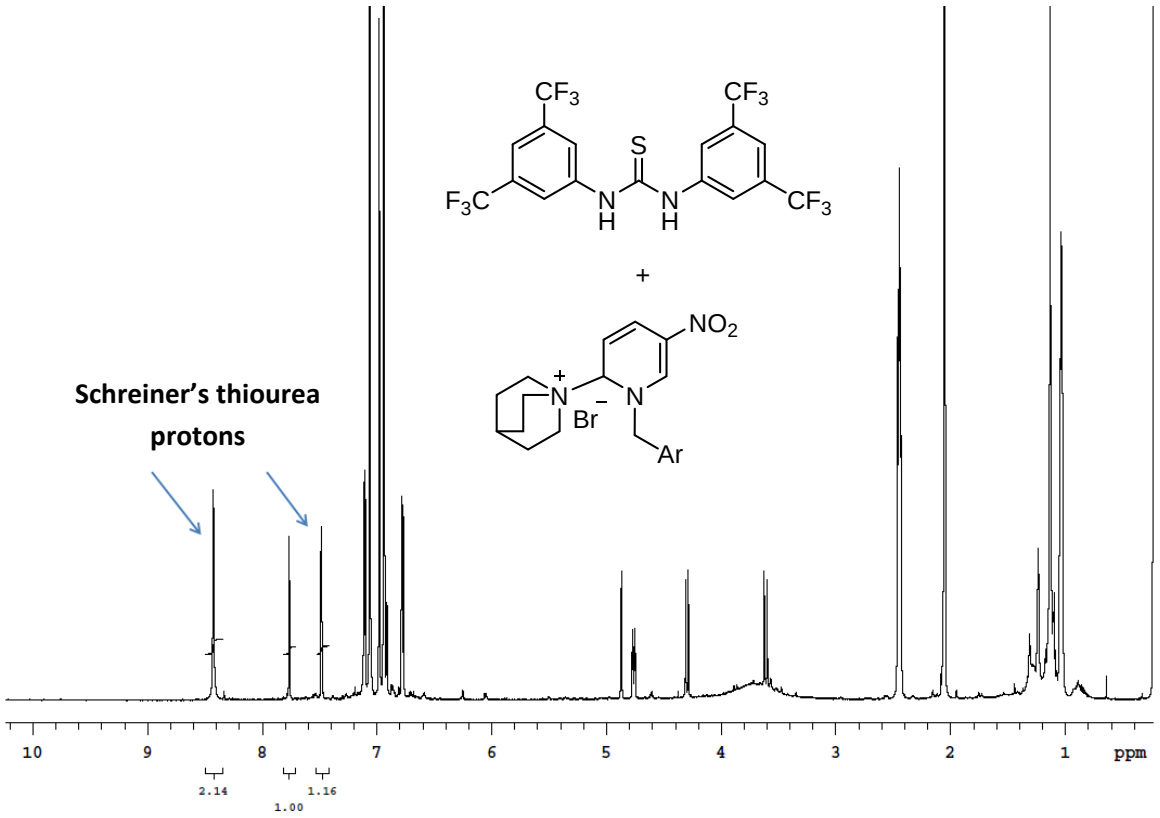


**Figure S16.** $^{1}$H NMR spectrum of Schreiner's thiourea and quinuclidine derived dihydropyridine intermediate in toluene-*d*8

All the previous results considered, we believe that catalyst **3a**, which bears both the thioureidic and the quinuclidinic moieties, acts in this way: nucleophilic addition at C-6 and bromide coordination. It is worth stressing that reactions performed with the quinuclidine alone are slower than reactions performed with a combination of quinuclidine and Schreiner's thiourea as catalyst, highlighting the role of a thiourea moiety in the promotion of the reaction.

On these grounds, we can propose the reaction pathway sketched in Scheme S3, involving the intermediacy of adduct **I** undergoing an $S_N2$'-like[7] reaction with indole. A concerted $S_N2$' mechanism does not seem likely, and an addition-elimination pathway has to be excluded (stabilization of the resulting negative charge is not possible due to the loss of conjugation with EWG group). An elimination-addition sequence seems instead more reasonable. In other words, attack of the indole would occur either as the catalyst is already leaving its position, on an electrophile that resembles more the free cation (**III**) than the dihydropyridine **I**, or even on the free pyridinium (**II**). Even if, according to the latter hypothesis, intermediate **I** is not involved in the regio- and stereo-determining step of the reaction (the addition of indole), its formation plays a crucial role in the catalytic cycle, "increasing" the concentration of the electrophile in the reaction medium.

To complete the proposed mechanism, we investigated if the indole had some interactions with the catalyst in the enantiodetermining step. Since the catalytic reaction performed with *N*-methylindole afforded only a small amount of product (<15%), in racemic form, it is likely that the N-H plays a crucial role in the catalytic mechanism. To account for these experimental data, we can propose two ways of coordination of the indole N-H moiety: either to the bromide anion exclusively, in its turn coordinated by the thiourea, as previously proposed by Porco and Jacobsen,[8] while the nitrogen of the quinuclidinic portion is leaving the previously attached C-6 position (**III**); or by the quinuclidine nitrogen and the bromide anion coordinated by the thiourea together (**II**, in this case addition of indoles **2** occurs on free pyridinium cation **1**). Coordination of the thiourea to the EWG can be instead excluded, considering the similar results obtained with substrates **1g-i** where EWG = $NO_2$, and **1j** where EWG = CN.

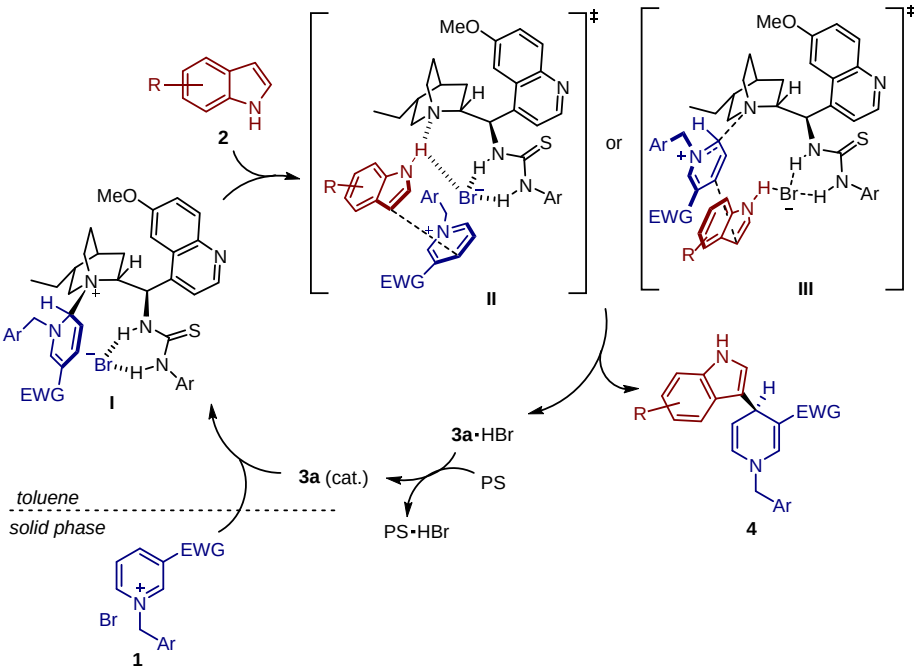


**Scheme S3.** Proposed reaction pathway and transition state.

Regarding the regioselectivity of the addition: in substrates **1** the C-6 position is generally considered to be the most reactive, while the C-4 gives the thermodynamically favoured 1,4-dihydropyridine products.[9] However, the regioselectivity in nucleophilic additions to **1** is often highly depending on the nature of the nucleophilic species, with soft nucleophiles preferentially undergoing addition at C-4, and hard nucleophiles at C-6.[10] From the collected NMR data it seems that the C6-adduct **I** of a tertiary amine catalyst to pyridinium ions **1** is favoured both kinetically and thermodynamically (absence of NOE between quinuclidine protons and dihydropyridine portion of **I** might indicate a fast equilibration between adduct **I** and the two parent species, thus **I** is also the thermodynamic addition product). In contrast, indoles **2** react selectively at C-4. It has been previously reported that the regioselectivity in addition of indoles to pyridinium ions **1** depends on reaction conditions (inorganic base and solvent).[3] While it can be concluded that the mild reaction conditions used in our work guarantee full regioselectivity towards C-4, the reasons for this selectivity are not fully clear. Different speculations can be done, taking into account *e.g.* the C-6 intermediates **I** undergoing an $S_N2'$-like reaction (through **III**), the mildness of the basic conditions used rendering indole rearomatization perhaps a non-negligible step for the selectivity of this reaction, etc. At this stage, we do not have a fully reliable mechanistic picture accounting for the results obtained. A more thorough and in depth investigation, beyond the scope of the present work, would be required.

Finally, to give some mechanistic explanation for the formation of isomers **5**, a reaction was performed with proton sponge only (see *"Preparation, characterization and structural assignment of isomers **4aa** and **5aa**"* page S5). Exclusively *N*-alkylation products were observed in the crude mixture by $^1$H NMR: **5aa**, which could be isolated and characterized, along with a highly unstable, not isolable isomer that was tentatively assigned to the C-6 adduct **5'aa** (presence of diastereotopic benzylic protons in the $^1$H NMR spectrum might

suggest the presence of a chiral centre near the $CH_2$). Since additions to such type of pyridinium ions can occur first at the C-6 position in a reversible fashion, yielding an unstable C-6 adduct which slowly isomerizes to the most stable C-4 isomer, we propose that the same equilibration occurs in this PS-promoted reaction (Scheme S4). The reasons for the selectivity in the *N*-alkylated products **5** *vs* C-alkylated **4**, displayed by the PS-promoted reactions are not clear at this stage.

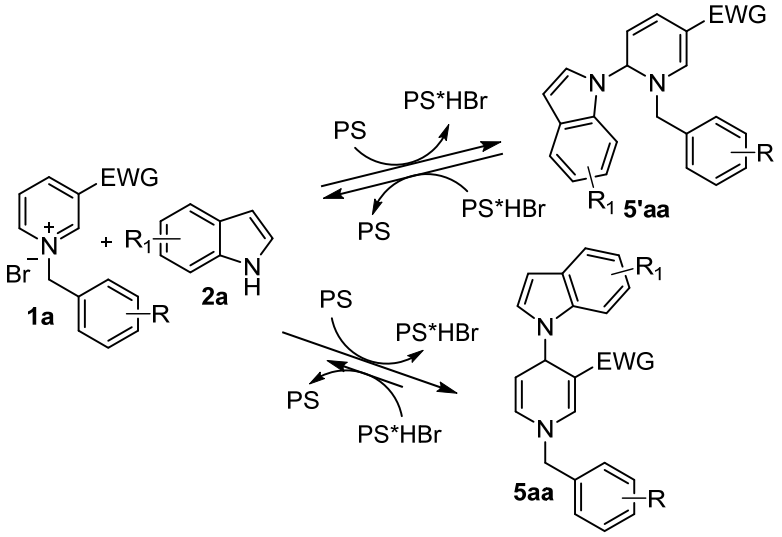


**Scheme S4.** Formation of product **5aa**

## Organocatalytic asymmetric dearomatization of pyridinium salts 1 with indoles 2.

**General procedure.** In a test tube equipped with a magnetic stirring bar, catalyst **3a** (0.015 mmol; 9.0 mg; 10 mol% or 0.023 mmol; 13.8 mg; 15 mol%) and indole **2a-f** (0.195 mmol; 1.3 equiv.) were dissolved in toluene (0.75 mL). The resulting mixture was stirred at the desired temperature for 5 minutes, after which pyridinium salt **1** (0.15 mmol) was added in one portion. Then, every 2 hours PS (0.03 mmol; 6.4 mg; 0.2 equiv.) was added as solid, until, after 10 hours, 1 equivalent was reached. The resulting mixture was then left stirring overnight.

Hereafter, $CH_2Cl_2$ was added (5 mL), the solution was filtered through a short plug of silica gel, and the plug was washed with $Et_2O$ (4x). After removal of the solvents, the reaction crude was analysed by $^1H$ NMR spectroscopy to determine the isomeric ratio of the dhydropyridines (**4**/**5**). The residue was then purified by chromatography on silica gel (*n*-hexane/EtOAc mixtures) to afford the desired products **4**. Finally, the enantiomeric excess was determined by chiral stationary phase HPLC (*n*-hexane/*i*-PrOH mixtures).

**(*S*)-3-(1-(4-(*tert*-Butyl)benzyl)-3-nitro-1,4-dihydropyridin-4-yl)-1*H*-indole (4ga)**

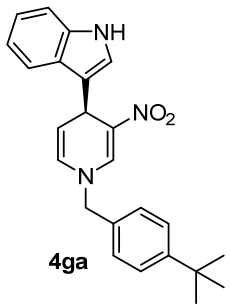

4ga

Following the general procedure (T = -20 °C, **3a** 10 mol%), from *N*-(4-*tert*-butylbenzyl)-3-nitropyridinium bromide (**1g**) and indole (**2a**), product **4ga** was obtained as a bright yellow solid in 80% yield after column chromatography on silica gel (*n*-hexane/EtOAc = 2.5:1). Isomeric ratio **4ga**/**5ga** was evaluated from the $^1H$ NMR spectrum of the crude mixture and was found to be 91:9. The enantiomeric excess of **4ga** was determined by chiral stationary phase HPLC (AS, *n*-hexane/*i*-PrOH 70:30, 1.00 mL/min, λ = 254 nm, $t_{maj}$ = 15.3 min, $t_{min}$ = 21.9 min, 91% *ee*). $[\alpha]_D^{25\ °C}$ = -279.1 (c = 0.4, $CHCl_3$); $^1H$ NMR (400 MHz, $CDCl_3$) δ = 8.10 (d, J = 1.4 Hz, 1H), 8.06 (bs, 1H), 7.51 (d, J = 8.0 Hz, 1H), 7.48-7.45 (m, 2H), 7.33 (d, J = 8.2 Hz, 1H), 7.30-7.26 (m, 2H), 7.15 (t, J = 7.6 Hz, 1H), 7.07 (s, 1H), 6.98 (t, J = 7.4 Hz, 1H), 6.01 (dt, $J_1$ = 7.8 Hz, $J_2$ = 1.2 Hz, 1H), 5.31 (dd, $J_1$ = 8.2 Hz, $J_2$ = 5.0 Hz, 1H), 5.25 (d, J = 4.8 Hz, 1H), 4.57 (s, 2H), 1.36 (s, 9H) ppm; $^{13}C$ NMR (100 MHz, $CDCl_3$) δ = 151.9, 138.9, 136.5, 132.3, 127.5, 126.2, 126.0, 125.6, 125.3, 122.7, 121.8, 119.4, 119.2, 118.5, 113.0, 111.4, 58.5, 34.7, 31.5, 31.3 ppm; ESI-MS: 410 [M + $Na^+$]; HRMS(ESI) calcd. for $C_{24}H_{25}N_3O_2Na$ (M + $Na^+$): 410.1844; found: 410.1844.

**(*S*)-3-(1-(4-Isopropylbenzyl)-3-nitro-1,4-dihydropyridin-4-yl)-1*H*-indole (4ha)**

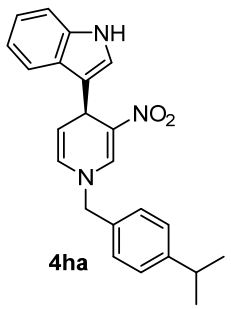

4ha

Following the general procedure (T = -20 °C, **3a** 10 mol%), from indole (**2a**) and *N*-(4-isopropylbenzyl)-3-nitropyridinium bromide (**1h**), product **4ha** was obtained as a bright yellow solid in 75% yield after column chromatography on silica gel (*n*-hexane/EtOAc = 3:1). Isomeric ratio **4ha**/**5ha** was evaluated from the $^1H$ NMR spectrum of the crude mixture and was found to be 80:20. The enantiomeric excess of **4ha** was determined by

chiral stationary phase HPLC (AS, *n*-hexane/*i*-PrOH 70:30, 1.00 mL/min, λ = 254 nm, $t_{maj}$ = 18.1 min, $t_{min}$ = 27.3 min, 91% *ee*). $[\alpha]_D^{25\ °C}$ = -285 (c = 0.410, $CHCl_3$); $^1$H NMR (400 MHz, $CDCl_3$) δ = 8.08 (d, J = 1.3 Hz, 1H), 8.06 (bs, 1H), 7.49 (d, J = 8.0 Hz, 1H), 7.31-7.28 (m, 3H), 7.26-7.24 (m, 2H), 7.13 (t, J = 7.5 Hz, 1H), 7.04 (d, J = 1.8 Hz, 1H), 6.97 (d, J = 7.4 Hz, 1H), 5.99 (dt, $J_1$ = 7.7 Hz, $J_2$ = 1.2 Hz, 1H), 5.29 (dd, $J_1$ = 7.6 Hz, $J_2$ = 4.9 Hz, 1H), 5.23 (d, J = 4.9 Hz, 1H), 4.54 (s, 2H), 2.95 (sept, J = 7.1 Hz, 1H), 1.28 (d, J = 7.1 Hz, 6H) ppm; $^{13}$C NMR (100 MHz, $CDCl_3$) δ = 149.6, 138.9, 136.5, 132.7, 127.8, 127.3, 126.1, 125.5, 125.3, 122.7, 121.8, 119.4, 119.2, 118.5, 113.0, 111.4, 58.6, 33.9, 31.5, 23.9 ppm; ESI-MS: 396 [M + $Na^+$].

**(*S*)-3-(1-(3,5-di-*tert*-Butylbenzyl)-3-nitro-1,4-dihydropyridin-4-yl)-1*H*-indole (4ia)**

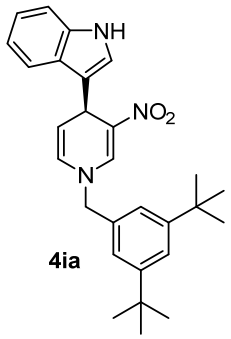


Following the general procedure (T = -20 °C, **3a** 10 mol%), from *N*-(3,5-di-*tert*-butylbenzyl)-3-nitropyridinium bromide (**1i**) and indole (**2a**), product **4ia** was obtained as a dark red solid in 70% yield after column chromatography on silica gel (*n*-hexane/EtOAc = 3.5:1). Isomeric ratio **4ia**/**5ia** was evaluated from the $^1$H NMR spectrum of the crude mixture and was found to be 82:18. The enantiomeric excess of **4ia** was determined by chiral stationary phase HPLC (AS, *n*-hexane/*i*-PrOH 80:20, 1.00 mL/min, λ = 254 nm, $t_{maj}$ = 11.3 min, $t_{min}$ = 16.8 min, 90% *ee*). $[\alpha]_D^{25\ °C}$ = -188 (c = 0.4, $CHCl_3$); $^1$H NMR (400 MHz, $CDCl_3$) δ = 8.13 (d, J = 1.4 Hz, 1H), 8.10 (bs, 1H), 7.57 (d, J = 8.0 Hz, 1H), 7.49 (t, J = 1.9 Hz, 1H), 7.32 (d, J = 8.2 Hz, 1H), 7.17-7.13 (m, 3H), 7.05-7.00 (m, 2H), 6.01 (dt, $J_1$ = 7.7 Hz, $J_2$ = 1.2 Hz, 1H), 5.34 (dd, $J_1$ = 7.8 Hz, $J_2$ = 4.9 Hz, 1H), 5.27 (d, J = 4.9 Hz, 1H), 4.60 (s, 2H), 1.36 (s, 18H) ppm; $^{13}$C NMR (100 MHz, $CDCl_3$) δ = 152.0, 139.1, 136.5, 134.4, 126.0, 125.5, 125.3, 122.8, 121.85, 121.76, 119.6, 119.1, 118.8, 113.1, 111.4, 59.3, 34.9, 31.5, 31.4 ppm; ESI-MS: 466 [M + $Na^+$].

**(*S*)-3-(1-(4-(*tert*-Butyl)benzyl)-3-nitro-1,4-dihydropyridin-4-yl)-5-methyl-1*H*-indole (4gb)**

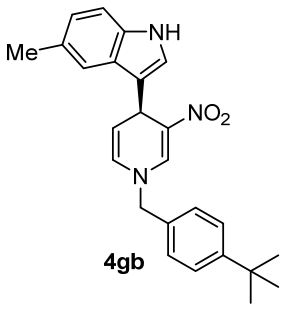


Following the general procedure (T = -20 °C, **3a** 10 mol%), from *N*-(4-*tert*-butylbenzyl)-3-nitropyridinium bromide (**1g**) and 5-methylindole (**2b**), product **4gb** was obtained as a bright yellow solid in 76% yield after column chromatography on silica gel (*n*-hexane/EtOAc = 3:1). Isomeric ratio **4gb**/**5gb** was evaluated from the $^1$H NMR spectrum of the crude mixture and was found to be 80:20. The enantiomeric excess of **4gb** was determined by chiral stationary phase HPLC (AS, *n*-hexane/*i*-PrOH 70:30, 1.00 mL/min, λ = 254 nm, $t_{maj}$ = 14.0 min, $t_{min}$ = 29.1 min, 91% *ee*). $[\alpha]_D^{25\ °C}$ = -339 (c = 0.4, $CHCl_3$); $^1$H NMR ($CDCl_3$, 400 MHz) δ = 8.09 (d, J = 1.6 Hz, 1H), 7.98 (bs, 1H), 7.47-7.43 (m, 2H), 7.38 (bs, 1H), 7.30-7.26 (m, 2H), 7.22 (d, J = 8.6 Hz, 1H), 7.02 (d, J = 2,5 Hz, 1H), 6.98 (dd, $J_1$ = 8.3 Hz, $J_2$ = 1.5 Hz, 1H), 5.99 (dt, $J_1$ = 7.8 Hz, $J_2$ = 1.4 Hz, 1H), 5.31 (dd, $J_1$ = 7.7 Hz, $J_2$ = 4.8 Hz, 1H), 5.23 (d, J = 4.9 Hz, 1H), 4.56 (s, 2H), 2.39 (s, 3H), 1.35 (s, 9H) ppm; $^{13}$C NMR (100 MHz, $CDCl_3$) δ = 150.8, 137.9, 133.9, 131.3, 127.6, 126.4, 125.2, 124.4, 124.4, 122.5, 121.9, 117.7, 117.1, 112.1, 110.0, 57.4, 33.6, 30.5, 30.2, 20.7 ppm; ESI-MS: 424 [M + $Na^+$].

**(*S*)-3-(1-(4-(*tert*-Butyl)benzyl)-3-nitro-1,4-dihydropyridin-4-yl)-5-methoxy-1*H*-indole (4gc)**

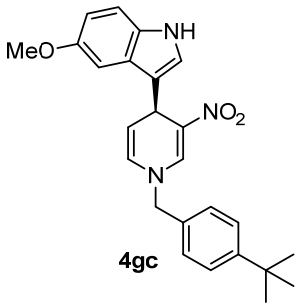


Following the general procedure (T = -20 °C, **3a** 10 mol%), from *N*-(4-*tert*-butylbenzyl)-3-nitropyridinium bromide (**1g**) and 5-methoxyindole (**2c**), product **4gc** was obtained as a yellow solid in 73% yield after column chromatography on silica gel (*n*-hexane/EtOAc = 2.5:1). Isomeric ratio **4gc**/**5gc** was evaluated from the $^1$H NMR spectrum of the crude mixture and was found to be 80:20. The enantiomeric excess of **4gc** was determined by chiral stationary phase HPLC (AD-H, *n*-hexane/*i*-PrOH 80:20, 0.75 mL/min, λ = 254 nm, $t_{maj}$ = 20.2 min, $t_{min}$ = 27.3 min, 87% *ee*). $[\alpha]_D^{25\ °C}$ = -280 (c = 0.2, $CHCl_3$); $^1$H NMR (400 MHz, $CDCl_3$) δ = 8.07 (d, J = 1.5 Hz,1H), 7.96 (bs, 1H), 7.46-7.42 (m, 2H), 7.26-7.23 (m, 3H), 7.22 (s, 1H), 7.15 (d, J = 2.5 Hz, 1H), 7.02 (d, J = 2.3 Hz, 1H), 6.00 (dt, $J_1$ = 7.8 Hz, $J_2$ = 1.4 Hz, 1H), 5.32 (dd, $J_1$ = 7.8 Hz, $J_2$ = 4.9 Hz, 1H), 5.22 (d, J = 4.9 Hz, 1H), 4.57 (s, 2H), 3.82 (s, 3H), 1.34 (s, 9H) ppm; $^{13}$C NMR (100 MHz, $CDCl_3$) δ = 154.0, 151.8, 138.8, 132.2, 131.7, 127.3, 126.4, 126.2, 125.55, 125.46, 123.7, 118.9, 112.9, 111.9, 111.8, 101.7, 58.3, 55.9, 34.7, 31.3, 31.2 ppm; ESI-MS: 440 [M + $Na^+$].

**(*S*)-3-(1-(4-(*tert*-Butyl)benzyl)-3-nitro-1,4-dihydropyridin-4-yl)-5-chloro-1*H*-indole (4gd)**

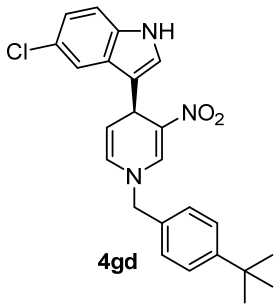


Following the general procedure (T = 0 °C, **3a** 15 mol%), from *N*-(4-*tert*-butylbenzyl)-3-nitropyridinium bromide (**1g**) and 5-chloroindole (**2d**), product **4gd** was obtained as an orange solid in 66% yield after column chromatography on silica gel (*n*-hexane/EtOAc = 3:1). Isomeric ratio **4gd**/**5gd** was evaluated from the $^1$H NMR spectrum of the crude mixture and was found to be > 95:5. The enantiomeric excess of **4gd** was determined by chiral stationary phase HPLC (AD-H, *n*-hexane/*i*-PrOH 90:10, 0.75 mL/min, λ = 254 nm, $t_{maj}$ = 34.6 min, $t_{min}$ = 37.3 min, 80% *ee*). Crystals suitable for X-ray diffraction experiment were grown by slow diffusion of a layer of *n*-hexane into a solution of **4gd** in EtOAc. The red crystals obtained were found to be enantiomerically pure (> 99% *ee*). $[\alpha]_D^{25\ °C}$ = -197 (c = 0.4, $CHCl_3$); $^1$H NMR (400 MHz, $CDCl_3$) δ = 8.16 (bs, 1H), 8.08 (d, J = 1.6 Hz, 1H), 7.57 (d, J = 2.1 Hz, 1H), 7.49-7.45 (m, 2H), 7.32-7.27 (m, 2H), 7.22 (d, J = 9.0 Hz, 1H), 7.12-7.06 (m, 2H), 6.01 (dt, $J_1$ = 7.8 Hz, $J_2$ = 1.1Hz, 1H), 5.26 (dd, $J_1$ = 7.8 Hz, $J_2$ = 4.8 Hz, 1H), 5.20 (d, J = 5.0 Hz, 1H), 4.59 (s, 2H), 1.34 (s, 9H) ppm; $^{13}$C NMR (100 MHz, $CDCl_3$) δ = 151.9, 139.1, 134.9, 131.9, 127.5, 127.1, 126.3, 125.8, 125.2, 125.1, 124.1, 122.2, 118.7, 118.1, 112.7, 112.4, 58.4, 34.7, 31.6, 31.3 ppm; ESI-MS: 444-446 [M + $Na^+$].

**(*S*)-3-(1-(4-(*tert*-Butyl)benzyl)-3-nitro-1,4-dihydropyridin-4-yl)-6-chloro-1*H*-indole (4ge)**

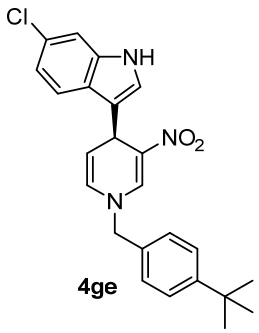

**4ge**

Following the general procedure (T = 0 °C, **3a** 15 mol%), from *N*-(4-*tert*-butylbenzyl)-3-nitropyridinium bromide (**1g**) and 6-chloroindole (**2e**), product **4ge** was obtained as an orange solid in 67% yield after column chromatography on silica gel (*n*-hexane/EtOAc = 3:1). Isomeric ratio **4ge**/**5ge** was evaluated from the $^{1}$H NMR spectrum of the crude mixture and was found to be > 95:5. The enantiomeric excess of **4ge** was determined by chiral stationary phase HPLC (OD, *n*-hexane/*i*-PrOH 80:20, 1.00 mL/min, λ = 254 nm, $t_{maj}$ = 32.4 min, $t_{min}$ = 25.4 min, 80% *ee*). The product was crystallized by slow diffusion of a layer of *n*-hexane into a solution of **4ge** in EtOAc. The red crystals obtained were found to have 93 % *ee*. $[\alpha]_D^{25\ °C}$ = -186 (c = 0.395, $CHCl_3$); $^{1}$H NMR (400 MHz, $CDCl_3$) δ = 8.12 (bs, 1H), 8.09 (d, J = 1.3 Hz, 1H), 7.49-7.45 (m, 2H), 7.33 (d, J = 8.5 Hz, 1H), 7.30-7.25 (m, 3H), 7.03 (s, 1H), 6.87 (dd, $J_1$ = 8.4 Hz, $J_2$ = 1.56 Hz, 1H), 6.02 (dt, $J_1$ = 7.8 Hz, $J_2$ = 1.2 Hz, 1H), 5.26 (dd, $J_1$ = 7.7 Hz, $J_2$ = 4.8 Hz, 1H), 5.19 (d, J = 4.8 Hz, 1H), 4.56 (s, 2H), 1.37 (s, 9H) ppm; $^{13}$C NMR (100 MHz, $CDCl_3$) δ = 152.0, 138.8, 136.8, 132.2, 127.7, 127.5, 126.3, 125.7, 125.2, 124.6, 123.4, 120.1, 120.0, 118.6, 112.8, 111.3, 58.6, 34.7, 31.4, 31.3 ppm; ESI-MS: 444-446 [M + $Na^+$].

**(*S*)-3-(1-(4-(*tert*-Butyl)benzyl)-3-nitro-1,4-dihydropyridin-4-yl)-2-methyl-1*H*-indole (4gf)**

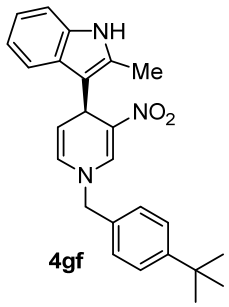

**4gf**

Following the general procedure (T = -20 °C, **3a** 10 mol%), from *N*-(4-*tert*-butylbenzyl)-3-nitropyridinium bromide (**1g**) and 2-methylindole (**2f**), product **4gf** was obtained as an orange solid in 79% yield after column chromatography on silica gel (*n*-hexane/EtOAc = 2.5:1). Isomeric ratio **4gf**/**5gf** was evaluated from the $^{1}$H NMR spectrum of the crude mixture and was found to be 89:11. The enantiomeric excess of **4gf** was determined by chiral stationary phase HPLC (AD-H, *n*-hexane/*i*-PrOH 90:10, 0.75 mL/min, λ = 254 nm, $t_{maj}$ = 33.8 min, $t_{min}$ = 36.2 min, 75% *ee*). $[\alpha]_D^{25\ °C}$ = -110 (c = 0.2, $CHCl_3$); $^{1}$H NMR (400 MHz, $CDCl_3$) δ = 8.09 (d, J = 1.6 Hz, 1H), 7.78 (bs, 1H), 7.50-7.46 (m, 2H), 7.35-7.30 (m, 2H), 7.28-7.21 (m, 2H), 7.04 (t, J = 7.7 Hz, 1H), 6.86 (t, J = 7.6 Hz, 1H), 6.05 (dt, $J_1$ = 7.7 Hz, $J_2$ = 1.4 Hz, 1H), 5.18 (d, J = 4.8 Hz, 1H), 5.14 (dd, $J_1$ = 7.6 Hz, $J_2$ = 4.8 Hz, 1H), 4.60 (s, 2H), 2.47 (s, 3H), 1.36 (s, 9H) ppm; $^{13}$C NMR (100 MHz, $CDCl_3$) δ = 151.9, 138.7, 135.2, 132.3, 131.9, 127.7, 127.6, 126.2, 125.7, 124.9, 120.7, 119.0, 118.3, 113.0, 112.3, 110.4, 58.6, 34.7, 31.3, 30.8, 11.8 ppm; ESI-MS: 424 [M + $Na^+$].

**(*S*)-3-(1-(4-(*tert*-Butyl)benzyl)-3-cyano-1,4-dihydropyridin-4-yl)-1*H*-indole (4ja)**

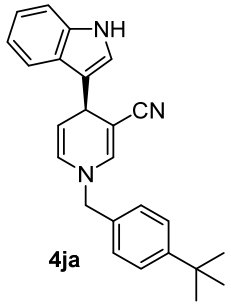


Following the general procedure (T = RT, **3a** 15 mol%), from *N*-(4-*tert*-butylbenzyl)-3-cyanopyridinium bromide (**1j**) and indole (**2a**), product **4ja** was obtained as a light yellow solid in 50% yield after column chromatography on silica gel (*n*-hexane/EtOAc = 4:1). Isomeric ratio **4ja** /**5ja** was evaluated from the $^1$H NMR spectrum of the crude mixture and was found to be 75:25. The enantiomeric excess of **4ja** was determined by chiral stationary phase HPLC (AS, *n*-hexane/*i*-PrOH 80:20, 1.00 mL/min, λ = 254 nm, $t_{maj}$ = 16.0 min, $t_{min}$ = 28.8 min, 83% *ee*). $[\alpha]_D^{25\ °C}$ = -7 (c = 0.563, $CHCl_3$); $^1$H NMR (400 MHz, $CDCl_3$) δ = 8.07 (bs, 1H), 7.65 (d, J = 8.0 Hz, 1H), 7.46-7.43 (m, 2H), 7.36 (d, J = 8.0 Hz, 1H), 7.25-7.22 (m, 2H), 7.18 (dt, $J_1$ = 7.7 Hz, $J_2$ = 1.1 Hz, 1H), 7.07-7.03 (m, 2H), 6.74 (d, J = 1.6 Hz, 1H), 5.93 (dt, $J_1$ = 8.1 Hz, $J_2$ = 1.4 Hz, 1H), 4.87 (dd, $J_1$ = 8.2 Hz, $J_2$ = 4.1 Hz, 1H), 4.66 (d, J = 4.1 Hz, 1H), 4.38 (s, 2H), 1.35 (s, 9H) ppm; $^{13}$C NMR (100 MHz, $CDCl_3$) δ = 151.4, 141.6, 136.9, 133.4, 127.2, 127.1, 126.1, 126.0, 122.1, 121.8, 121.4, 120.7, 119.42, 119.40, 111.3, 106.0, 82.9, 57.5, 34.6, 31.32, 31.27 ppm; ESI-MS: 390 [M + $Na^+$].

**(*S*)-3-(1-(4-(*tert*-Butyl)benzyl)-3-cyano-1,4-dihydropyridin-4-yl)-5-methyl-1*H*-indole (4jb)**

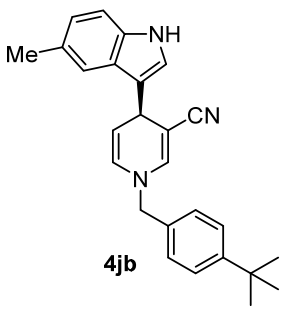


Following the general procedure (T = RT, **3a** 15 mol%), from *N*-(4-*tert*-butylbenzyl)-3-cyanopyridinium bromide (**1j**) and 5-methylindole (**2b**), product **4jb** was obtained as a light yellow solid in 45% yield after column chromatography on silica gel (*n*-hexane/EtOAc = 4:1). Isomeric ratio **4jb**/**5jb** was evaluated from the $^1$H NMR spectrum of the crude mixture and was found to be 75:25. The enantiomeric excess of **4jb** was determined by chiral stationary phase HPLC (AS, *n*-hexane/*i*-PrOH 80:20, 1.00 mL/min, λ = 254 nm, $t_{maj}$ = 14.0 min, $t_{min}$ = 30.0 min, 89% *ee*). $[\alpha]_D^{25\ °C}$ = -11 (c = 0.468, $CHCl_3$); $^1$H NMR ($CDCl_3$, 400 MHz) δ = 7.98 (bs, 1H), 7.48 (s, 1H), 7.45-7.42 (m, 2H), 7.27-7.25 (m, 2H), 7.24 (d, J = 2.3 Hz, 1H), 7.03-7.00 (m, 2H), 6.73 (d, J = 1.8 Hz, 1H), 5.92 (dt, $J_1$ = 8.1 Hz, $J_2$ = 1.4 Hz, 1H), 4.87 (dd, $J_1$ = 8.2 Hz, $J_2$ = 4.0 Hz, 1H), 4.64 (dd, $J_1$ = 4.0 Hz, $J_2$ = 1.2 Hz, 1H), 4.38 (s, 2H), 1.34 (s, 9H) ppm; $^{13}$C NMR (100 MHz, $CDCl_3$) δ = 151.3, 141.7, 135.3, 133.4, 128.6, 127.2, 127.0, 126.3, 126.0, 123.8, 122.0, 121.4, 120.2, 118.9, 111.0, 106.2, 83.0, 57.4, 34.6, 31.3, 31.3, 21.7 ppm; ESI-MS: 404 [M + $Na^+$].

**(*S*)-3-(1-(4-(*tert*-Butyl)benzyl)-3-cyano-1,4-dihydropyridin-4-yl)-5-methoxy-1*H*-indole (4jc)**

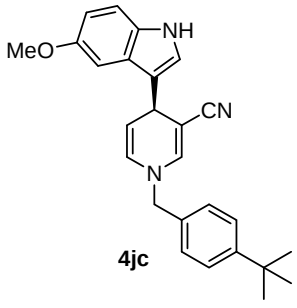


Following the general procedure (T = RT, **3a** 15 mol%), from *N*-(4-*tert*-butylbenzyl)-3-cyanopyridinium bromide (**1j**) and 5-methoxyindole (**2c**), product **4jc** was obtained as a pale yellow solid in 55% yield after column chromatography on silica gel (*n*-hexane/EtOAc = 3:1). Isomeric ratio **4jc**/**5jc** was evaluated from the $^1$H NMR spectrum of the crude mixture and was found to be 75:25. The enantiomeric excess of **4jc** was determined by chiral stationary phase

HPLC (AS, *n*-hexane/*i*-PrOH 80:20, 1.00 mL/min, λ = 254 nm, $t_{maj}$ = 31.4 min, $t_{min}$ = 34.1 min, 80% *ee*). $[\alpha]_D^{25\ °C}$ = -15 (c = 0.5, $CHCl_3$); $^1H$ NMR ($CDCl_3$, 400 MHz) δ = 8.00 (bs, 1H), 7.43-7.40 (m, 2H), 7.26 (d, J = 8.3 Hz, 1H), 7.23-7.19 (m, 2H), 7.18 (d, J = 4.5 Hz, 1H), 7.05 (d, J = 2.5 Hz, 1H), 6.86 (dd, $J_1$ = 9 Hz, $J_2$ = 2.5 Hz, 1H), 6.73 (d, J =1.7 Hz, 1H), 5.93 (dt, $J_1$ = 8.0 Hz, $J_2$ = 1.5 Hz, 1H), 4.88 (dd, $J_1$ = 8.0 Hz, $J_2$ = 4.0 Hz, 1H), 4.65 (dd, $J_1$ = 3.9 Hz, $J_2$ = 1.0 Hz, 1H), 4.38 (s, 2H), 3.82 (s, 3H), 1.34 (s, 9H) ppm; $^{13}C$ NMR (100 MHz, $CDCl_3$) δ = 153.9, 151.3, 141.7, 133.3, 132.1, 127.1, 126.5, 126.0, 122.9, 121.5, 120.6, 112.1, 111.9, 105.9, 101.6, 83.0, 57.4, 55.9, 34.6, 31.3, 31.1 ppm; ESI-MS: 420 [$M + Na^+$].

**Preparation of 3-((3*S*,4*S*)-1-(4-(*tert*-butyl)benzyl)-3-nitropyridin-4-yl)-1*H*-indole (6)**

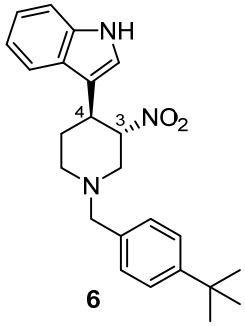


**6**

In a small vial, equipped with a magnetic stirring bar, product **4ga** (91% *ee*; 31.4 mg, 0.08 mmol) was suspended in MeOH (0.75 mL). $NaBH_4$ was then added in small portions until TLC showed complete conversion of the reagent (overall 37.8 mg added, 10 mmol). A saturated solution of $NH_4Cl$ (5 mL) and DCM (5 mL) were added and the organic layer separated, washed again with a saturated solution of $NH_4Cl$ (5 mL), dried over $MgSO_4$ and filtered. To this crude solution (containing a 50/50 diastereomeric mixture, by $^1H$ NMR analysis) $SiO_2$ (3.50 g) was added and the solvent was evaporated *in vacuo*. The product was left standing adsorbed on $SiO_2$ for 5 h. Then, $CHCl_3$ (20 mL) was added and the resulting suspension was stirred for 30 min. $SiO_2$ was filtered off and washed repeatedly with $CHCl_3$. The solvent was finally evaporated to afford 32.0 mg (quantitative yield) of pure product **6** as a white solid. Diastereomeric ratio was evaluated from the $^1H$ NMR spectrum and was found to be > 20:1. The enantiomeric excess of the product was determined by chiral stationary phase HPLC (ADH, *n*-hexane/*i*-PrOH 80:20, 0.75 mL/min, $\lambda$ = 254 nm, $t_{maj}$ = 8.8 min, $t_{min}$ = 10.2 min, 90% *ee*). $[\alpha]_D^{25\ °C}$ = -7.3 (c = 0.4, $CHCl_3$); $^1H$ NMR ($CDCl_3$, 400 MHz) $\delta$ = 8.03 (bs, 1H), 7.66 (d, J = 8.0 Hz, 1H), 7.39-7.36 (m, 2H), 7.34 (dt, $J_1$=8.0 Hz, $J_2$ = 0.8 Hz, 1H), 7.28-7.25 (m, 2H), 7.19 (ddd, $J_1$ = 8.1 Hz, $J_2$ = 7.1 Hz, $J_3$ = 1.2 Hz, 1H), 7.12 (ddd, $J_1$ = 8.0 Hz, $J_2$ = 7.1 Hz, $J_3$ = 1.1 Hz, 1H), 7.06 (d, J = 2.4 Hz, 1H), 5.03 (td, $J_1$ = 10.9 Hz, $J_2$ = 4 Hz, 1H), 3.68 (d, J = 13.1 Hz, 1H), 3.58 (d, J = 13.1 Hz, 1H), 3.54 (td, $J_1$ = 11.0 Hz, $J_2$ = 5.4 Hz, 1H), 3.43 (ddd, $J_1$ = 10.4 Hz, $J_2$ = 4.0 Hz, $J_3$ = 1.7 Hz, 1H), 3.06-3.01 (m, 1H), 2.59 (t, J = 10.4 Hz, 1H), 2.31 (td, $J_1$ =11.4 Hz, $J_2$ = 3.5 Hz, 1H), 2.14-2.04 (m, 2H), 1.34 (s, 9H) ppm; $^{13}C$ NMR (100 MHz, $CDCl_3$) $\delta$ = 150.4, 136.3, 134.2, 128.8, 126.1, 125.3, 122.3, 121.2, 119.7, 118.9, 115.0, 111.4, 88.1, 62.2, 57.0, 53.2, 38.5, 34.5, 31.7, 31.4 ppm; ESI-MS: 414 [M + $Na^+$]. HRMS(ESI) calcd. for $C_{24}H_{30}N_3O_2$ (M + $H^+$): 392.2338; found: 392.2338.

The relative configuration of the two stereogenic centres was determined by means of $^1H$ NMR spectroscopy, on the basis of the coupling constants of the signal at 5.03 ppm, belonging to H-3 ($\alpha$ to the nitro group, assigned for the chemical shift). A value of 10.9 Hz for $J_t$ clearly indicates two *trans*-diaxial relationships, of which one must be between H-3 and H-4 (proton $\alpha$ to the indole). In a chair-like conformation of the piperidine ring, this configuration allows the two bulky substituents at C-3 and C-4 (indole and the nitro group) to occupy the most favourable equatorial positions. This assignment also takes into account the major stability of this product, obtained after thermodynamic equilibration of the diastereomeric mixture.

**Preparation of 3-((2*S*,3*R*,4*S*)-1-(4-(*tert*-butyl)benzyl)-3-iodo-2-methoxy-5-nitro-1,2,3,4-tetrahydropyridin-4-yl)-1*H*-indole (7)[11]**

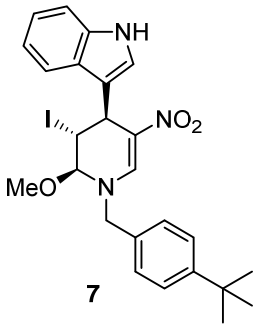


**7**

In a round bottomed flask equipped with a magnetic stirring bar and under $N_2$ flow, product **4ga** (91% *ee*, 31.4 mg, 0.08 mmol) was suspended in MeOH (1.6 mL). The resulting mixture was cooled to 0 °C and a solution of $I_2$ (38.5 mg, 0.152 mmol) in MeOH (4.4 mL) was added dropwise by means of an addition funnel, over a period of 15 minutes. The resulting mixture was stirred for additional 15 minutes at 0 °C, after which a saturated solution of $NaHCO_3$ was added dropwise (10 mL). The precipitated yellow solid was dissolved by addition of DCM (10 mL) and the two layers formed were separated. The aqueous layer was extracted again with DCM (2 x 10 mL). The organic extracts were then washed with a diluted solution of $Na_2S_2O_3$ (2 x 10 mL), dried over $MgSO_4$, filtered and evaporated *in vacuo*. Product **7** was obtained as a red solid in 72% yield (31.4 mg) after column chromatography on silica gel (*n*-hexane/EtOAc = 3:1). The diastereomeric ratio was evaluated from the $^1$H NMR spectrum of the crude mixture and was found to be > 20:1. The enantiomeric excess of the product was determined by chiral stationary phase HPLC (ADH, *n*-hexane/*i*-PrOH 80:20, 0.75 mL/min, $\lambda$ = 254 nm, $t_{maj}$ = 11.9 min, $t_{min}$ = 11.0 min, 87% *ee*). $[\alpha]_D^{25\ °C}$ = -77.9 (c = 0.450, $CHCl_3$); $^1$H NMR ($CDCl_3$, 400 MHz) $\delta$ = 8.41 (s, 1H), 8.02 (bs, 1H), 7.68-7.64 (m, 1H), 7.45-7.41 (m, 2H), 7.36-7.31 (m, 3H), 7.20 (dt, $J_1$ = 7.0 Hz, $J_2$ = 1.5 Hz, 1H), 7.16 (td, $J_1$ = 7.0 Hz, $J_2$ = 1.5 Hz, 1H), 6.87 (dd, $J_1$ = 2.5 Hz, $J_2$ = 0.9 Hz, 1H), 5.08-5.06 (m, 2H), 4.56 (s, 2H), 4.51 (t, J = 1.8 Hz, 1H), 2.67 (s, 3H), 1.34 (s, 9H) ppm; $^1$H NMR ($CD_3CN$, 600 MHz) $\delta$ = 9.15 (bs, 1H), 8.47 (s, 1H), 7.62 (d, J = 8.1 Hz, 1H), 7.51-7.49 (m, 2H), 7.44-7.42 (m, 2H), 7.41 (d, J = 8.4 Hz, 1H), 7.17 (ddd, $J_1$ = 8.2 Hz, $J_2$ = 7.0 Hz, $J_3$ = 1.2 Hz, 1H), 7.11 (ddd, $J_1$ = 7.9 Hz, $J_2$ = 7.2 Hz, $J_3$= 1.0 Hz, 1H), 6.64 (dd, $J_1$ = 2.8 Hz, $J_2$ = 0.9 Hz, 1H), 5.13 (t, J = 2.0 Hz, 1H), 4.92 ("pseudo-q" or ddd $J_1 = J_2 = J_3$ = 1.5 Hz, 1H), 4.69 (d, J = 14.6 Hz, 1H), 4.64 (t, J = 1.7 Hz, 1H), 4.62 (d, J = 14.6 Hz, 1H), 2.73 (s, 3H), 1.34 (s, 9H) ppm; $^{13}$C NMR (100 MHz, $CDCl_3$) $\delta$ = 152.0, 142.5, 136.3, 130.9, 128.8, 125.9, 122.6, 122.2, 121.9, 119.9, 117.9, 114.9, 111.6, 90.3, 57.8, 55.0, 38.7, 34.7, 31.3, 21.9 ppm; ESI-MS: 568 [M + $Na^+$].

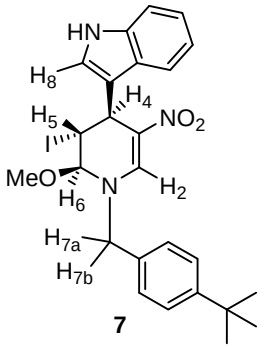


**7**

The relative configuration of the three stereogenic centres was assigned by means of NMR spectroscopy. First of all, since overlapping of the signals of interest was observed in the $^{1}$H NMR spectrum registered in $CDCl_3$ solution, we switched to $CD_3CN$, in which a better separation was obtained (Figure S17). Thus, complete characterization of the "aliphatic" region was achieved. On the basis of the gHSQC experiment in $CD_3CN$ (Figure S19), the signal at 4.64 ppm was assigned to H-6 (correlation with a carbon (CH) at 91.4 ppm, deshielded by the O and N atoms). The signals at 4.69 and 4.62 ppm were assigned to benzylic protons H-7a and H-7b for their correlation with the same carbon (58.5 ppm, $CH_2$). The signal at 5.13 ppm was assigned to H-5, due to the correlation with a carbon (CH) at 24.2 ppm, shielded by the I atom. The signal at 4.92 ppm was therefore assigned to H-4. Then, to account for the multiplicity observed in the H-4, H-5 and H-6 signals, a gCOSY experiment was carried out in $CD_3CN$ (Figure S18). The signal at 4.92 ppm (H-4), formally a ddd with three almost equivalent J constants (1.5 Hz), showed couplings with signals at 5.13 ppm (H-5, $^{3}$J) and 4.64 ppm (H-6, $^{4}$J), along with the one at 6.94 ppm ($^{4}$J), corresponding to H-8 (assigned for the multiplicity and the chemical shift: the sole signal showing only "small" J values in the aromatic region). This also confirms the gHSQC assignment. The signal at 5.13 ppm (H-5) showed couplings with the signal at 4.92 ppm (H-4, $^{3}$J) and 4.64 ppm (H-6, $^{3}$J); the signal at 4.64 ppm (H-6) showed therefore couplings with signals at 5.13 ppm (H-5, $^{3}$J) and 4.92 ppm (H-4, $^{4}$J).

Since the coupling constants of the signal corresponding to H-5 with signals corresponding to H-4 and H-6 are the same (the formal doublet of doublets has in fact the shape of a triplet; $^{3}J = 2.0$ Hz), the same dihedral angle between H-5 and H-6 is observed between H-5 and H-4. Building upon what was reported by Lavilla *et al.*,[11] the MeO and I substituents are in a *trans* relationship (*i.e.* H-5 and H-6 are *anti*): this implies that also H-5 and H-4 have to be *anti* to each other (*i.e.* the I and the indole substituents are *trans*).

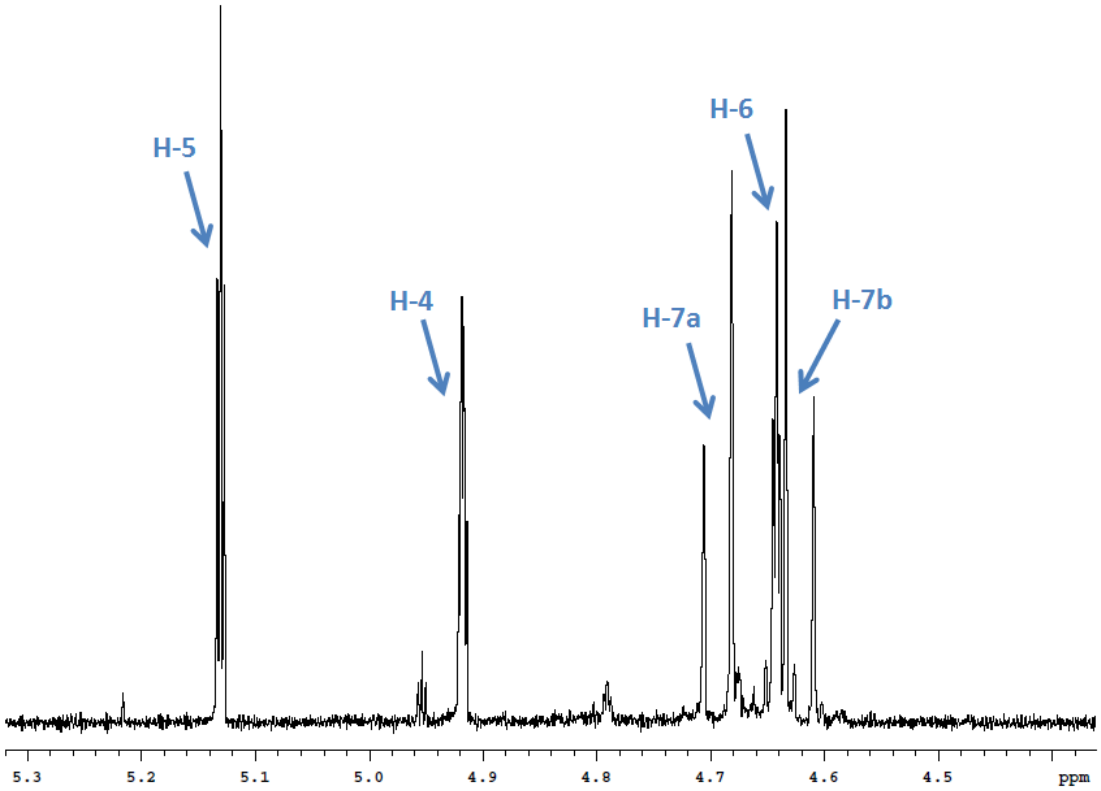


**Figure S17.** Expansion of the region of interest in the $^{1}$H NMR spectrum of product **7** in $CD_3CN$

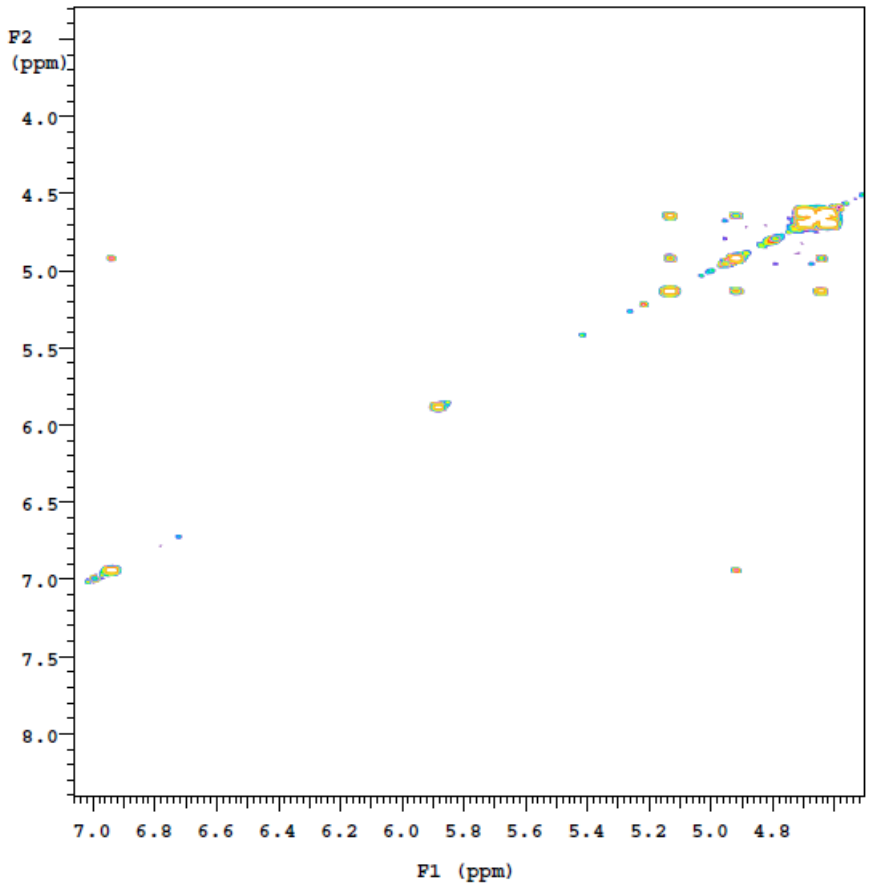


**Figure S18.** Expansion of the region of interest in the gCOSY spectrum of product **7** in $CD_3CN$

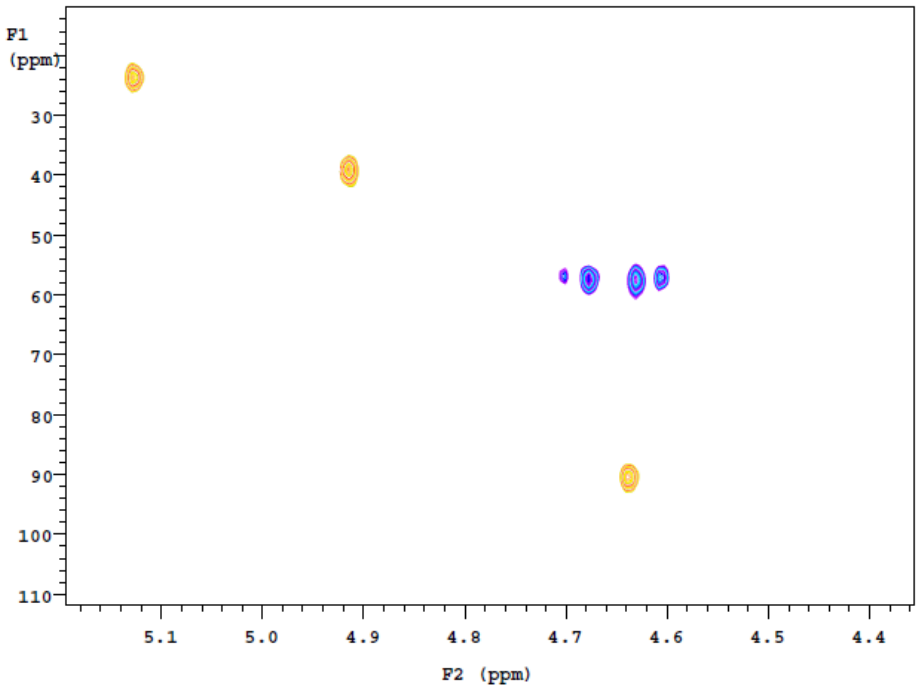


**Figure S19** Expansion of the region of interest in the gHSQC spectrum of product **7** in $CD_3CN$

## References and notes


(1) Venning, A. R. O.; Bohan, P. T.; Alexanian, E. J. *J. Am. Chem. Soc.* **2015**, *137*, 3731–3734.

(2) 9-Deoxy-9-amino-*epi*-dihydroquinidine: (a) Cassani, C.; Martín – Rapún, R.; Arceo, E.; Bravo, F.; Melchiorre, P. *Nat. Protoc.* **2013**, *8*, 325–344. Thiourea formation: (b) Vakulya, B.; Varga, S.; Csámpai, A.; Soós, T. *Org. Lett.* **2005**, *7*, 1967–1969.

(3) Lavilla, R.; Gotsens, T.; Guerrero, M.; Masdeu, C.; Santano, M. C.; Minguillón, C.; Bosch, J. *Tetrahedron* **1997**, *53*, 13959–13968.

(4) Additional enhancement was observed on the signals at 7.20 ppm and 7.57 ppm, each integrating for a single proton. This enhancement indicates that the other two overlapped signals generating the multiplet at 7.05 ppm together with H-2in belong to the indole core; otherwise, belonging to H-9, they would have produced enhancement of signal at 7.34 ppm (H-8). Therefore, the multiplet at 7.46 ppm is generated by the overlapping of H-9 and H-10 while signals at 7.20 ppm and 7.57 ppm belong to the indole ring.

(5) (a) Phipps, R. J.; Hamilton, G. L.; Toste, F. D. *Nat. Chem.* **2012**, *4*, 603-614. (b) Brak, K.; Jacobsen, E. N. *Angew. Chem., Int. Ed.* **2013**, *52*, 534–561.

(6) Kotek, J.; Herman, P.; Vojtisek, K.; Rohovec, J.; Lukes, I. *Collect. Czech. Chem. Commun.* **2000**, *65*, 243–266.

(7) Baidya, M.; Remennikov, G. Y.; Mayer, P.; Mayr, H. *Chem. Eur. J.* **2010**, *16*, 1365–1371.

(8) Yeung, C. S.; Ziegler, R. E.; Porco Jr., J. A.; Jacobsen, E. N. *J. Am. Chem. Soc.* **2014**, *136*, 13614–13617.

(9) Lyle, R. E.; Gauthier, G. J. *Tetrahedron Lett.* **1965**, *6*, 4615–4621.

(10) Bull, J. A.; Mousseau, J. J.; Pelletier, G.; Charette, A. B. *Chem. Rev.* **2012**, *112*, 2642–2713.

(11) Procedure adapted from: Lavilla, R.; Coll, O.; Kumar, R.; Bosch, J. *J. Org. Chem.* **1998**, *63*, 2728–2730.

## Copies of $^{1}H$ and $^{13}C$ NMR spectra and HPLC traces

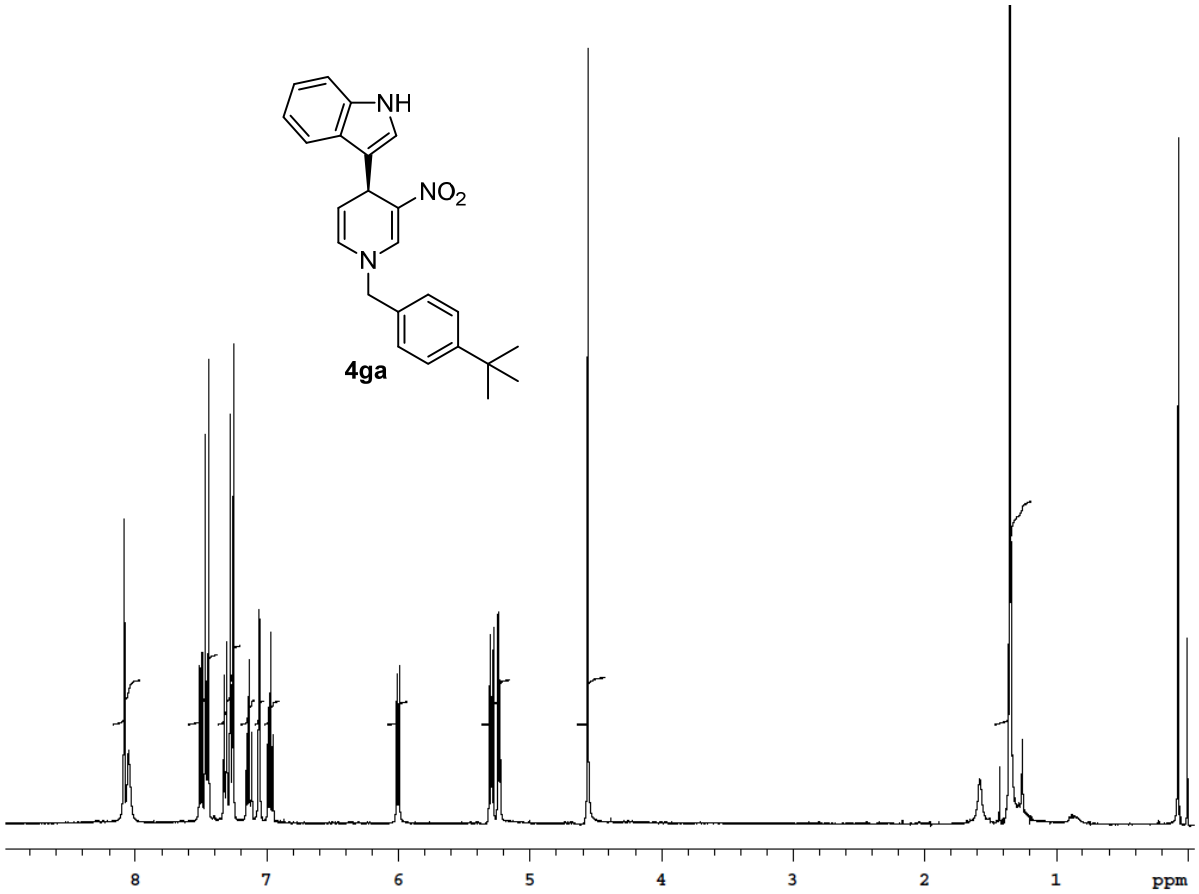


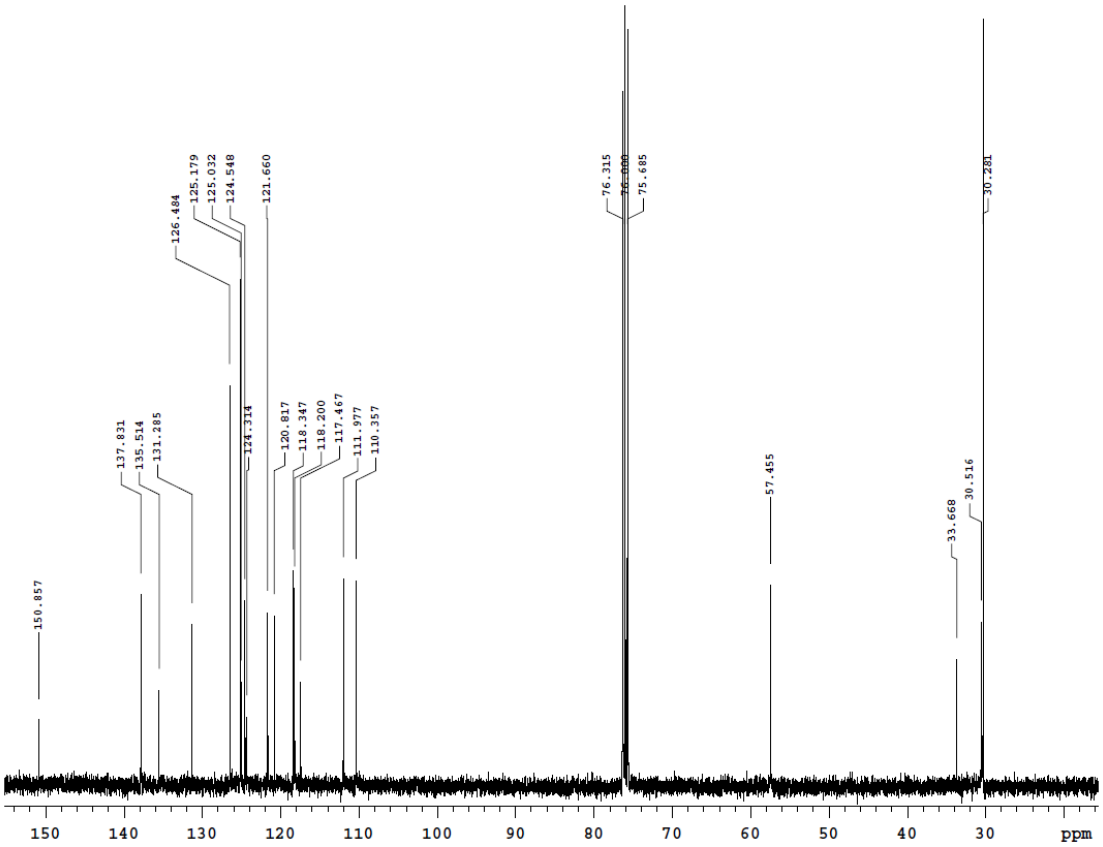

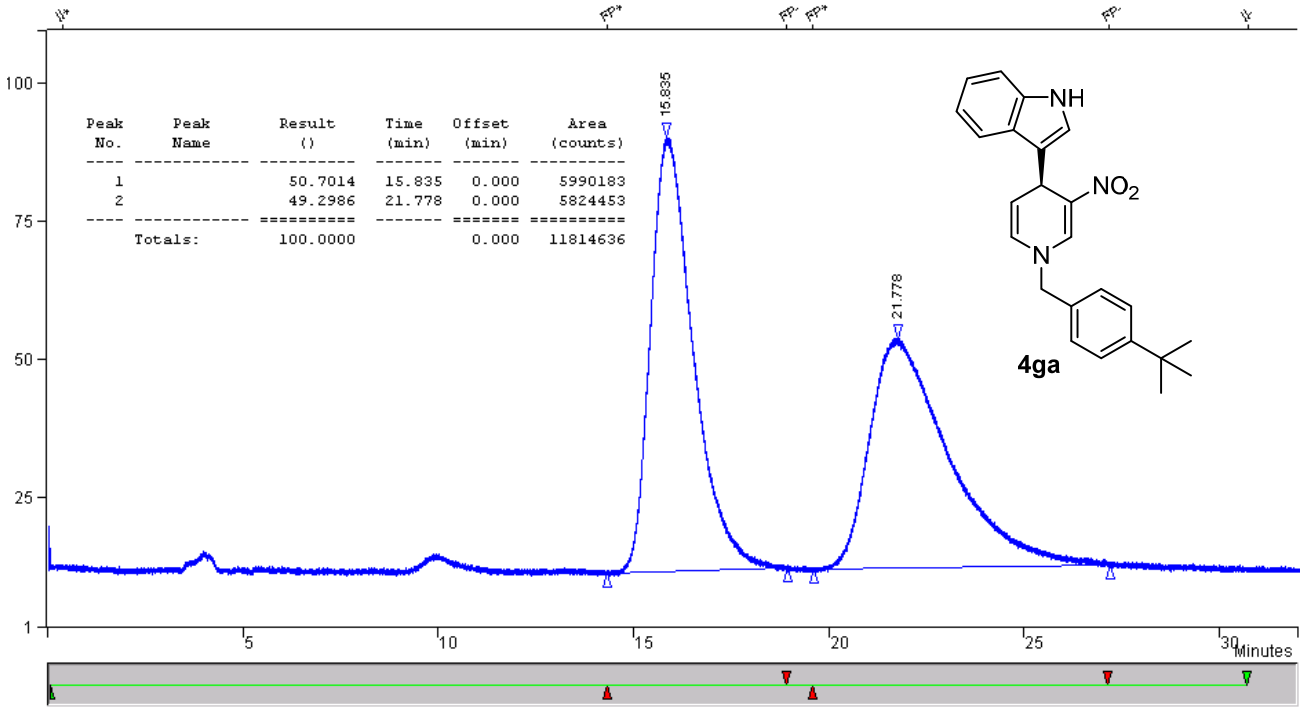
Peak No. | Peak Name | Result () | Time (min) | Offset (min) | Area (counts)
1 | 50.7014 | 15.835 | 0.000 | 5990183
2 | 49.2986 | 21.778 | 0.000 | 5824453
Totals: | 100.0000 | 0.000 | 11814636
15.835
21.778
NH
NO2
N
4ga
100
75
50
25
1
5
10
15
20
25
30
Minutes

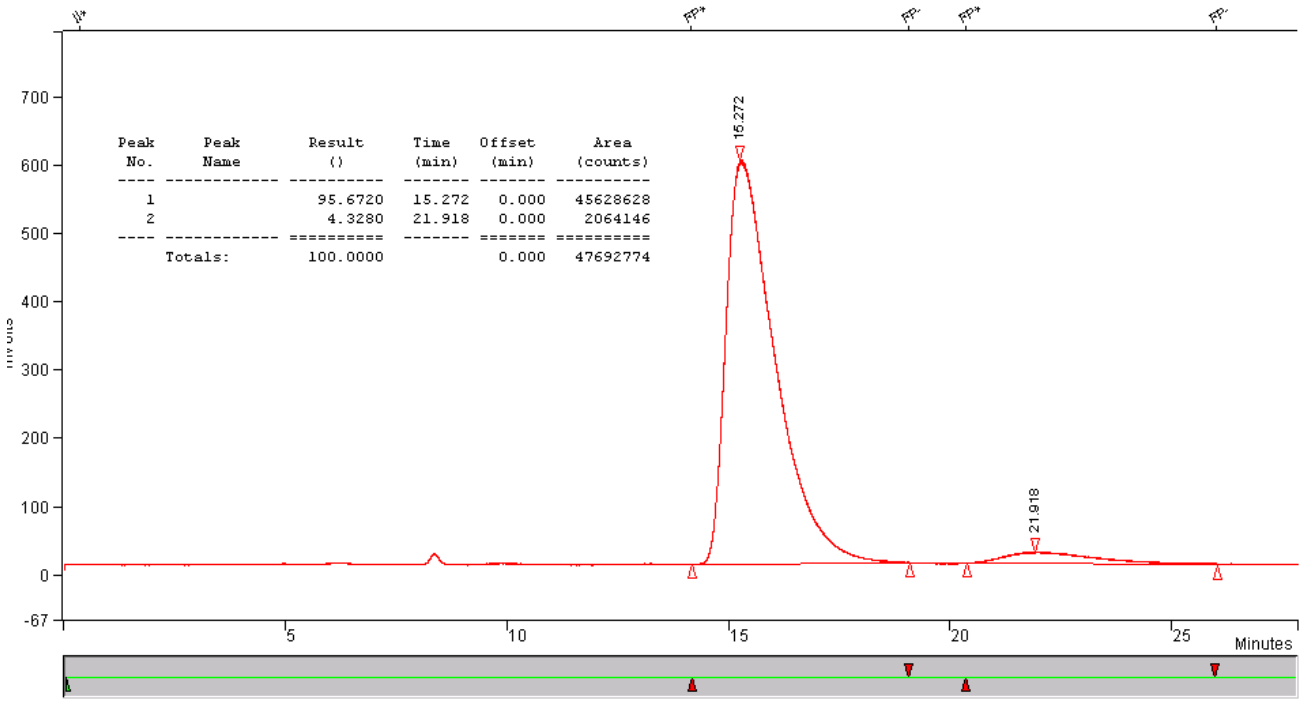
Peak No. | Peak Name | Result () | Time (min) | Offset (min) | Area (counts)
1 | 95.6720 | 15.272 | 0.000 | 45628628
2 | 4.3280 | 21.918 | 0.000 | 2064146
Totals: | 100.0000 | 0.000 | 47692774
15.272
21.918
700
600
500
400
300
200
100
0
-67
5
10
15
20
25
Minutes

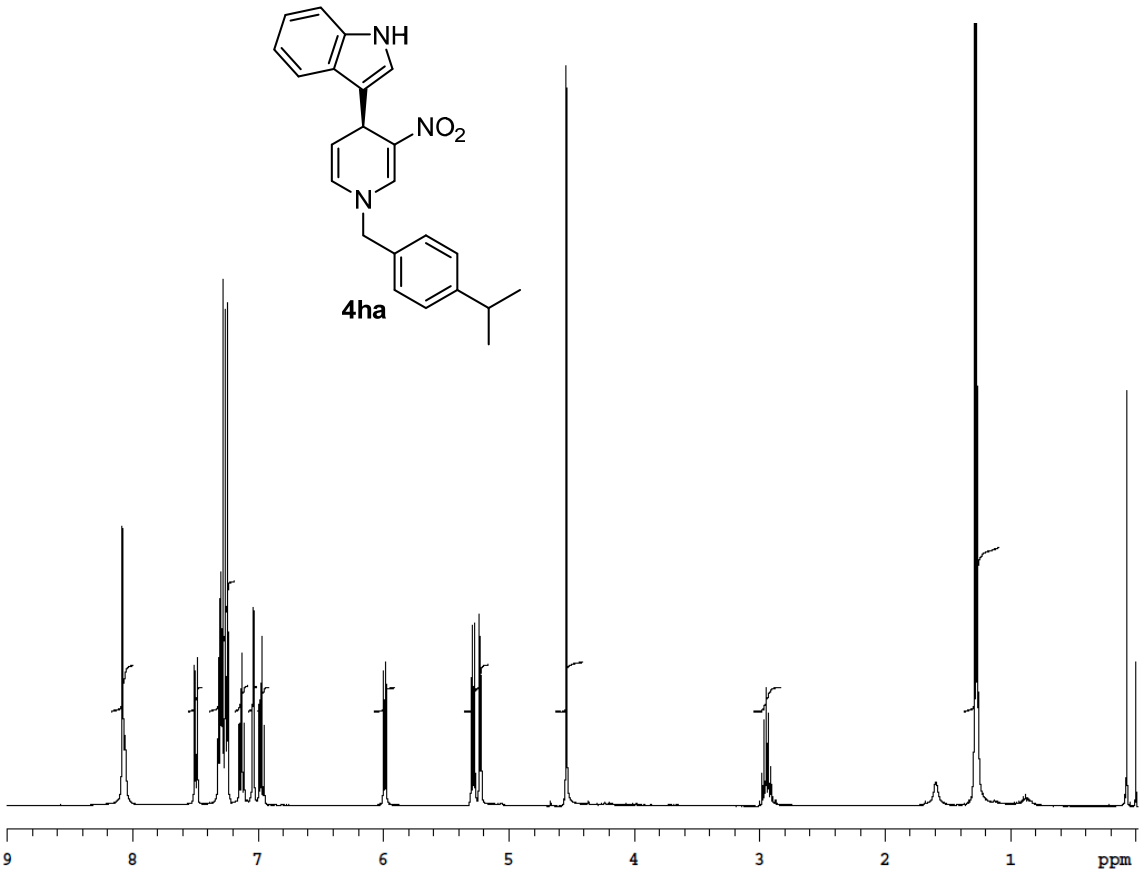
NH
NO2
N
4ha
9
8
7
6
5
4
3
2
1
ppm

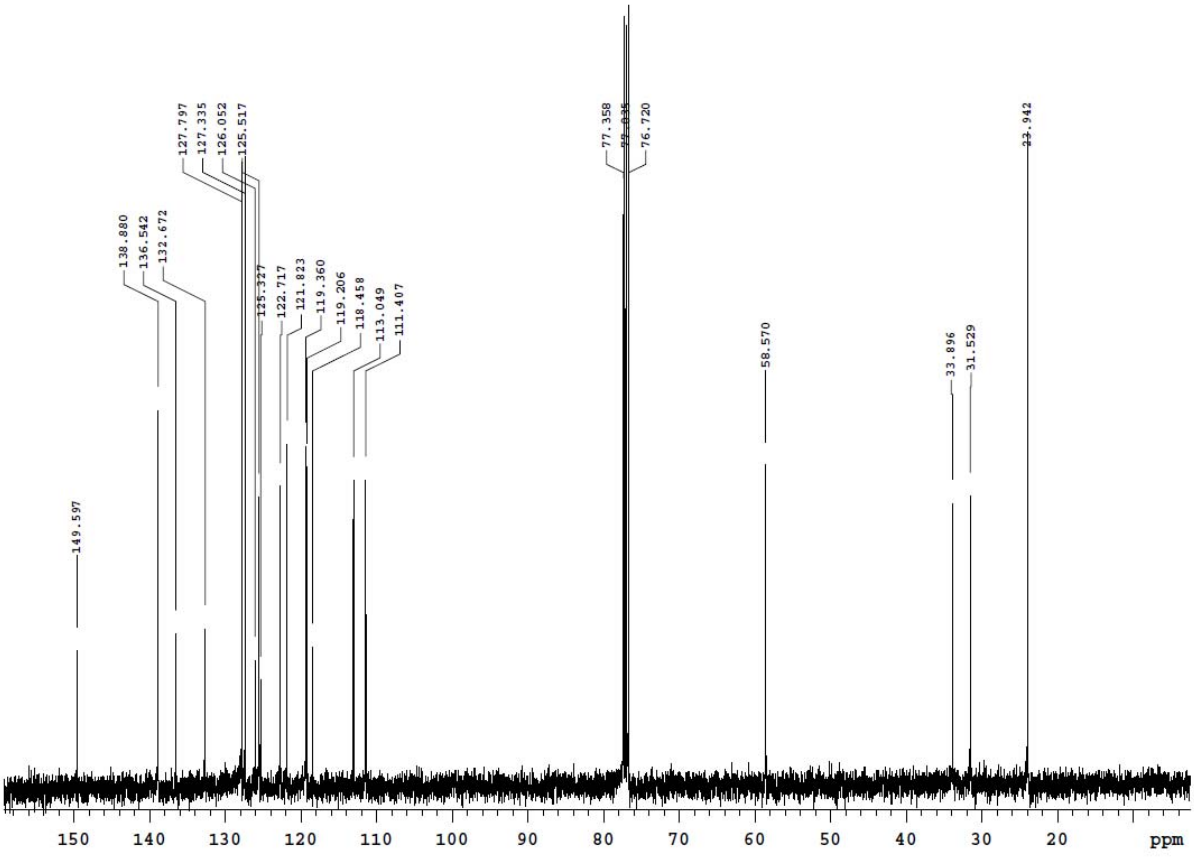
149.597
138.880
136.542
132.672
127.797
127.335
126.052
125.517
125.327
122.717
121.823
119.360
119.206
118.458
113.049
111.407
77.358
76.720
58.570
33.896
31.529
22.942
150
140
130
120
110
100
90
80
70
60
50
40
30
20
ppm

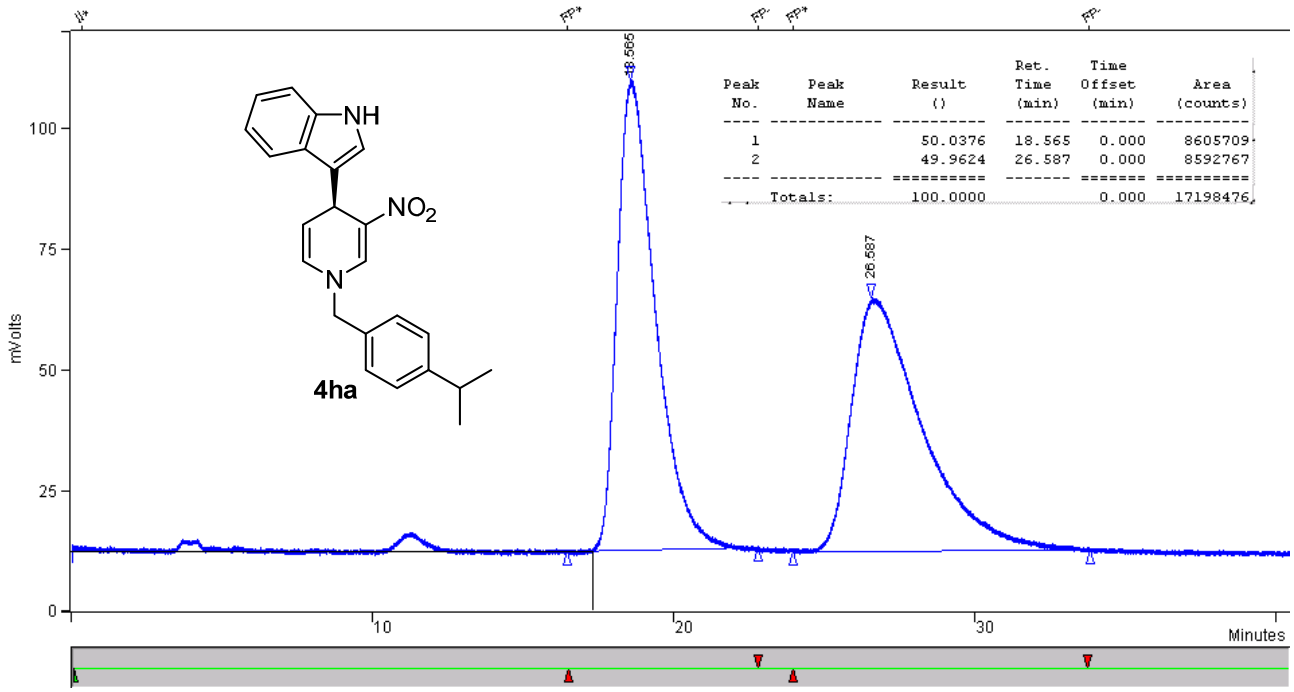


| Peak No. | Peak Name | Result () | Ret. Time (min) | Time Offset (min) | Area (counts) |
|---|---|---|---|---|---|
| 1 | | 50.0376 | 18.565 | 0.000 | 8605709 |
| 2 | | 49.9624 | 26.587 | 0.000 | 8592767 |
| | Totals: | 100.0000 | | 0.000 | 17198476 |

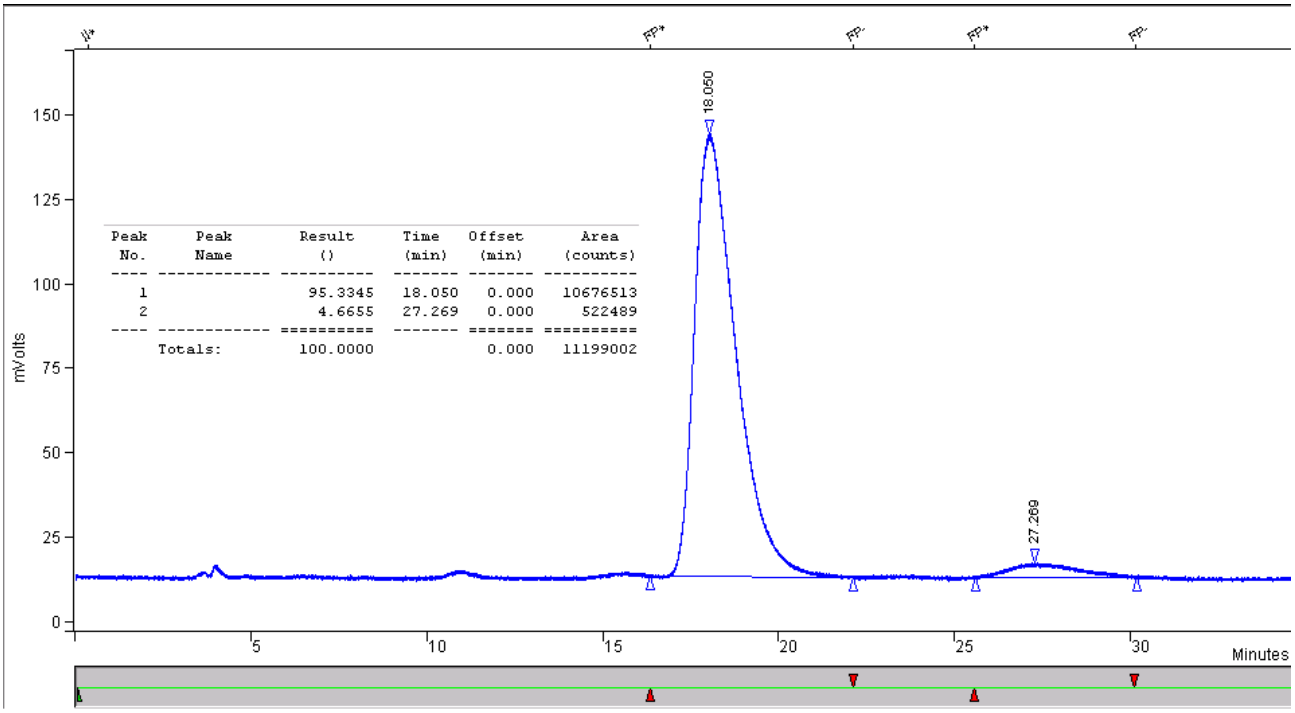


| Peak No. | Peak Name | Result () | Time (min) | Offset (min) | Area (counts) |
|---|---|---|---|---|---|
| 1 | | 95.3345 | 18.050 | 0.000 | 10676513 |
| 2 | | 4.6655 | 27.269 | 0.000 | 522489 |
| | Totals: | 100.0000 | | 0.000 | 11199002 |

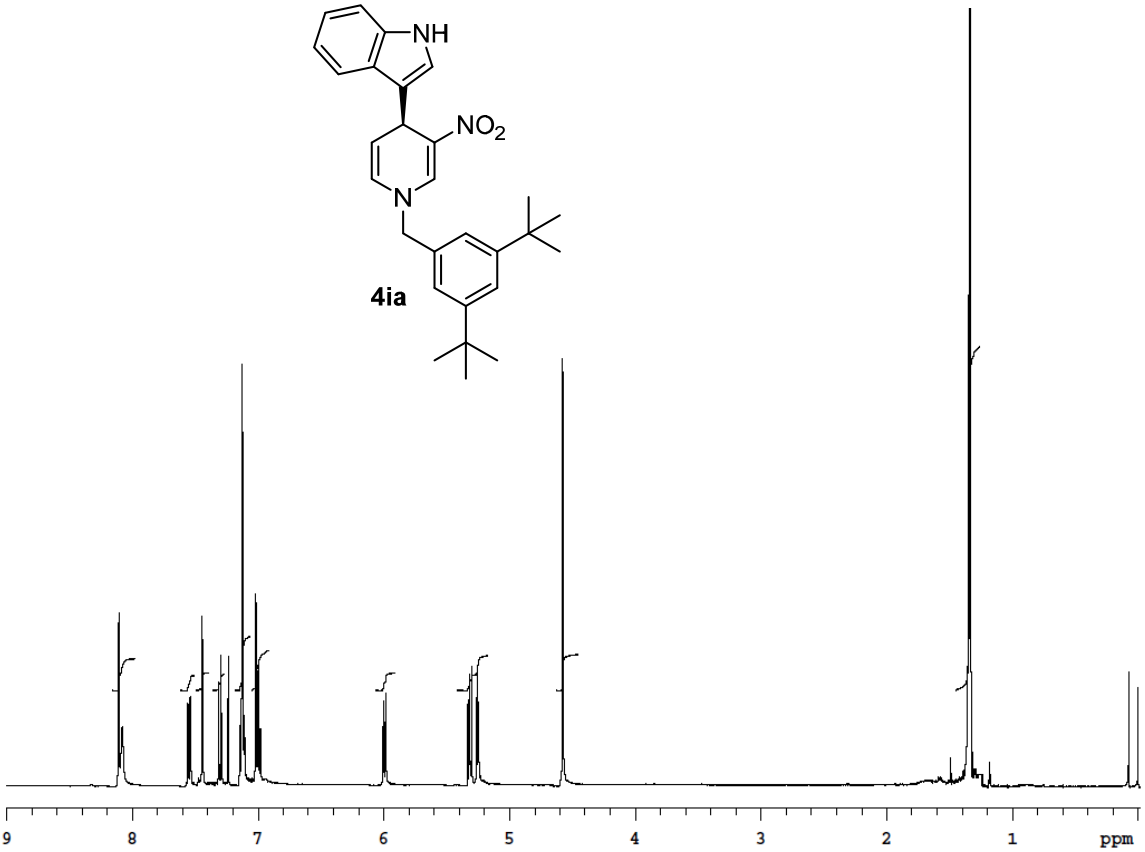
NH
NO2
N
4ia
9
8
7
6
5
4
3
2
1
ppm

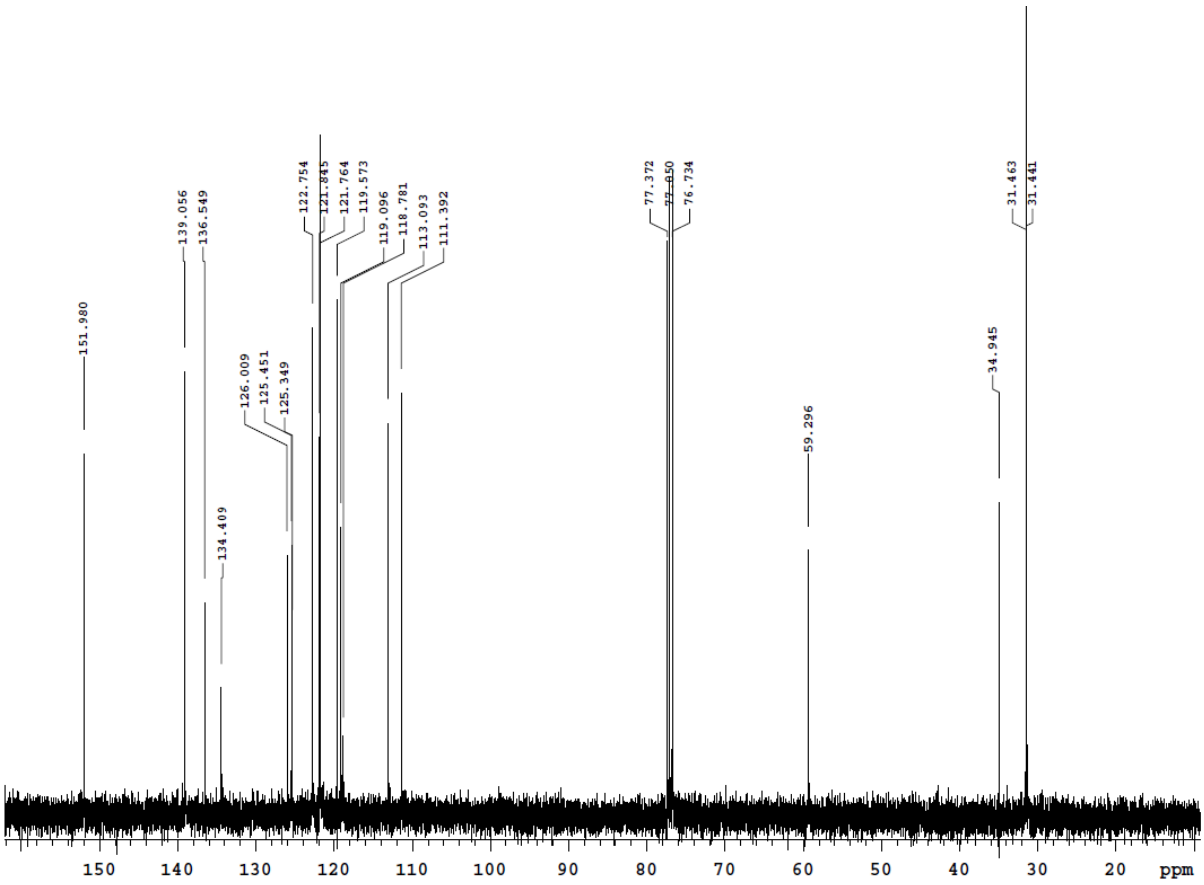
151.980
139.056
136.549
134.409
126.009
125.451
125.349
122.754
121.845
121.764
119.573
119.096
118.781
113.093
111.392
77.372
77.050
76.734
59.296
34.945
31.463
31.441
150
140
130
120
110
100
90
80
70
60
50
40
30
20
ppm

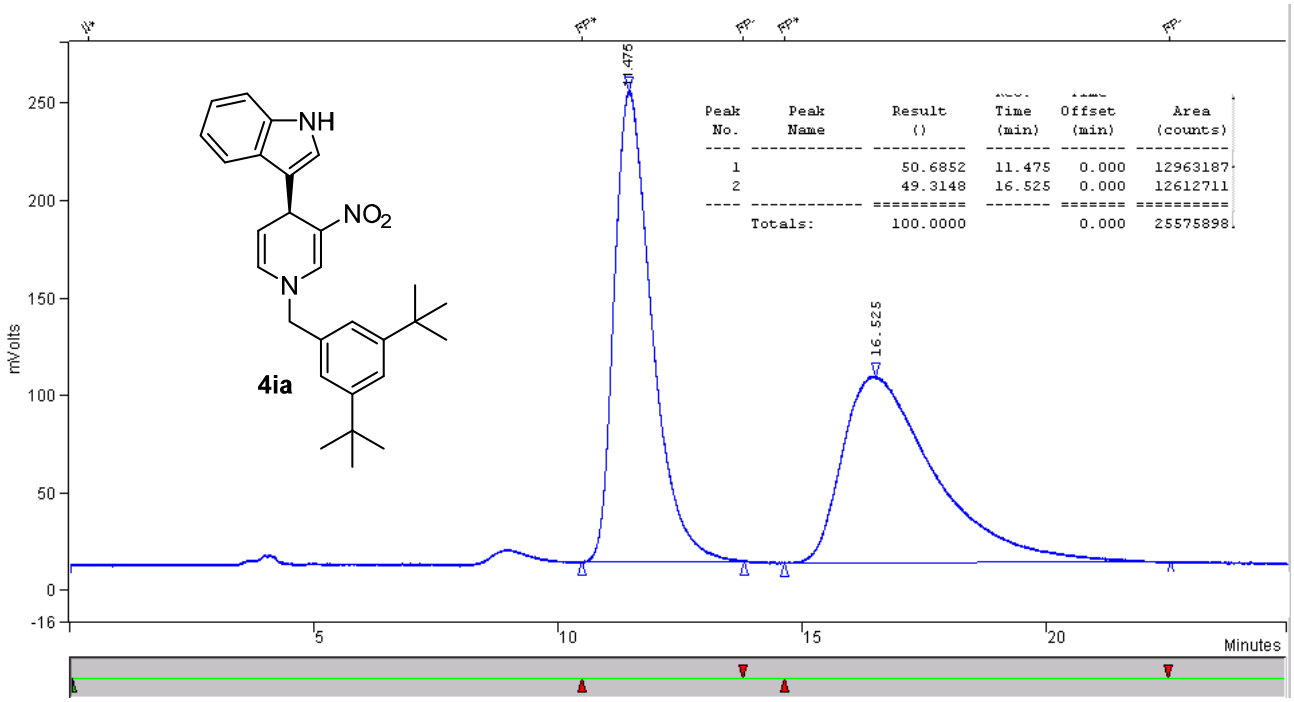
NH
NO2
N
4ia
11.475
16.525
mVolts
Minutes
Peak No. | Peak Name | Result () | Ret. Time (min) | Time Offset (min) | Area (counts)
1 | | 50.6852 | 11.475 | 0.000 | 12963187
2 | | 49.3148 | 16.525 | 0.000 | 12612711
Totals: | | 100.0000 | | 0.000 | 25575898

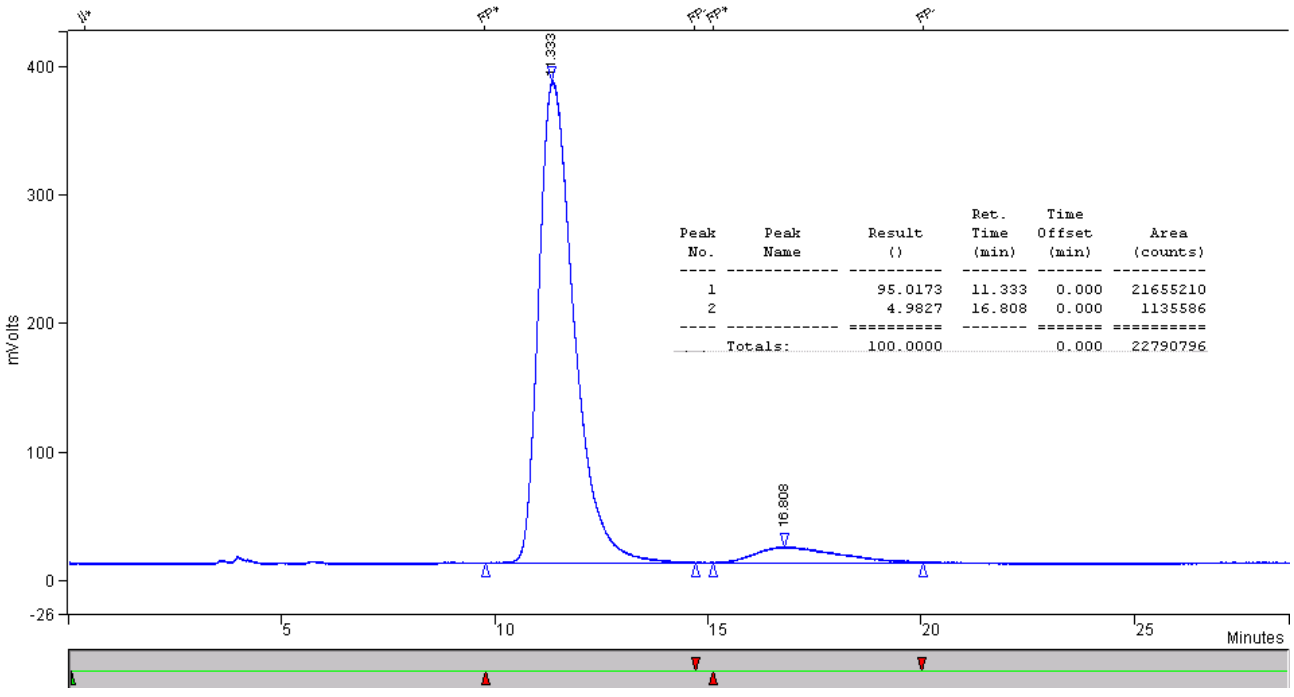
11.333
16.808
mVolts
Minutes
Peak No. | Peak Name | Result () | Ret. Time (min) | Time Offset (min) | Area (counts)
1 | | 95.0173 | 11.333 | 0.000 | 21655210
2 | | 4.9827 | 16.808 | 0.000 | 1135586
Totals: | | 100.0000 | | 0.000 | 22790796

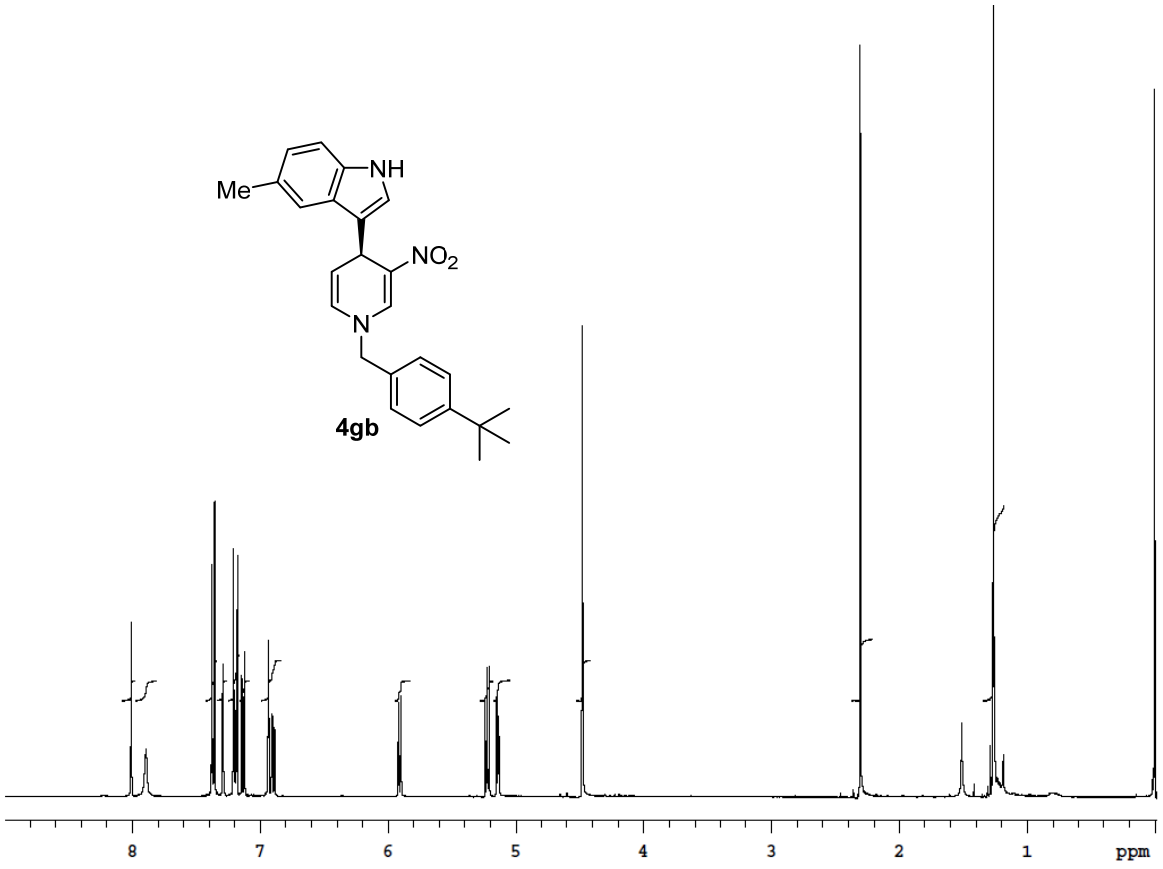
NH
Me
NO2
N
4gb
8
7
6
5
4
3
2
1
ppm

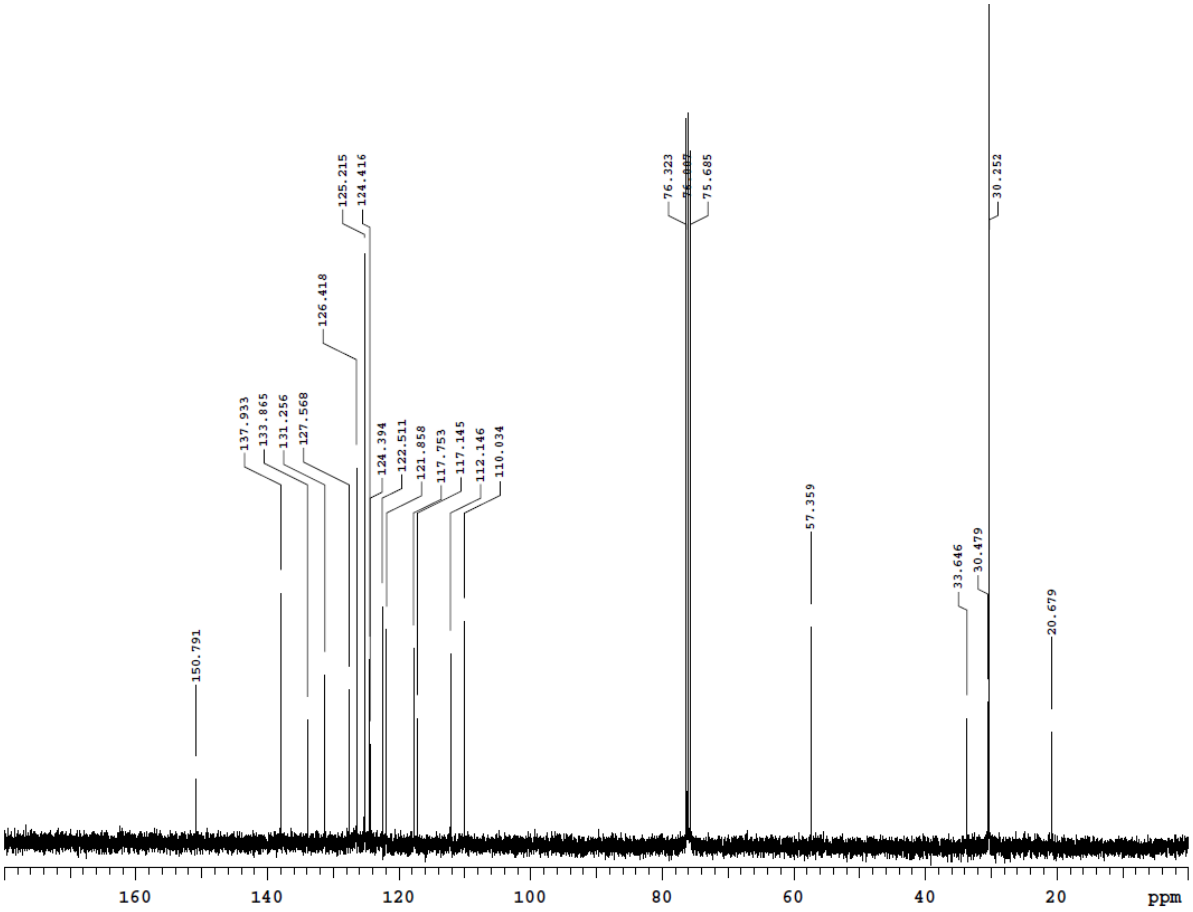
150.791
137.933
133.865
131.256
127.568
126.418
125.215
124.416
124.394
122.511
121.858
117.753
117.145
112.146
110.034
76.323
75.685
57.359
33.646
30.479
30.252
20.679
160
140
120
100
80
60
40
20
ppm

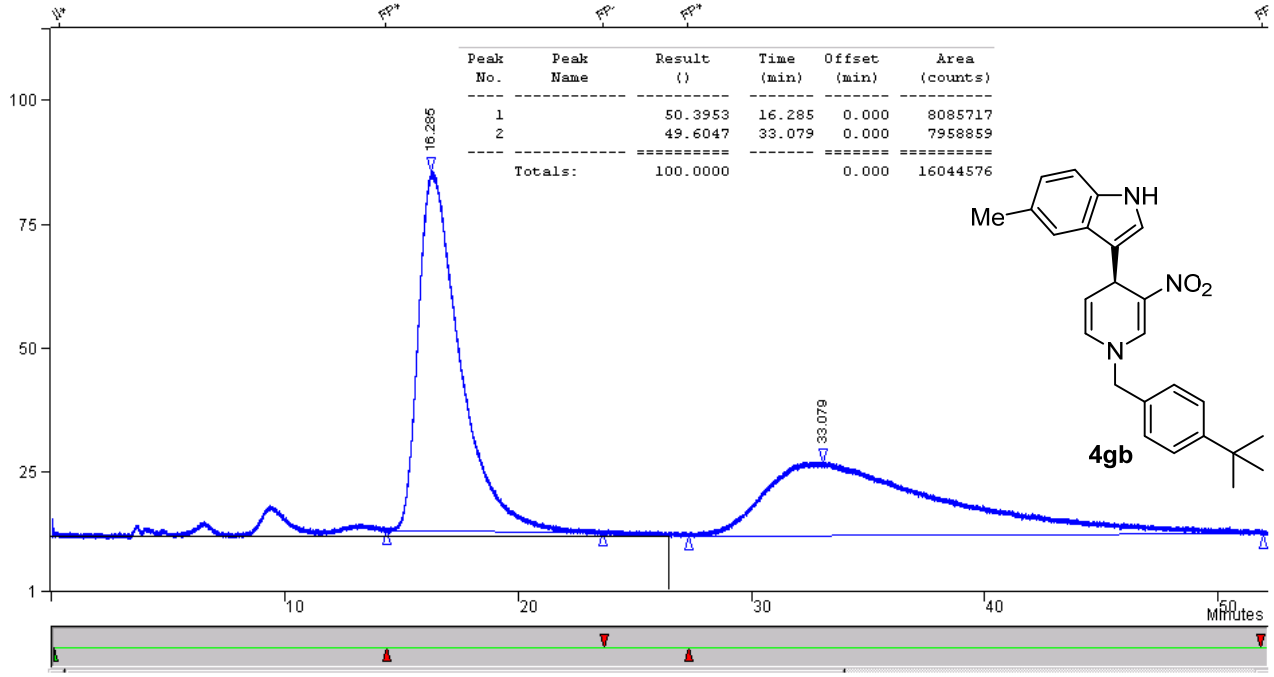
Peak No. | Peak Name | Result () | Time (min) | Offset (min) | Area (counts)
1 | | 50.3953 | 16.285 | 0.000 | 8085717
2 | | 49.6047 | 33.079 | 0.000 | 7958859
Totals: | | 100.0000 | | 0.000 | 16044576
16.285
33.079
Me
NH
NO2
N
4gb
100
75
50
25
1
10
20
30
40
50
Minutes

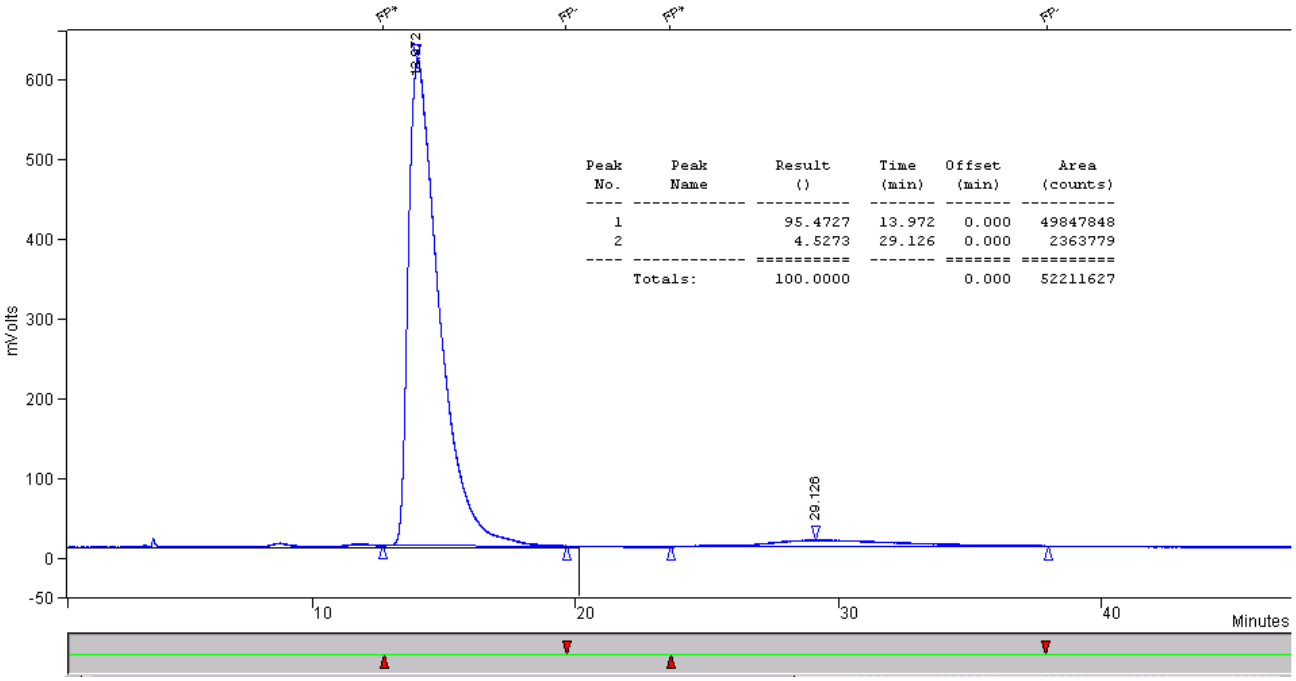
Peak No. | Peak Name | Result () | Time (min) | Offset (min) | Area (counts)
1 | | 95.4727 | 13.972 | 0.000 | 49847848
2 | | 4.5273 | 29.126 | 0.000 | 2363779
Totals: | | 100.0000 | | 0.000 | 52211627
29.126
mVolts
600
500
400
300
200
100
0
-50
10
20
30
40
Minutes

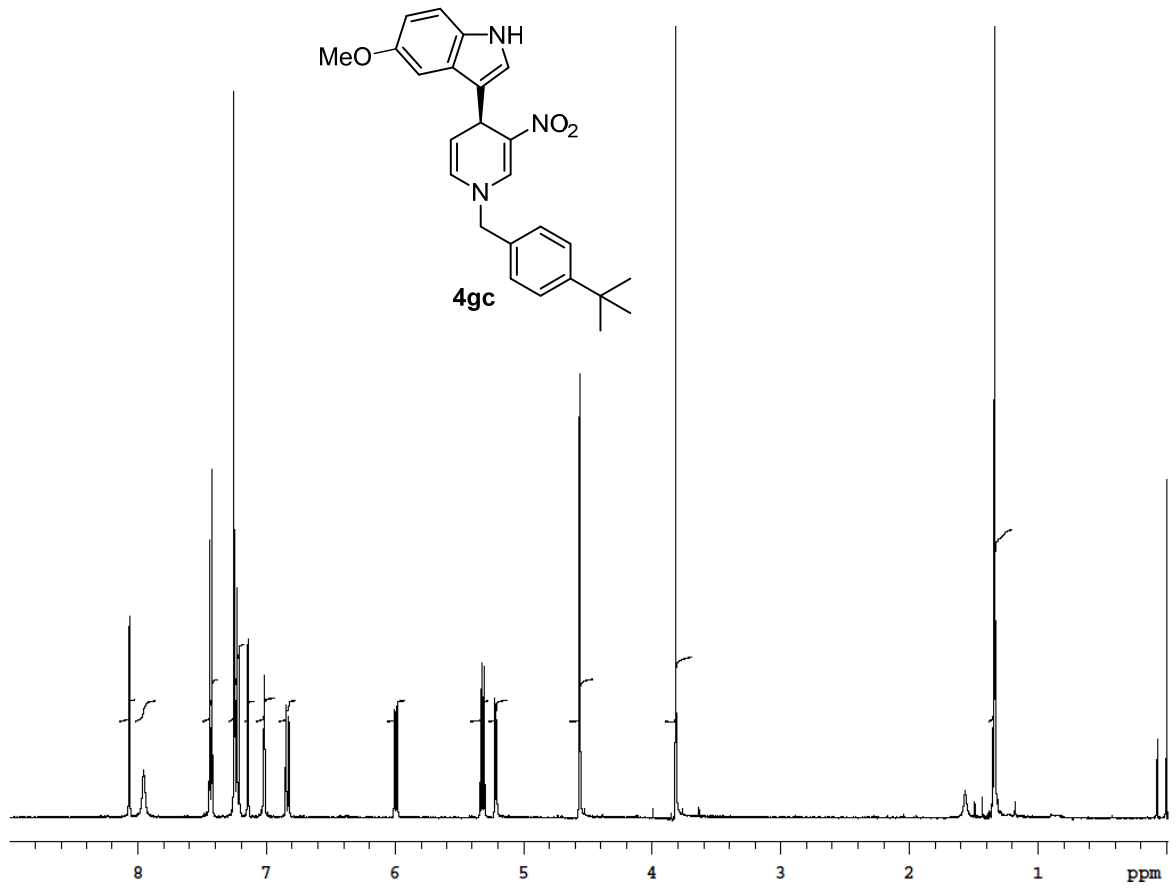
MeO
NH
NO2
N
4gc
8
7
6
5
4
3
2
1
ppm

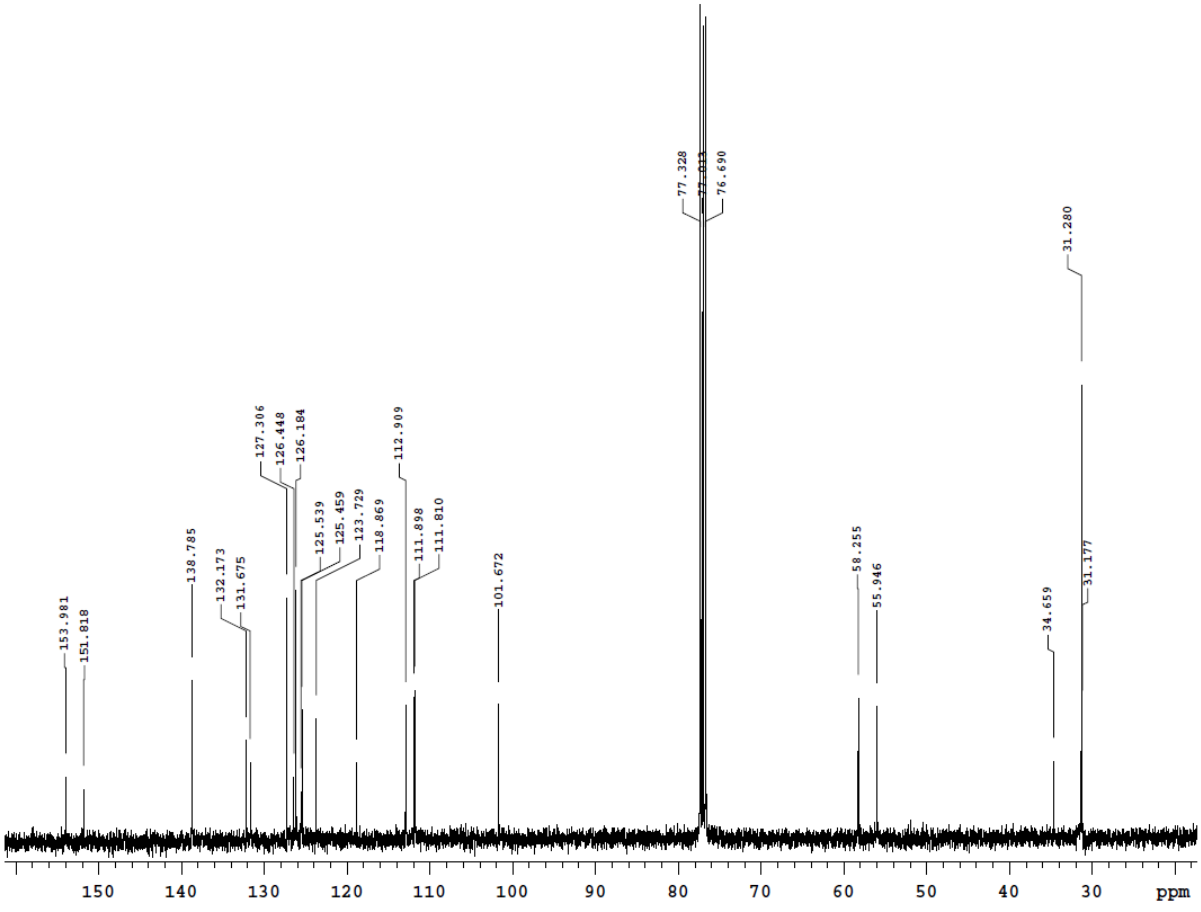
153.981
151.818
138.785
132.173
131.675
127.306
126.448
126.184
125.539
125.459
123.729
118.869
112.909
111.898
111.810
101.672
77.328
77.013
76.690
58.255
55.946
34.659
31.280
31.177
150
140
130
120
110
100
90
80
70
60
50
40
30
ppm

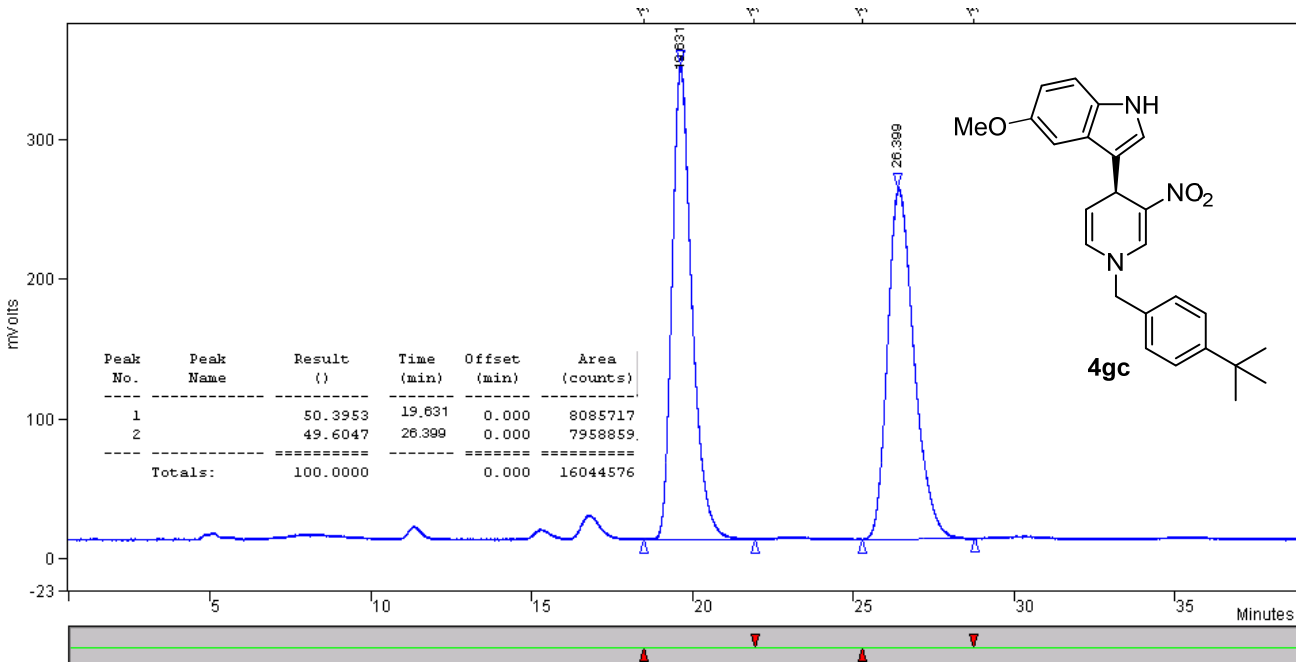
mVolts
300
200
100
0
-23
5
10
15
20
25
30
35
Minutes
19.631
26.399
MeO
NH
NO2
N
4gc
Peak No. | Peak Name | Result () | Time (min) | Offset (min) | Area (counts)
1 | | 50.3953 | 19.631 | 0.000 | 8085717
2 | | 49.6047 | 26.399 | 0.000 | 7958859
Totals: | | 100.0000 | | 0.000 | 16044576

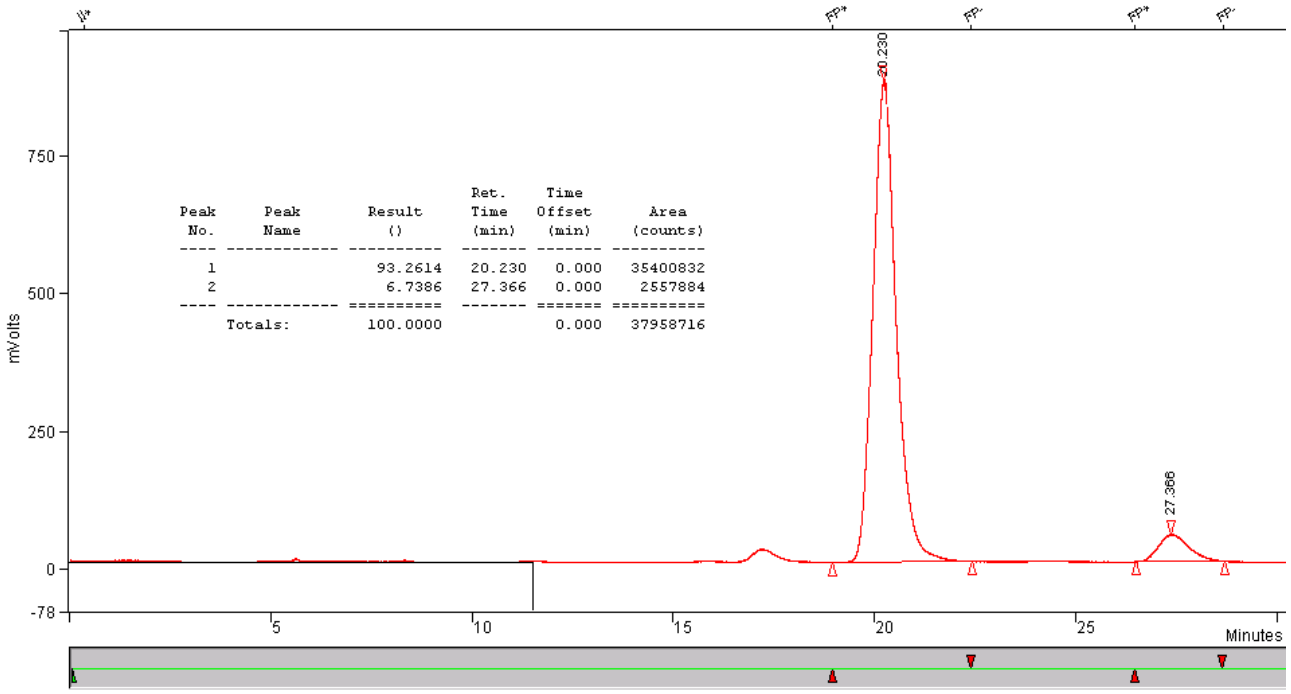
mVolts
750
500
250
0
-78
5
10
15
20
25
Minutes
20.230
27.366
Peak No. | Peak Name | Result () | Ret. Time (min) | Time Offset (min) | Area (counts)
1 | | 93.2614 | 20.230 | 0.000 | 35400832
2 | | 6.7386 | 27.366 | 0.000 | 2557884
Totals: | | 100.0000 | | 0.000 | 37958716

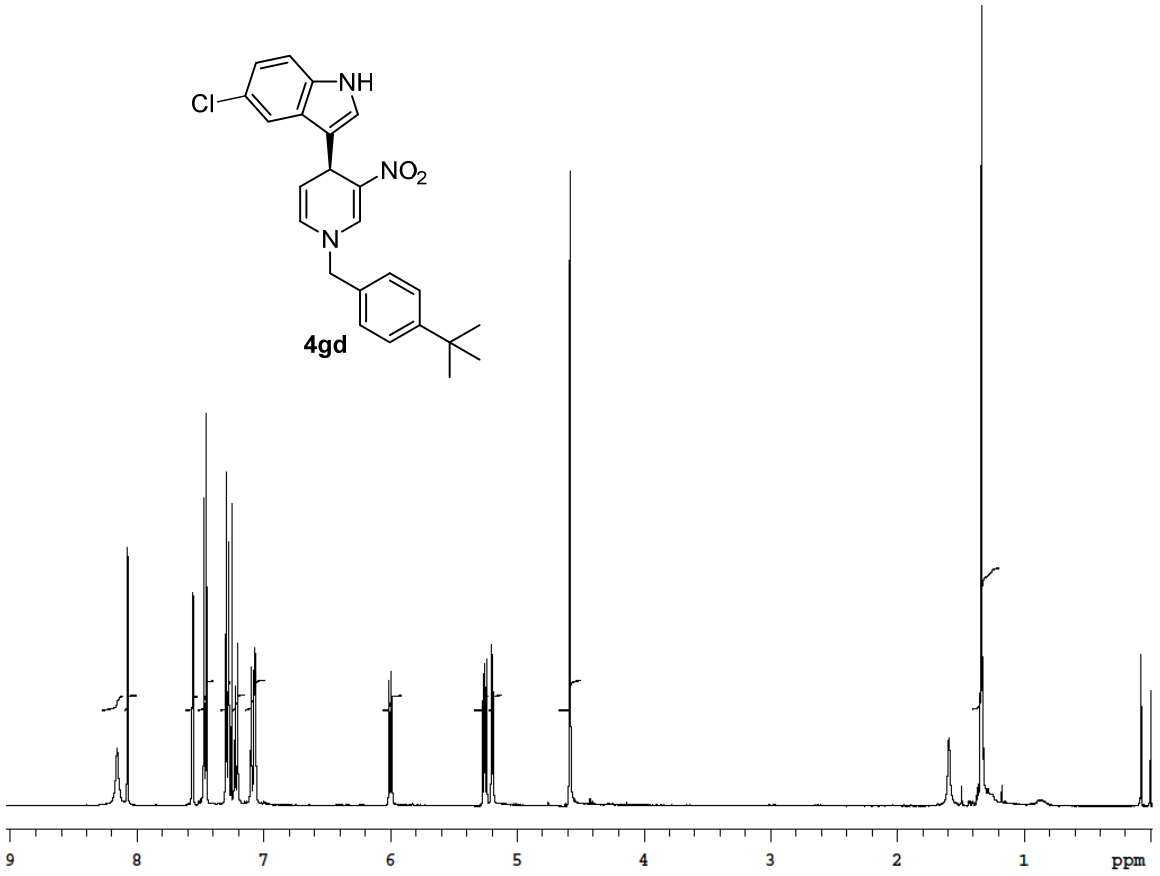
Cl
NH
NO2
N
4gd
9
8
7
6
5
4
3
2
1
ppm

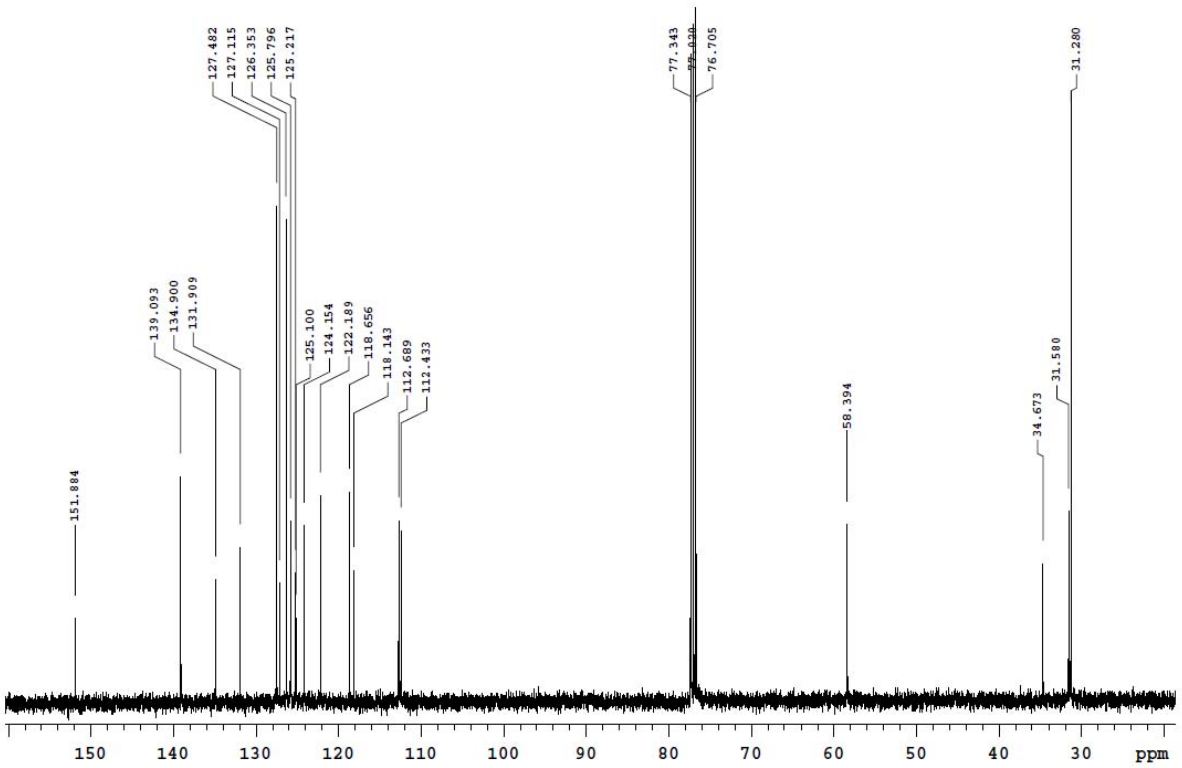
151.884
139.093
134.900
131.909
127.482
127.115
126.353
125.796
125.217
125.100
124.154
122.189
118.656
118.143
112.689
112.433
77.343
76.705
58.394
34.673
31.580
31.280
150
140
130
120
110
100
90
80
70
60
50
40
30
ppm

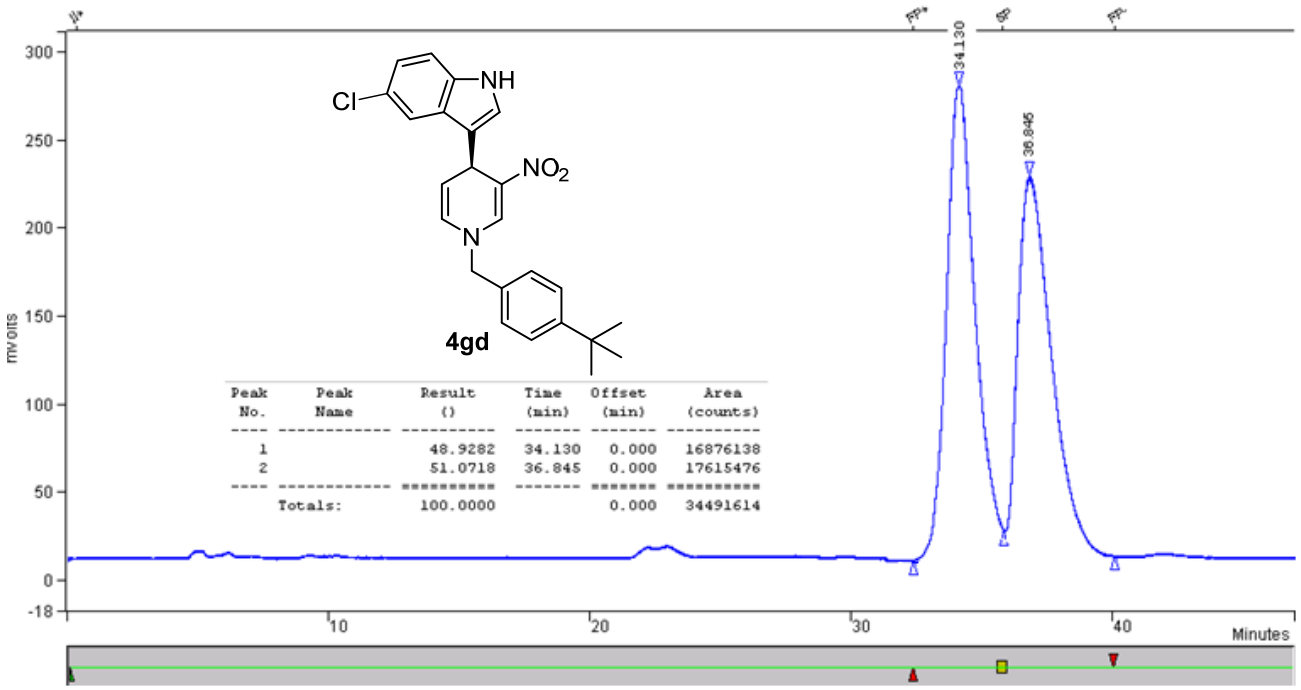


| Peak No. | Peak Name | Result () | Time (min) | Offset (min) | Area (counts) |
|---|---|---|---|---|---|
| 1 | | 48.9282 | 34.130 | 0.000 | 16876138 |
| 2 | | 51.0718 | 36.845 | 0.000 | 17615476 |
| Totals: | | 100.0000 | | 0.000 | 34491614 |

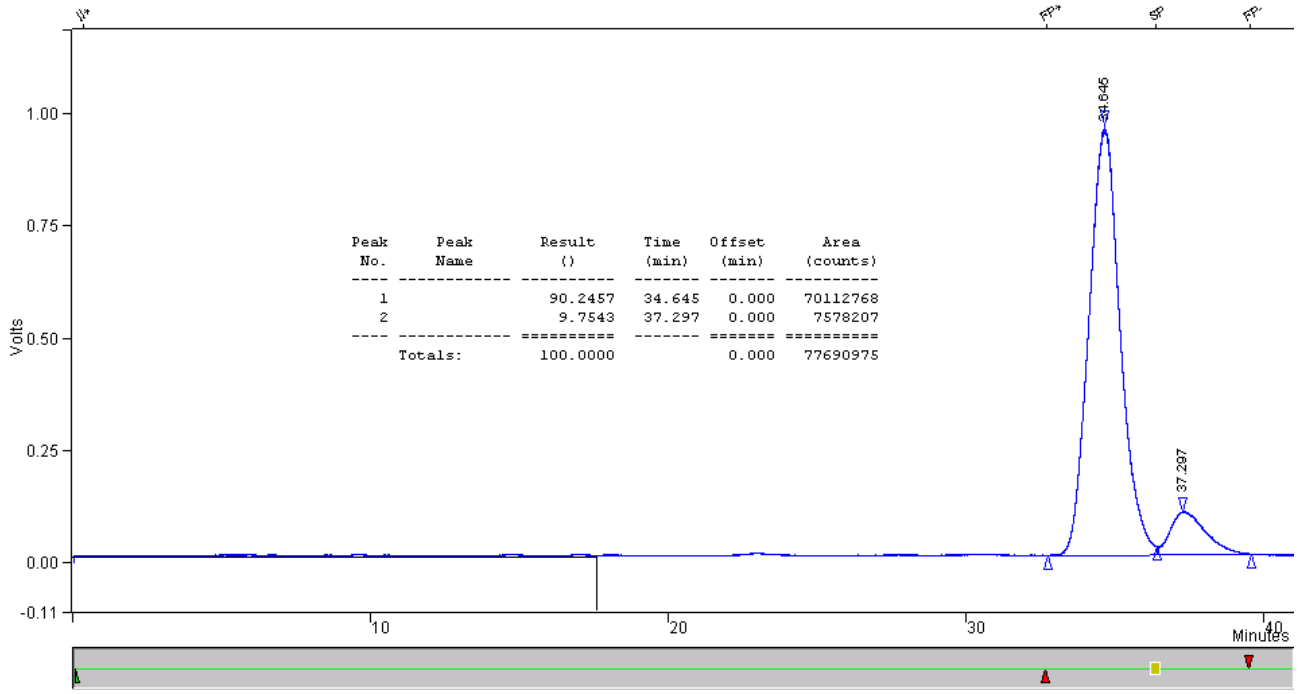


| Peak No. | Peak Name | Result () | Time (min) | Offset (min) | Area (counts) |
|---|---|---|---|---|---|
| 1 | | 90.2457 | 34.645 | 0.000 | 70112768 |
| 2 | | 9.7543 | 37.297 | 0.000 | 7578207 |
| Totals: | | 100.0000 | | 0.000 | 77690975 |

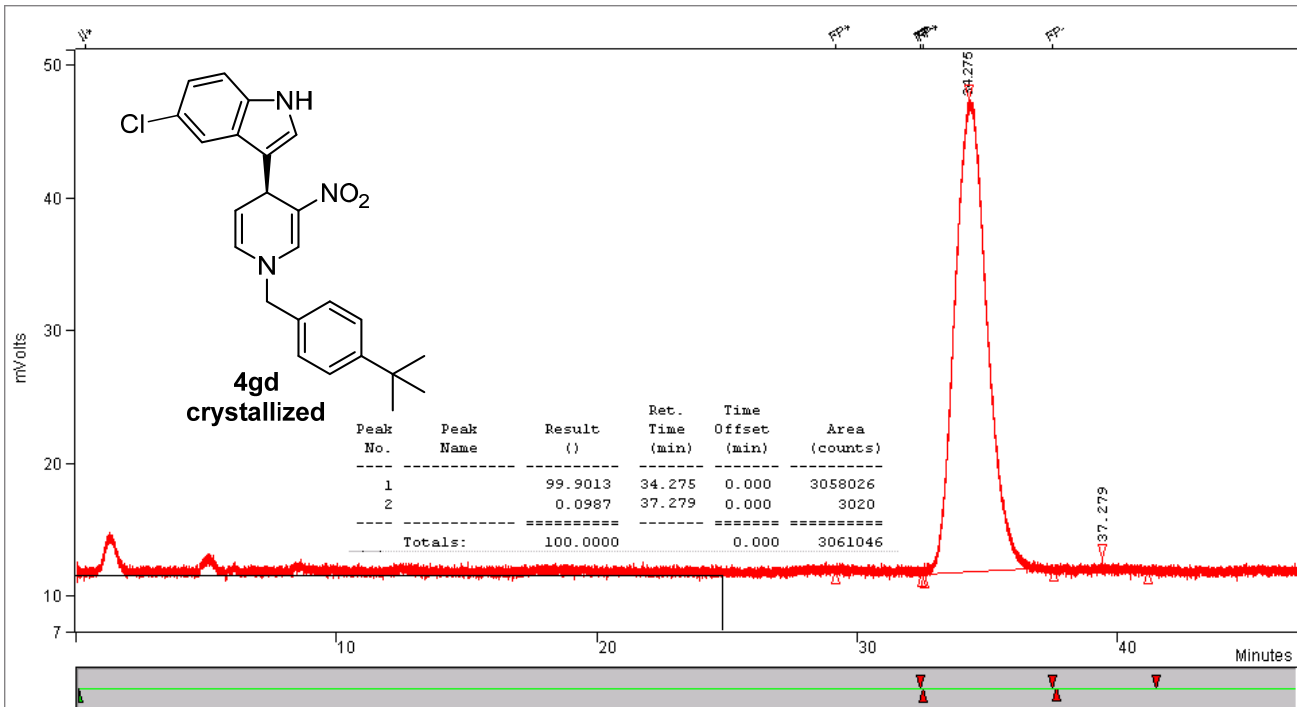


| Peak No. | Peak Name | Result () | Ret. Time (min) | Time Offset (min) | Area (counts) |
|---|---|---|---|---|---|
| 1 | | 99.9013 | 34.275 | 0.000 | 3058026 |
| 2 | | 0.0987 | 37.279 | 0.000 | 3020 |
| | Totals: | 100.0000 | | 0.000 | 3061046 |

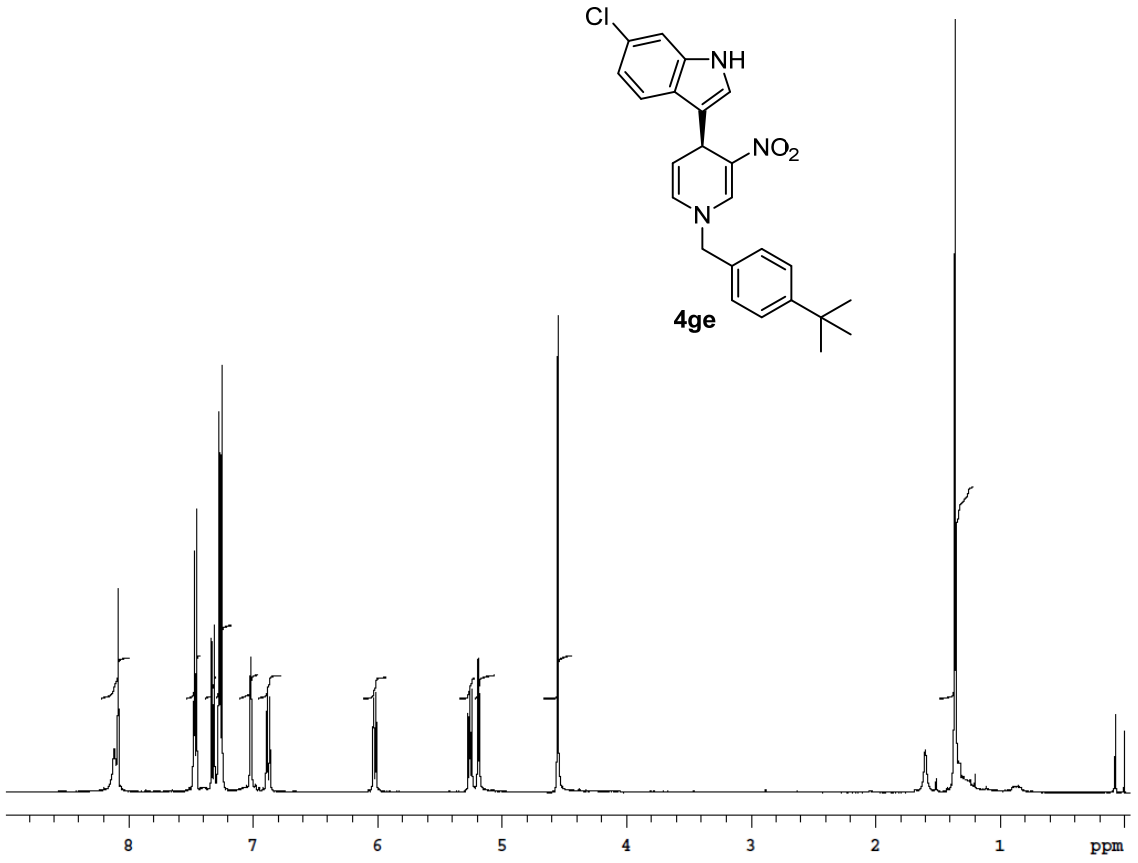
Cl
NH
NO2
N
4ge
8
7
6
5
4
3
2
1
ppm

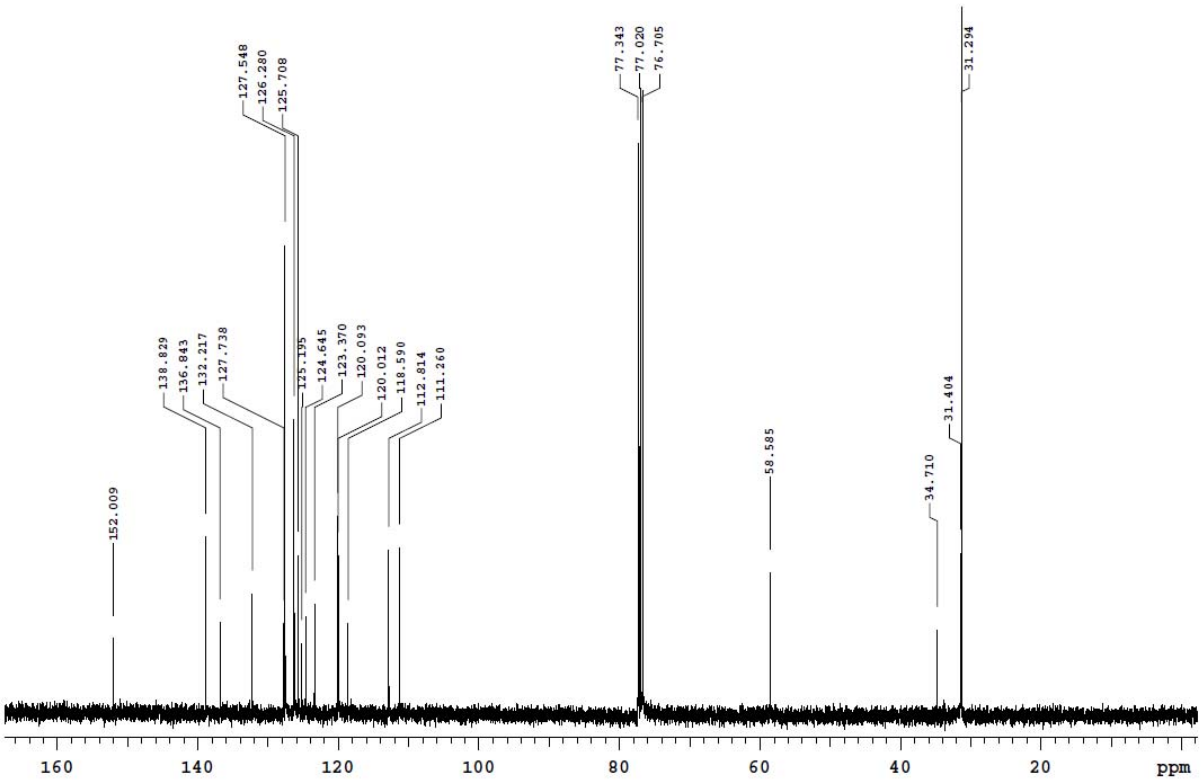
127.548
126.280
125.708
138.829
136.843
132.217
127.738
125.195
124.645
123.370
120.093
120.012
118.590
112.814
111.260
152.009
77.343
77.020
76.705
58.585
34.710
31.404
31.294
160
140
120
100
80
60
40
20
ppm

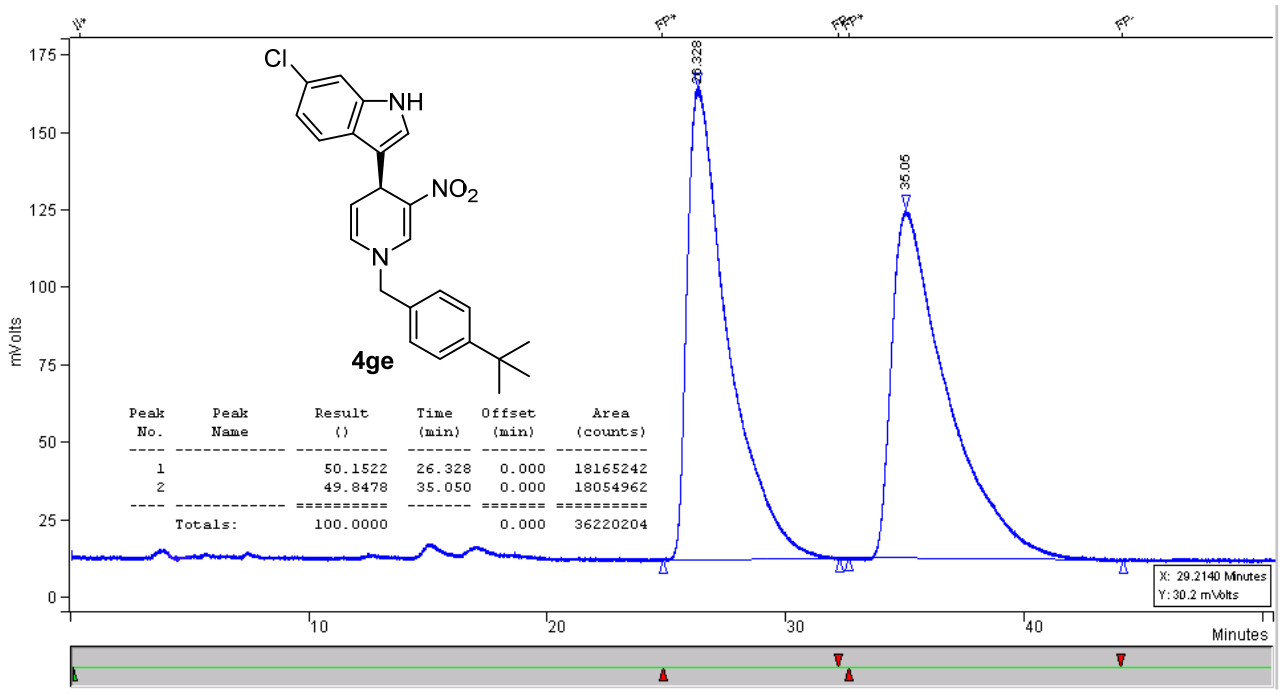


| Peak No. | Peak Name | Result () | Time (min) | Offset (min) | Area (counts) |
|---|---|---|---|---|---|
| 1 | | 50.1522 | 26.328 | 0.000 | 18165242 |
| 2 | | 49.8478 | 35.050 | 0.000 | 18054962 |
| | Totals: | 100.0000 | | 0.000 | 36220204 |

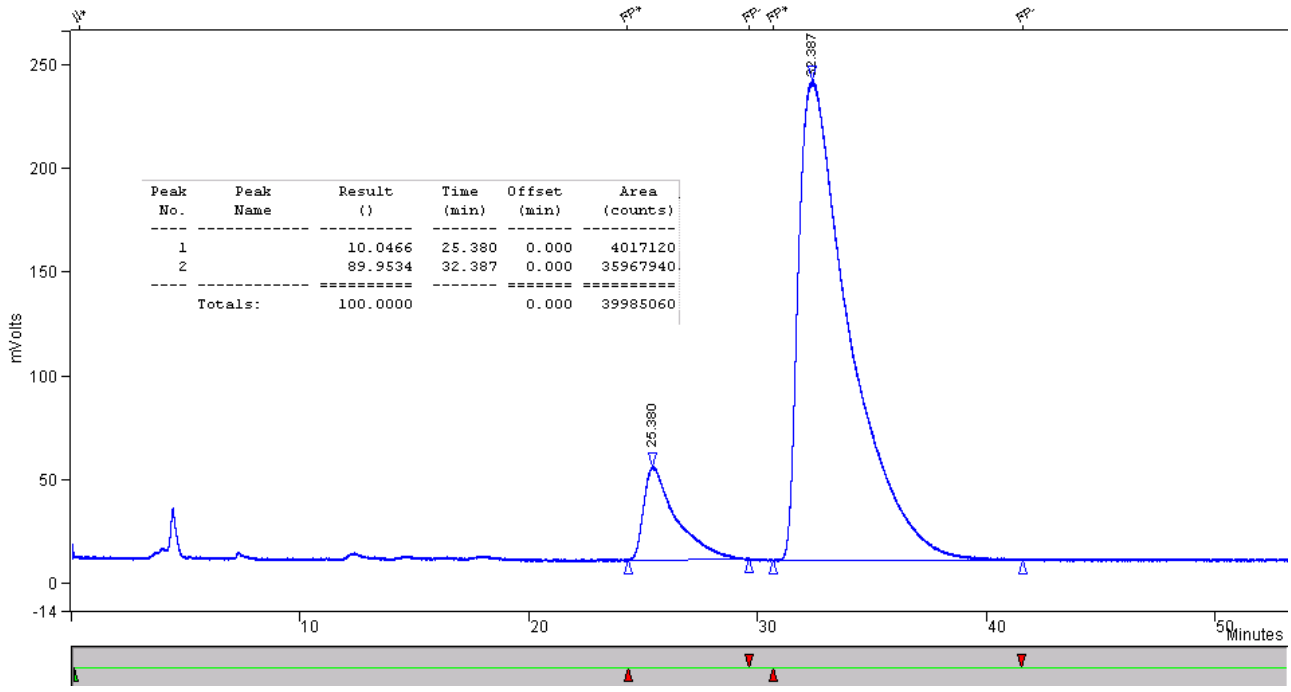


| Peak No. | Peak Name | Result () | Time (min) | Offset (min) | Area (counts) |
|---|---|---|---|---|---|
| 1 | | 10.0466 | 25.380 | 0.000 | 4017120 |
| 2 | | 89.9534 | 32.387 | 0.000 | 35967940 |
| | Totals: | 100.0000 | | 0.000 | 39985060 |

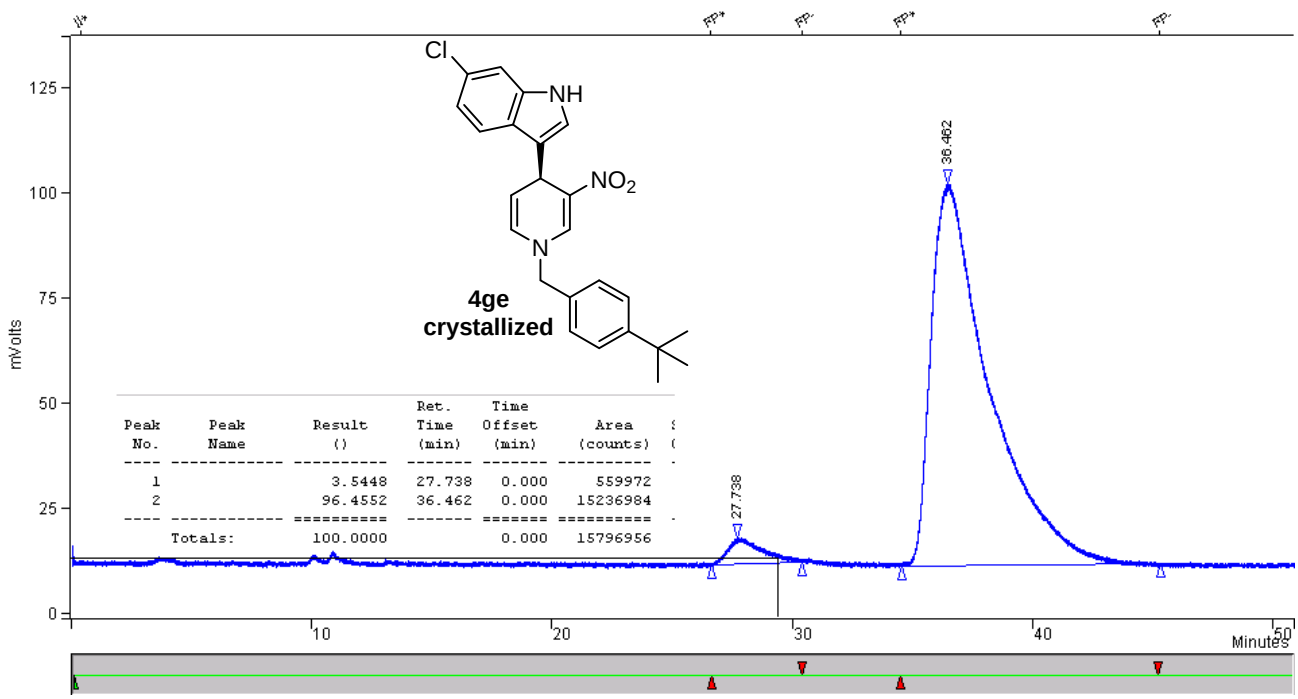


| Peak No. | Peak Name | Result () | Ret. Time (min) | Time Offset (min) | Area (counts) |
|---|---|---|---|---|---|
| 1 | | 3.5448 | 27.738 | 0.000 | 559972 |
| 2 | | 96.4552 | 36.462 | 0.000 | 15236984 |
| | Totals: | 100.0000 | | 0.000 | 15796956 |

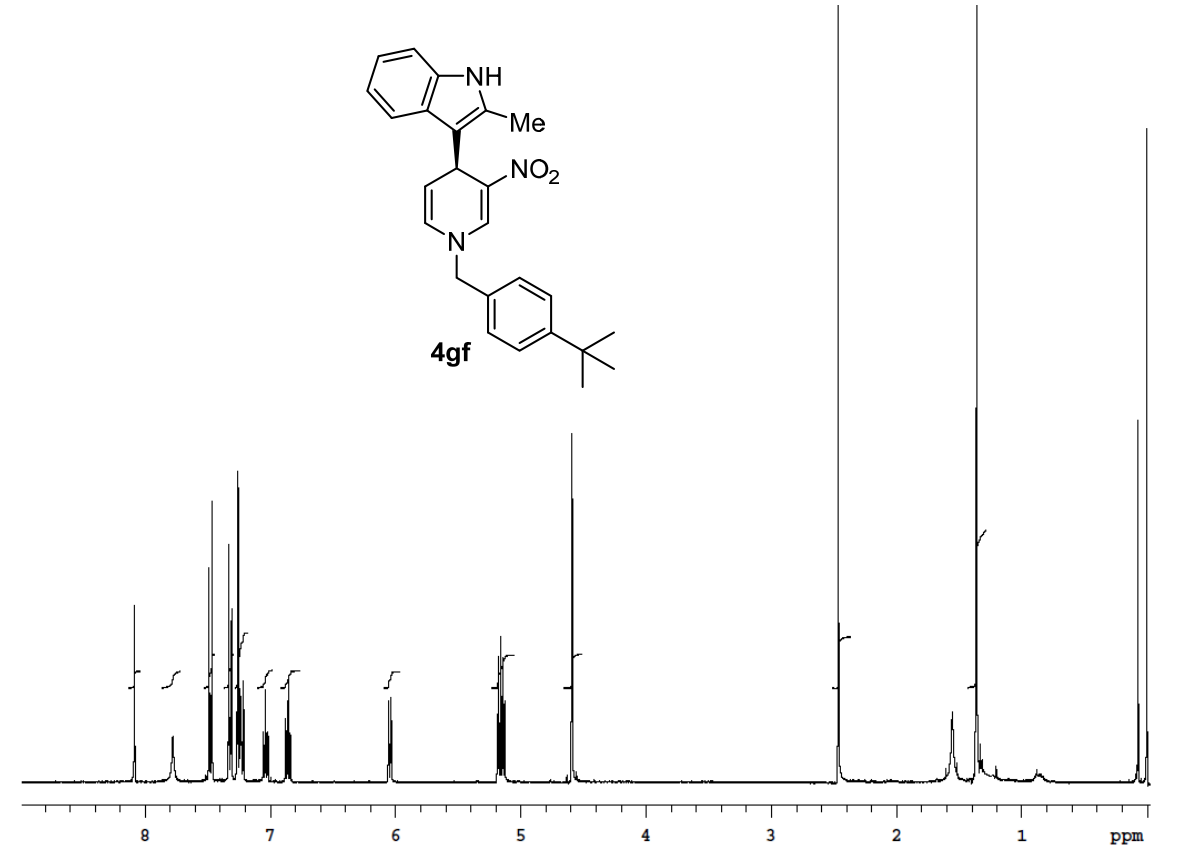
NH
Me
NO2
N
4gf
8
7
6
5
4
3
2
1
ppm

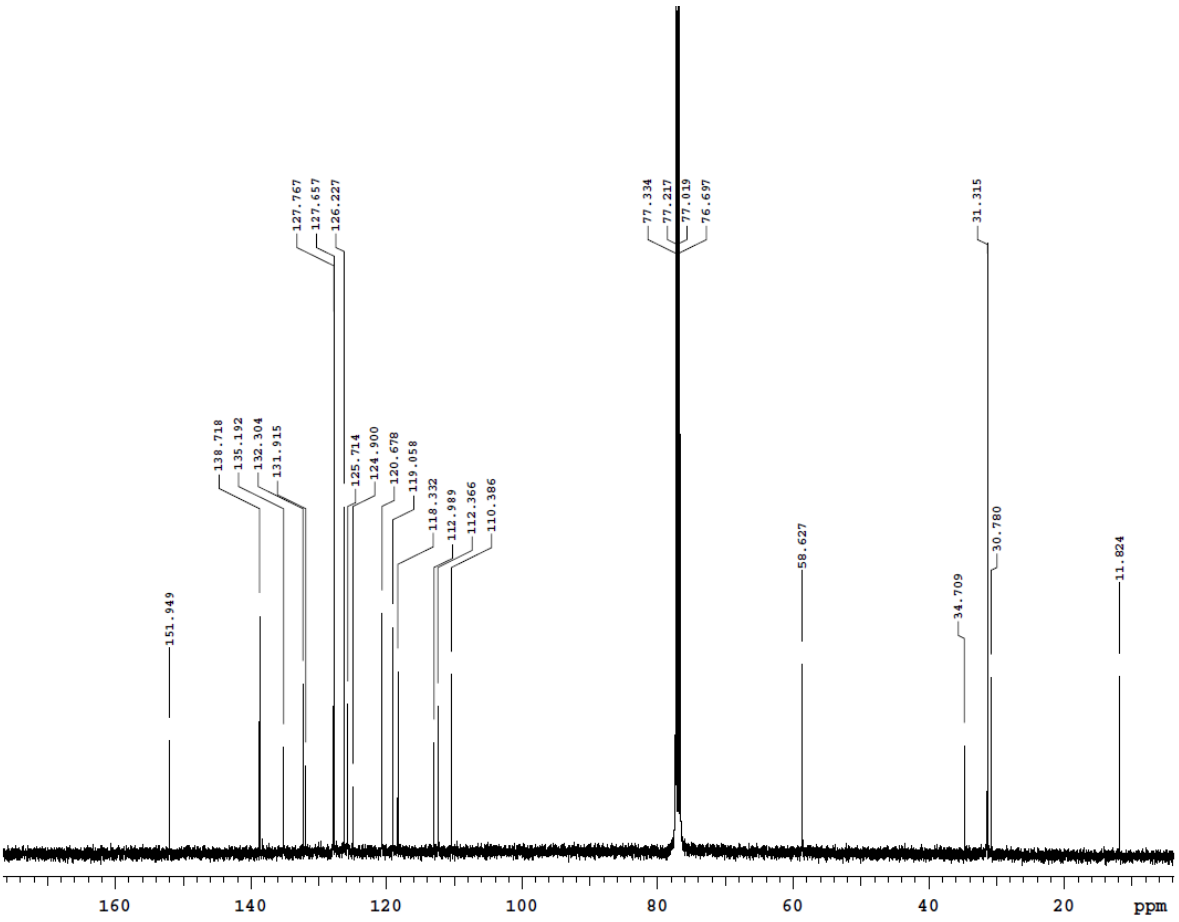
151.949
138.718
135.192
132.304
131.915
127.767
127.657
126.227
125.714
124.900
120.678
119.058
118.332
112.989
112.366
110.386
77.334
77.217
77.019
76.697
58.627
34.709
31.315
30.780
11.824
160
140
120
100
80
60
40
20
ppm

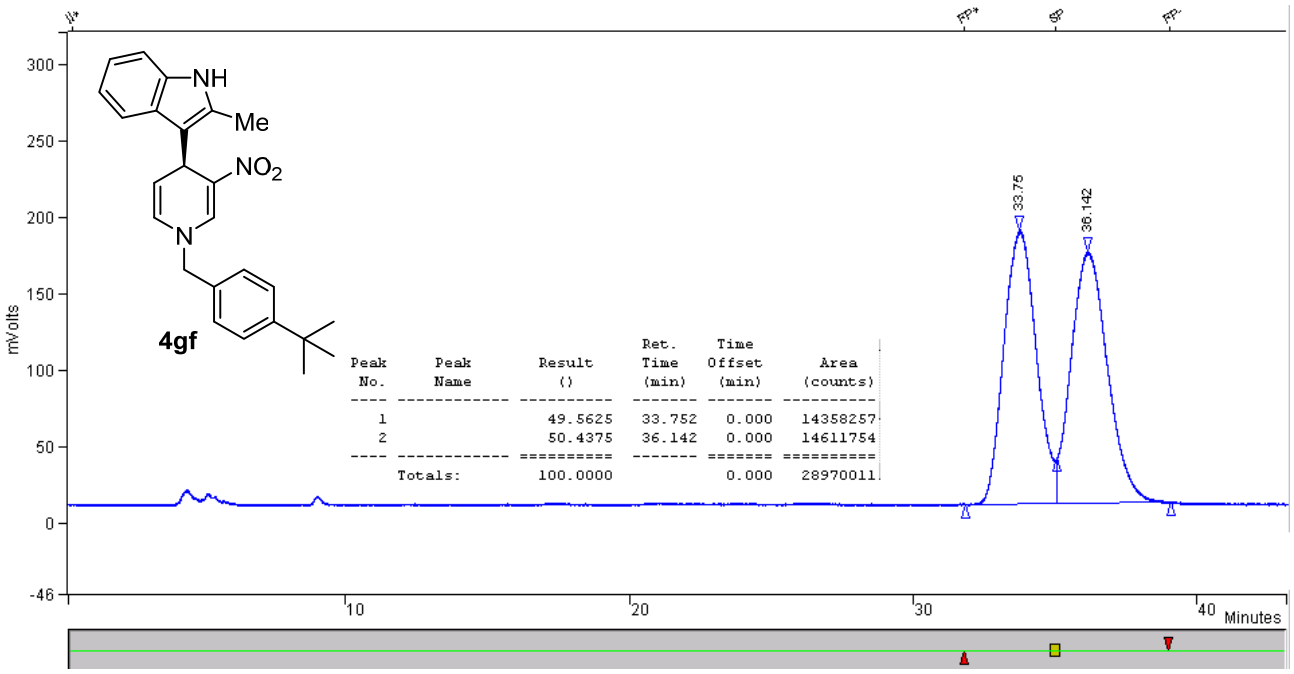


| Peak No. | Peak Name | Result () | Ret. Time (min) | Time Offset (min) | Area (counts) |
|---|---|---|---|---|---|
| 1 | | 49.5625 | 33.752 | 0.000 | 14358257 |
| 2 | | 50.4375 | 36.142 | 0.000 | 14611754 |
| Totals: | | 100.0000 | | 0.000 | 28970011 |

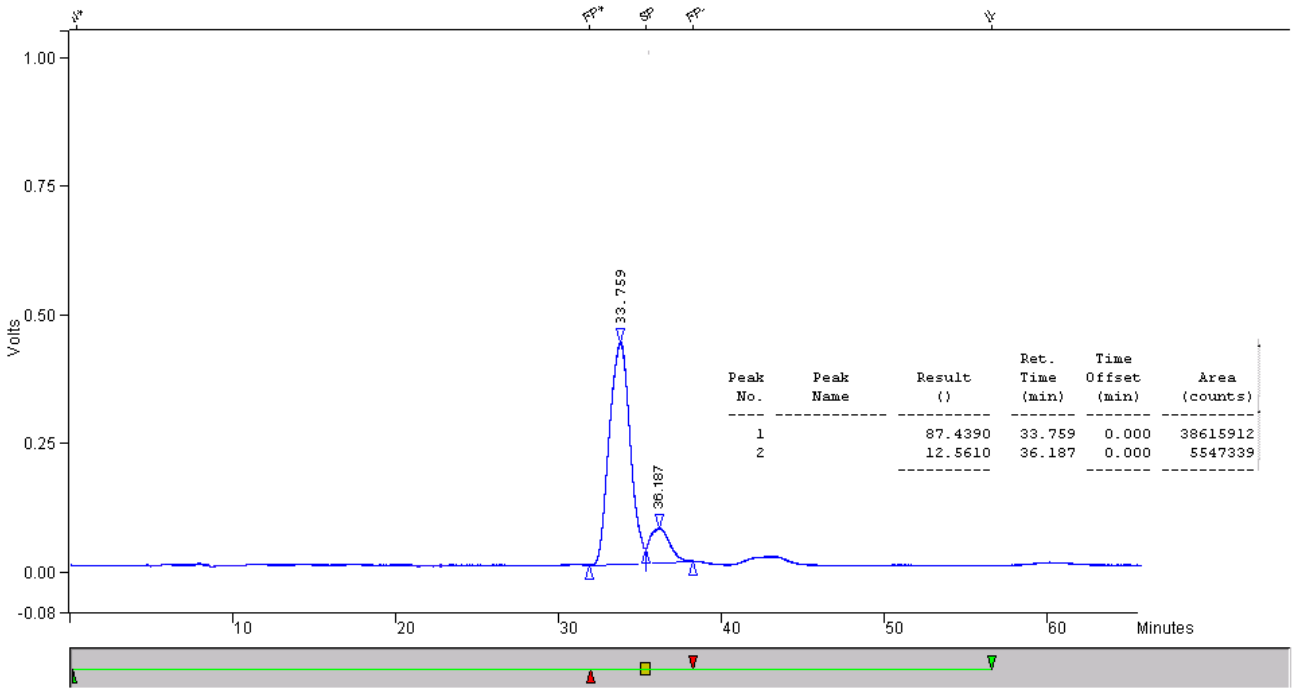


| Peak No. | Peak Name | Result () | Ret. Time (min) | Time Offset (min) | Area (counts) |
|---|---|---|---|---|---|
| 1 | | 87.4390 | 33.759 | 0.000 | 38615912 |
| 2 | | 12.5610 | 36.187 | 0.000 | 5547339 |

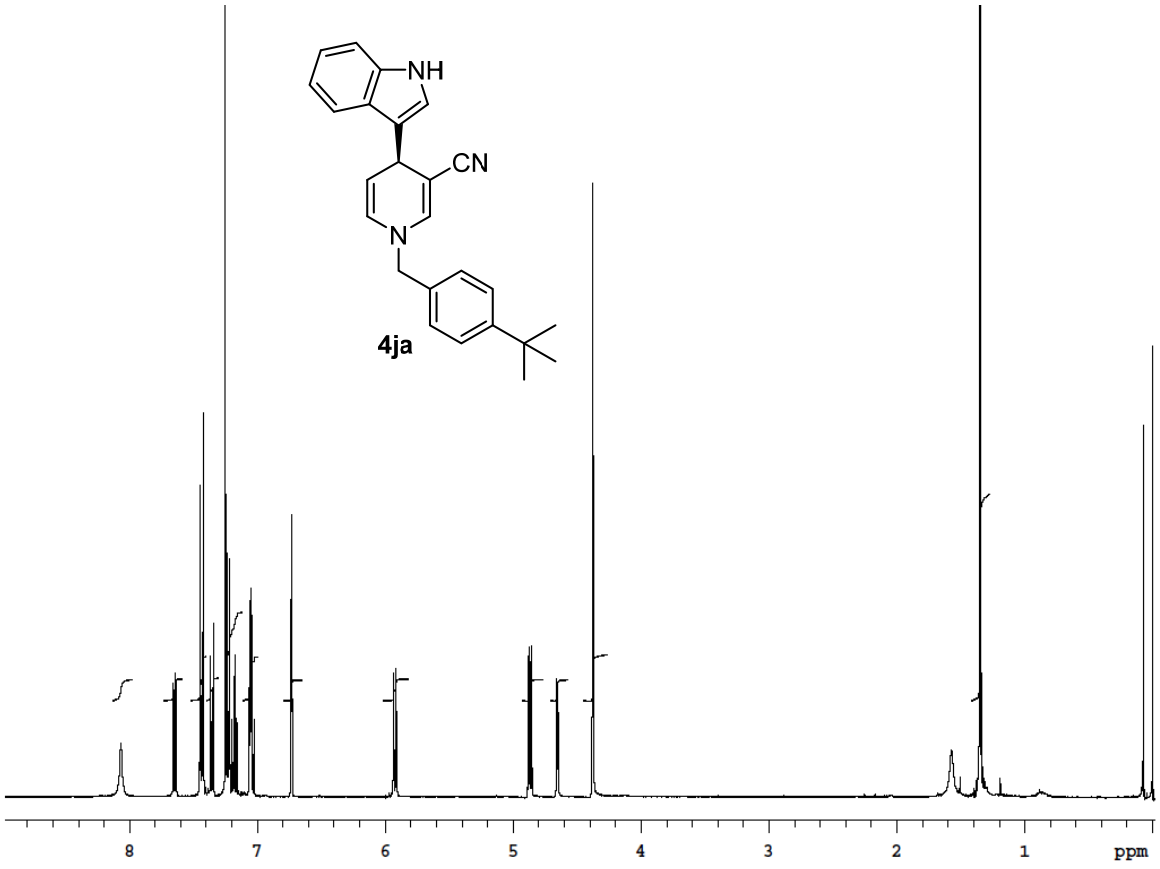
NH
CN
N
4ja
8
7
6
5
4
3
2
1
ppm

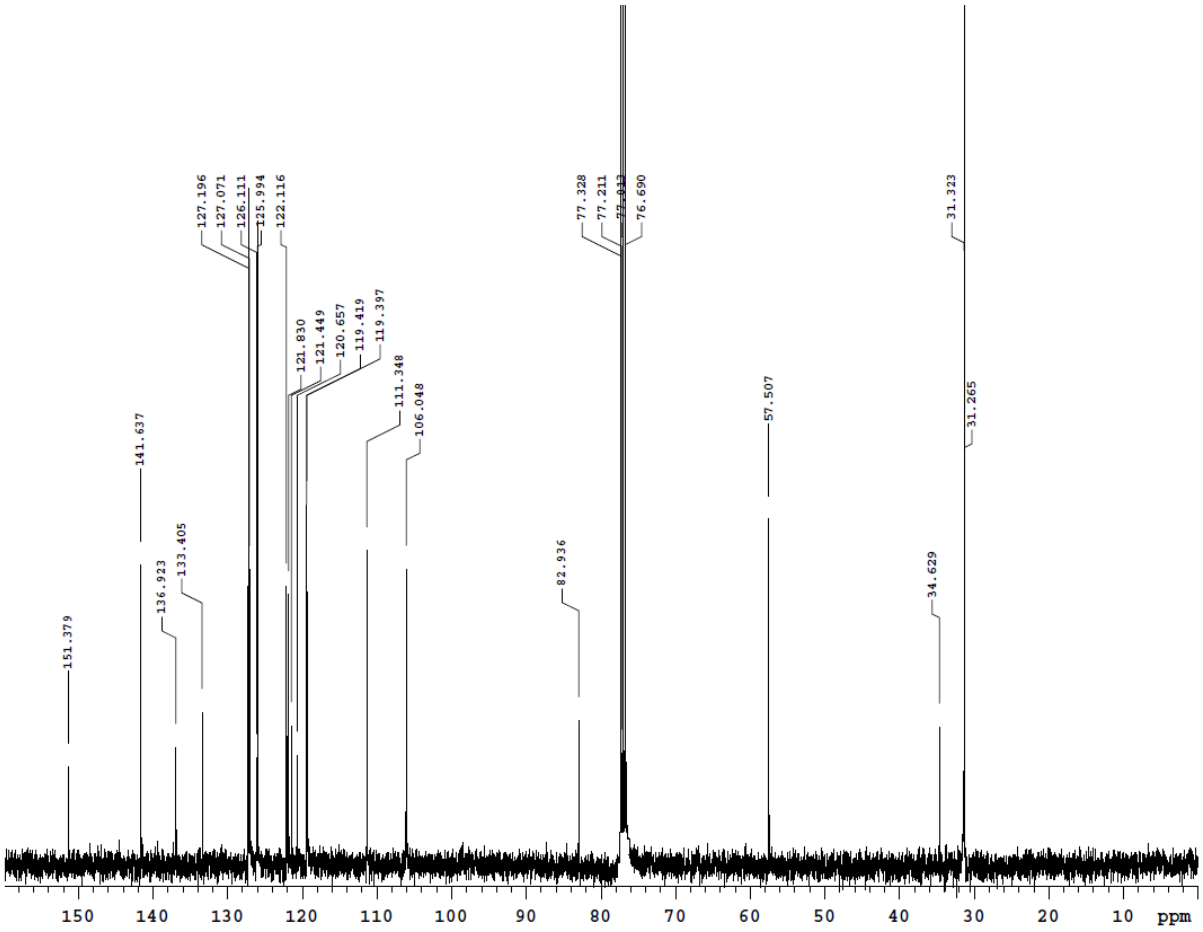
151.379
141.637
136.923
133.405
127.196
127.071
126.111
125.994
122.116
121.830
121.449
120.657
119.419
119.397
111.348
106.048
82.936
77.328
77.211
76.690
57.507
34.629
31.323
31.265
150
140
130
120
110
100
90
80
70
60
50
40
30
20
10
ppm

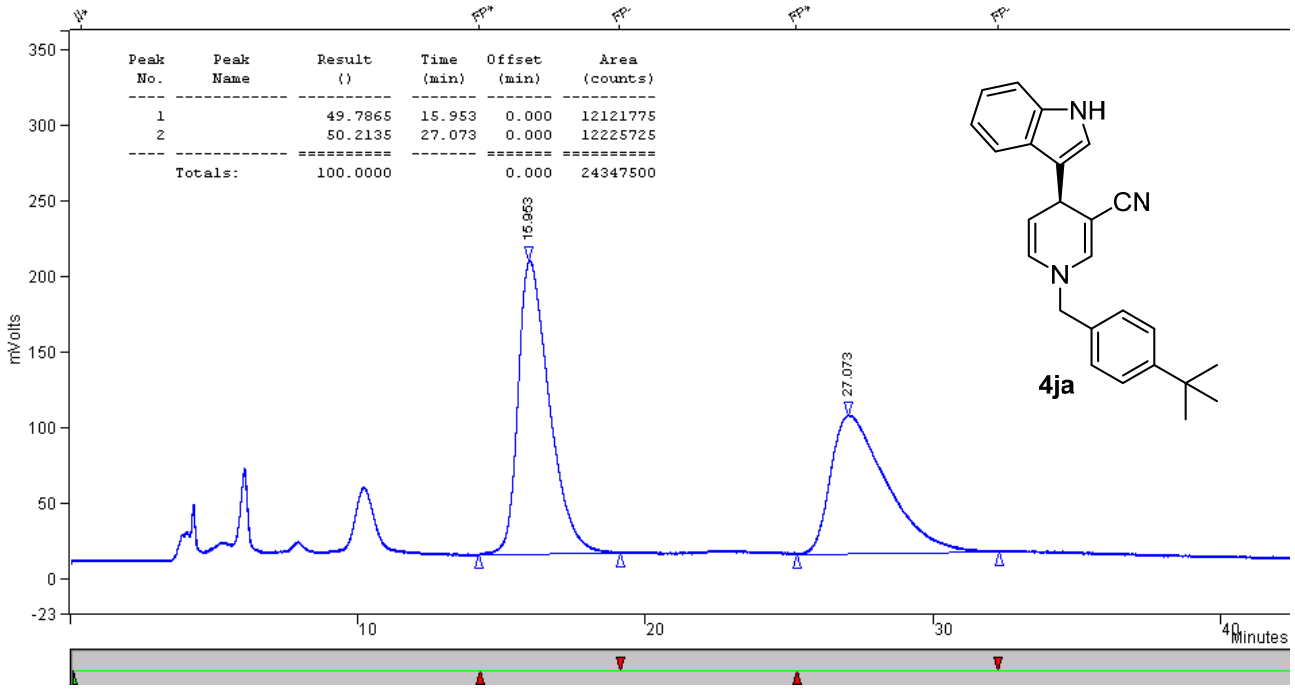
Peak No. | Peak Name | Result () | Time (min) | Offset (min) | Area (counts)
1 | 49.7865 | 15.953 | 0.000 | 12121775
2 | 50.2135 | 27.073 | 0.000 | 12225725
Totals: | 100.0000 | | 0.000 | 24347500
15.953
27.073
NH
CN
N
4ja
mVolts
Minutes

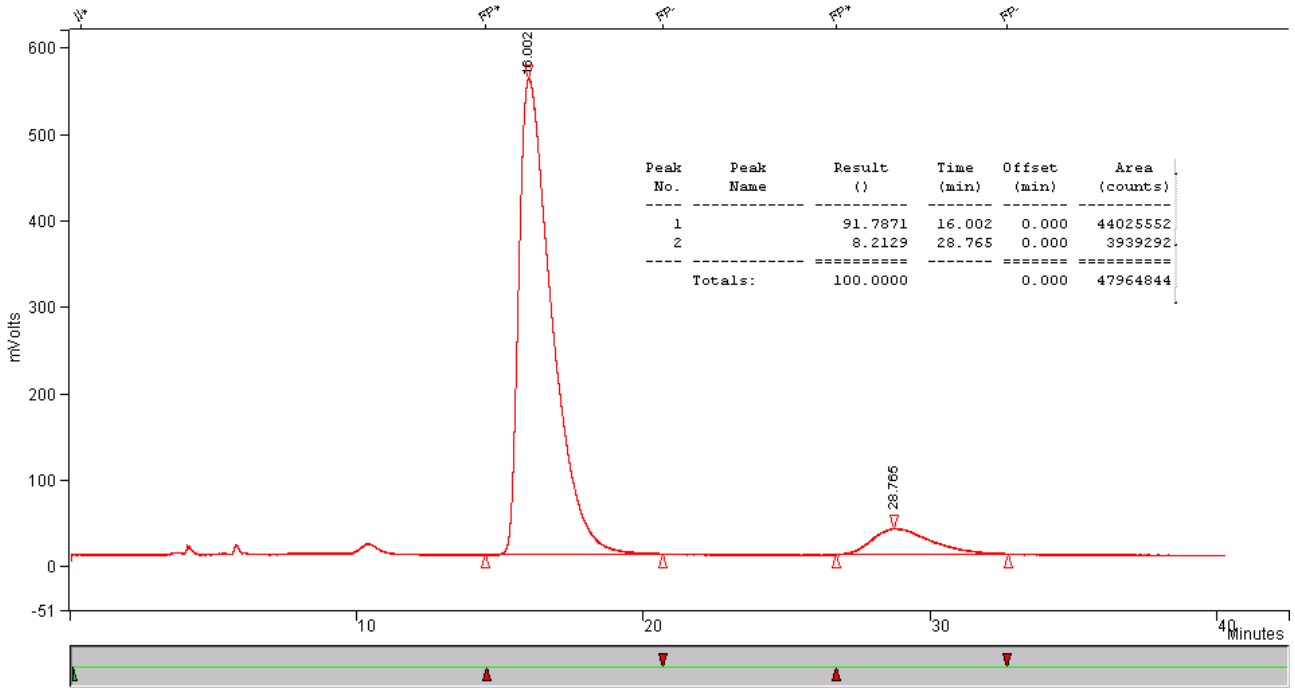
Peak No. | Peak Name | Result () | Time (min) | Offset (min) | Area (counts)
1 | 91.7871 | 16.002 | 0.000 | 44025552
2 | 8.2129 | 28.765 | 0.000 | 3939292
Totals: | 100.0000 | | 0.000 | 47964844
16.002
28.765
mVolts
Minutes

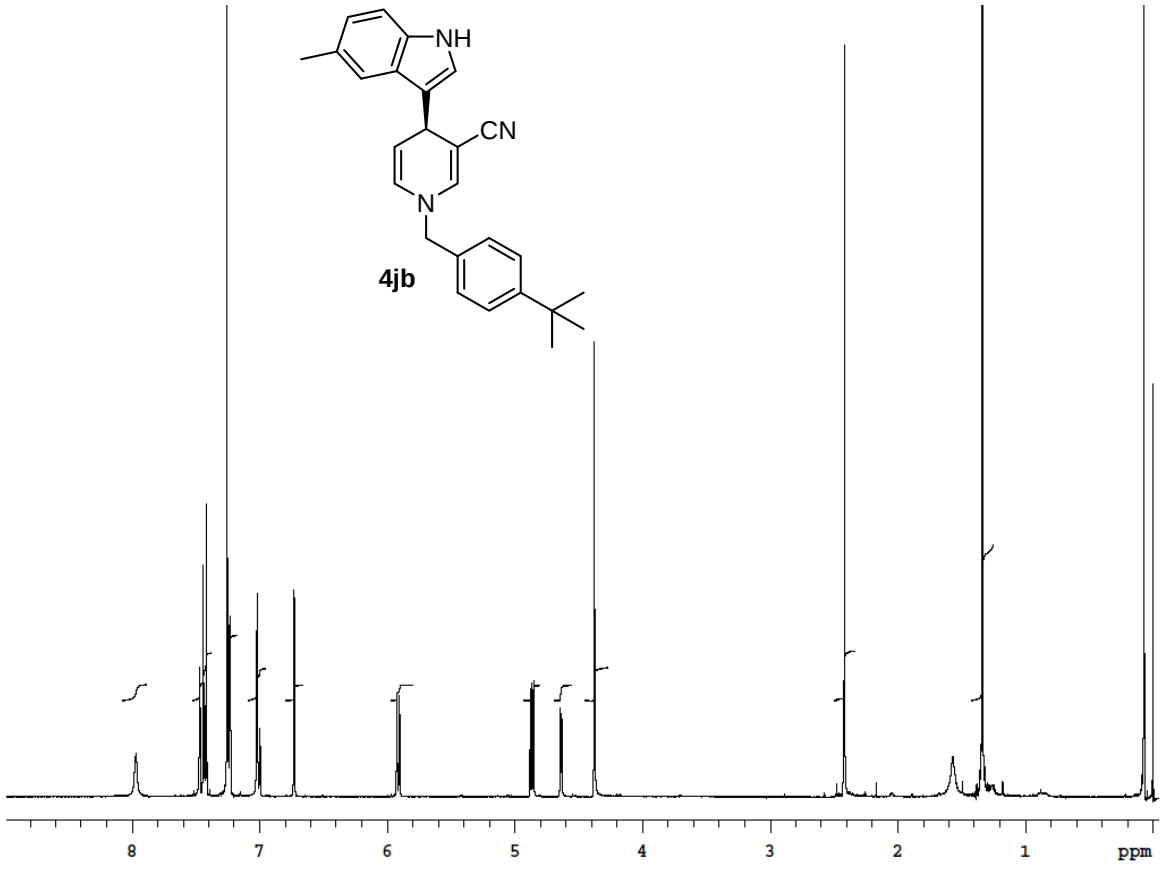
NH
CN
N
4jb
8
7
6
5
4
3
2
1
ppm

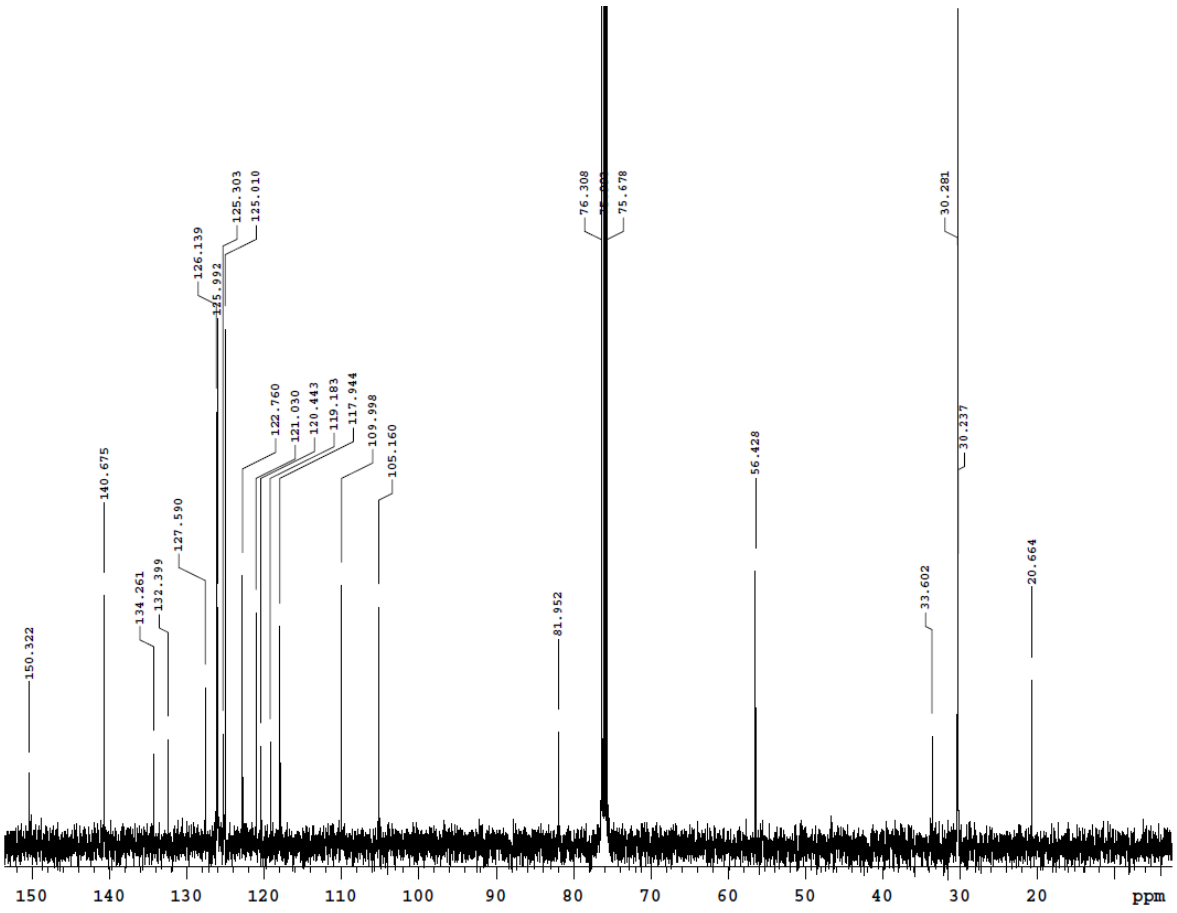
150.322
140.675
134.261
132.399
127.590
126.139
125.992
125.303
125.010
122.760
121.030
120.443
119.183
117.944
109.998
105.160
81.952
76.308
75.678
56.428
30.281
30.237
33.602
20.664
150
140
130
120
110
100
90
80
70
60
50
40
30
20
ppm

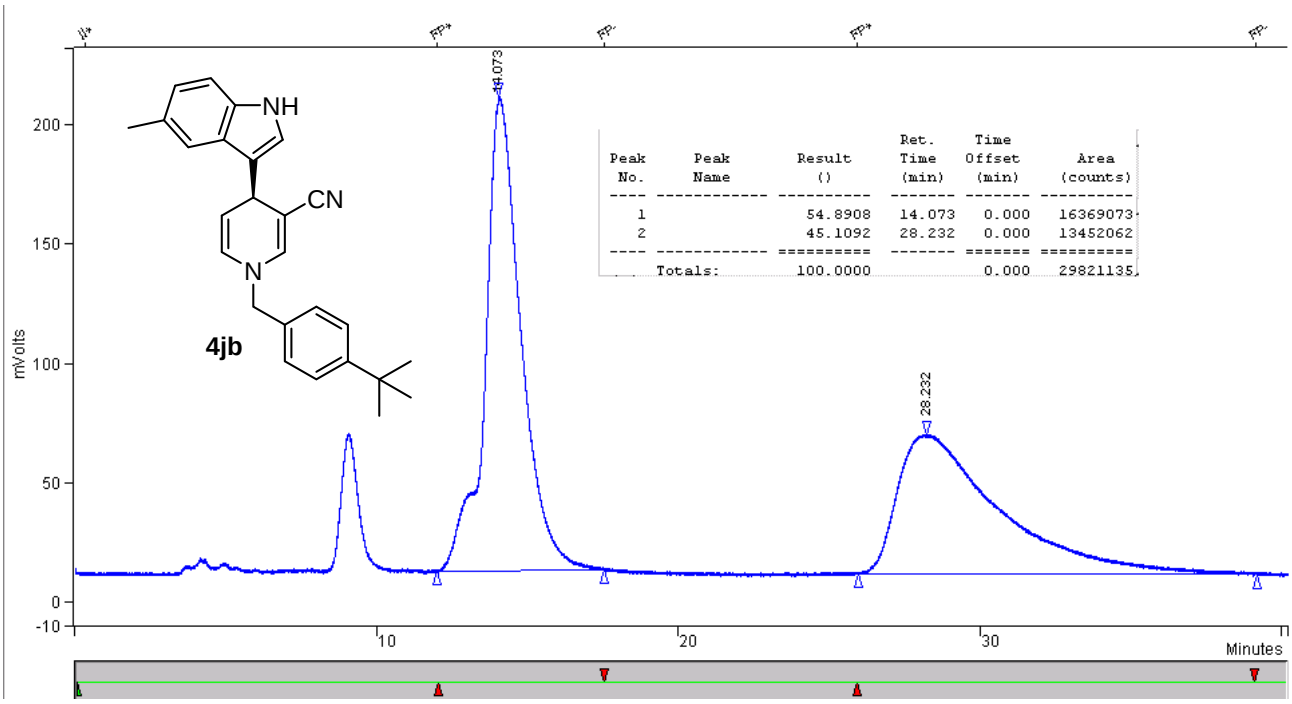


| Peak No. | Peak Name | Result () | Ret. Time (min) | Time Offset (min) | Area (counts) |
|---|---|---|---|---|---|
| 1 | | 54.8908 | 14.073 | 0.000 | 16369073 |
| 2 | | 45.1092 | 28.232 | 0.000 | 13452062 |
| | Totals: | 100.0000 | | 0.000 | 29821135 |

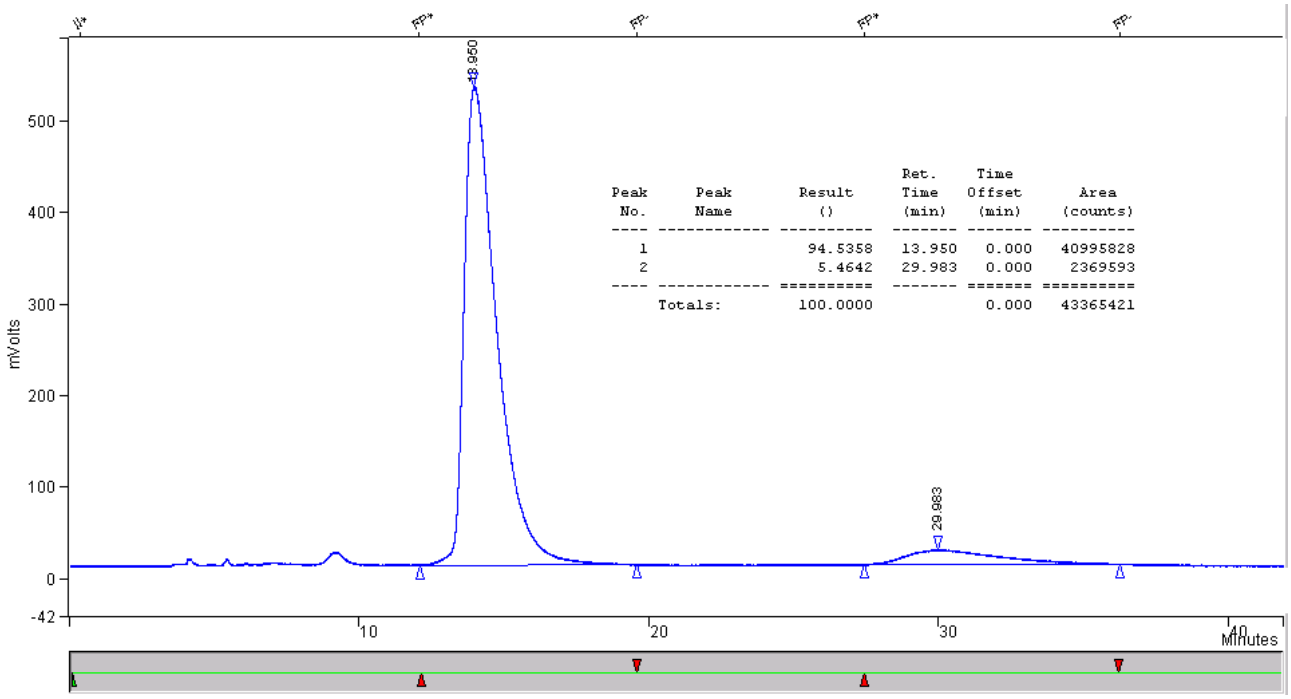


| Peak No. | Peak Name | Result () | Ret. Time (min) | Time Offset (min) | Area (counts) |
|---|---|---|---|---|---|
| 1 | | 94.5358 | 13.950 | 0.000 | 40995828 |
| 2 | | 5.4642 | 29.983 | 0.000 | 2369593 |
| | Totals: | 100.0000 | | 0.000 | 43365421 |

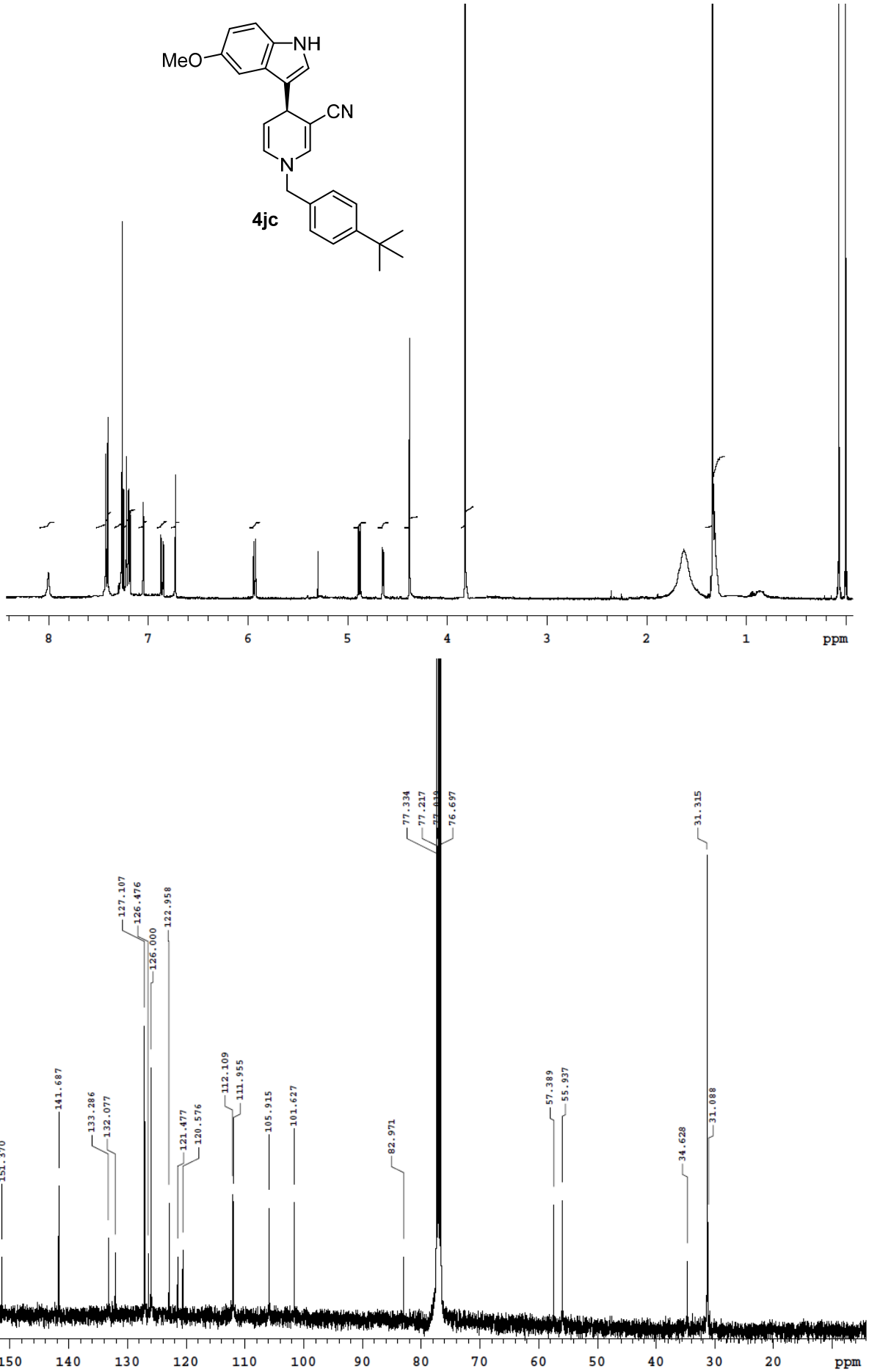
MeO
NH
CN
N
4jc
8
7
6
5
4
3
2
1
ppm
153.958
151.370
141.687
133.286
132.077
127.107
126.476
126.000
122.958
121.477
120.576
112.109
111.955
105.915
101.627
82.971
77.334
77.217
76.697
57.389
55.937
34.628
31.315
31.088
150
140
130
120
110
100
90
80
70
60
50
40
30
20
ppm

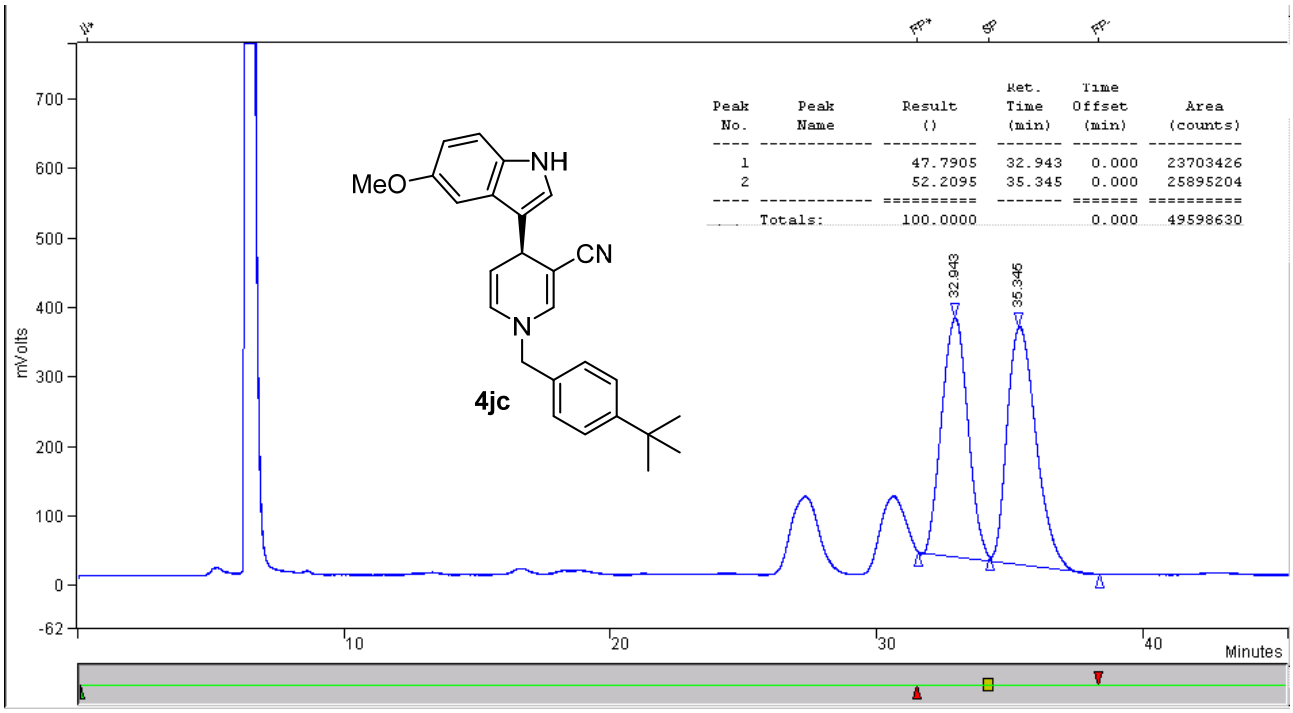
MeO
NH
CN
N
4jc
Peak No. | Peak Name | Result () | Ret. Time (min) | Time Offset (min) | Area (counts)
1 | | 47.7905 | 32.943 | 0.000 | 23703426
2 | | 52.2095 | 35.345 | 0.000 | 25895204
Totals: | | 100.0000 | | 0.000 | 49598630
32.943
35.345
mVolts
Minutes

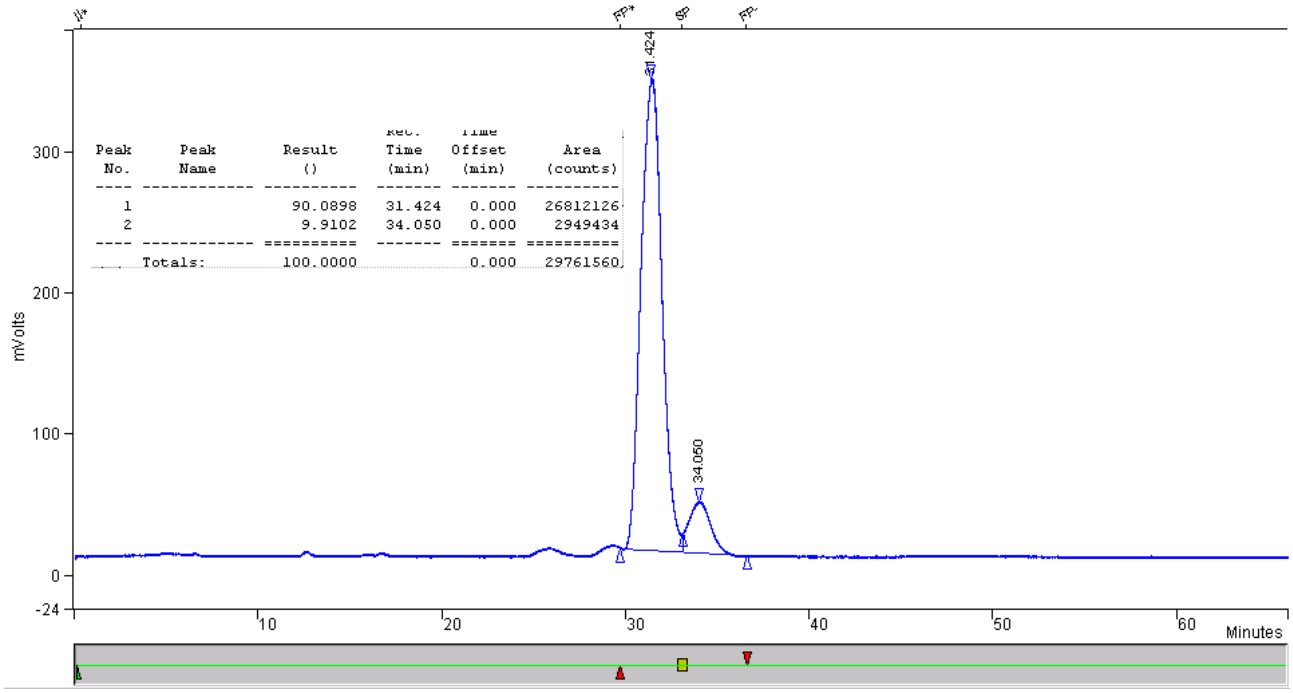
Peak No. | Peak Name | Result () | Ret. Time (min) | Time Offset (min) | Area (counts)
1 | | 90.0898 | 31.424 | 0.000 | 26812126
2 | | 9.9102 | 34.050 | 0.000 | 2949434
Totals: | | 100.0000 | | 0.000 | 29761560
31.424
34.050
mVolts
Minutes

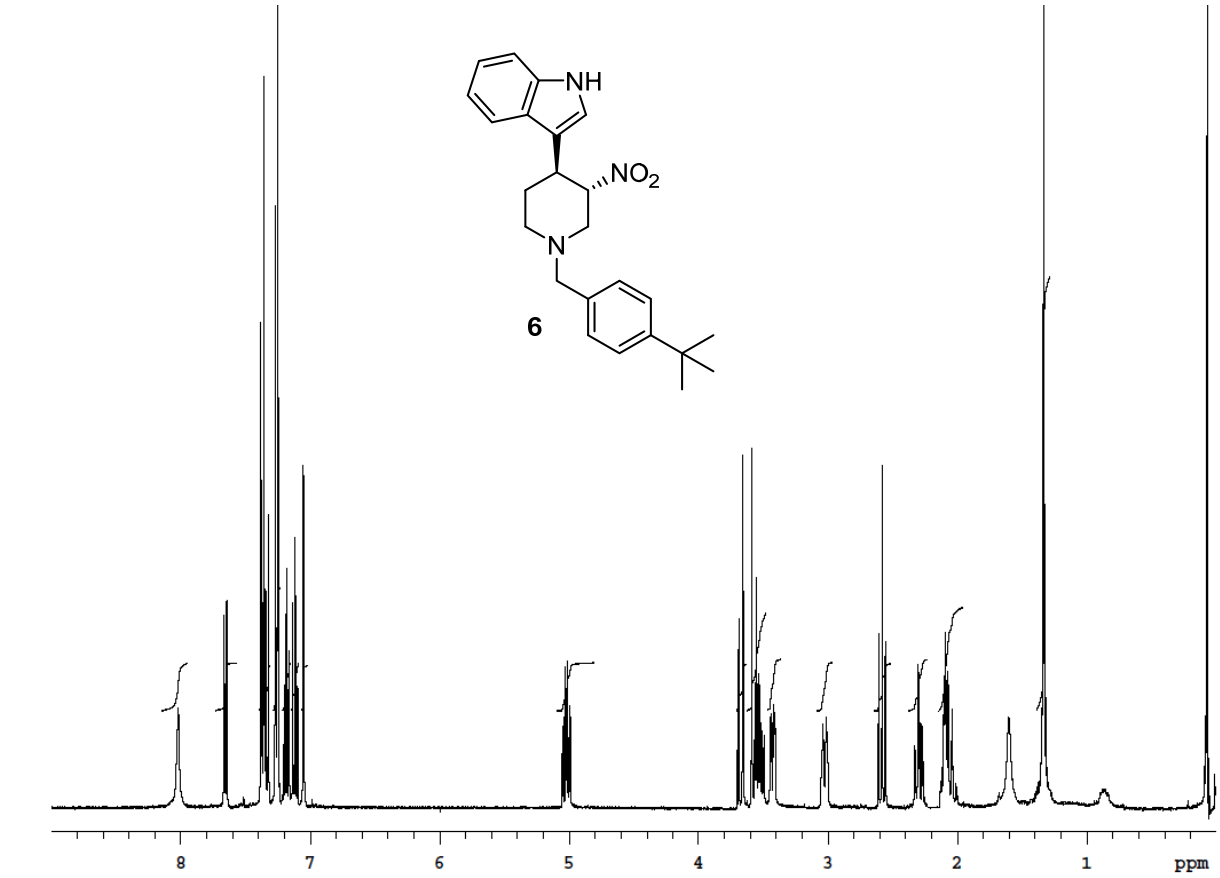
NH
NO2
N
6
8
7
6
5
4
3
2
1
ppm

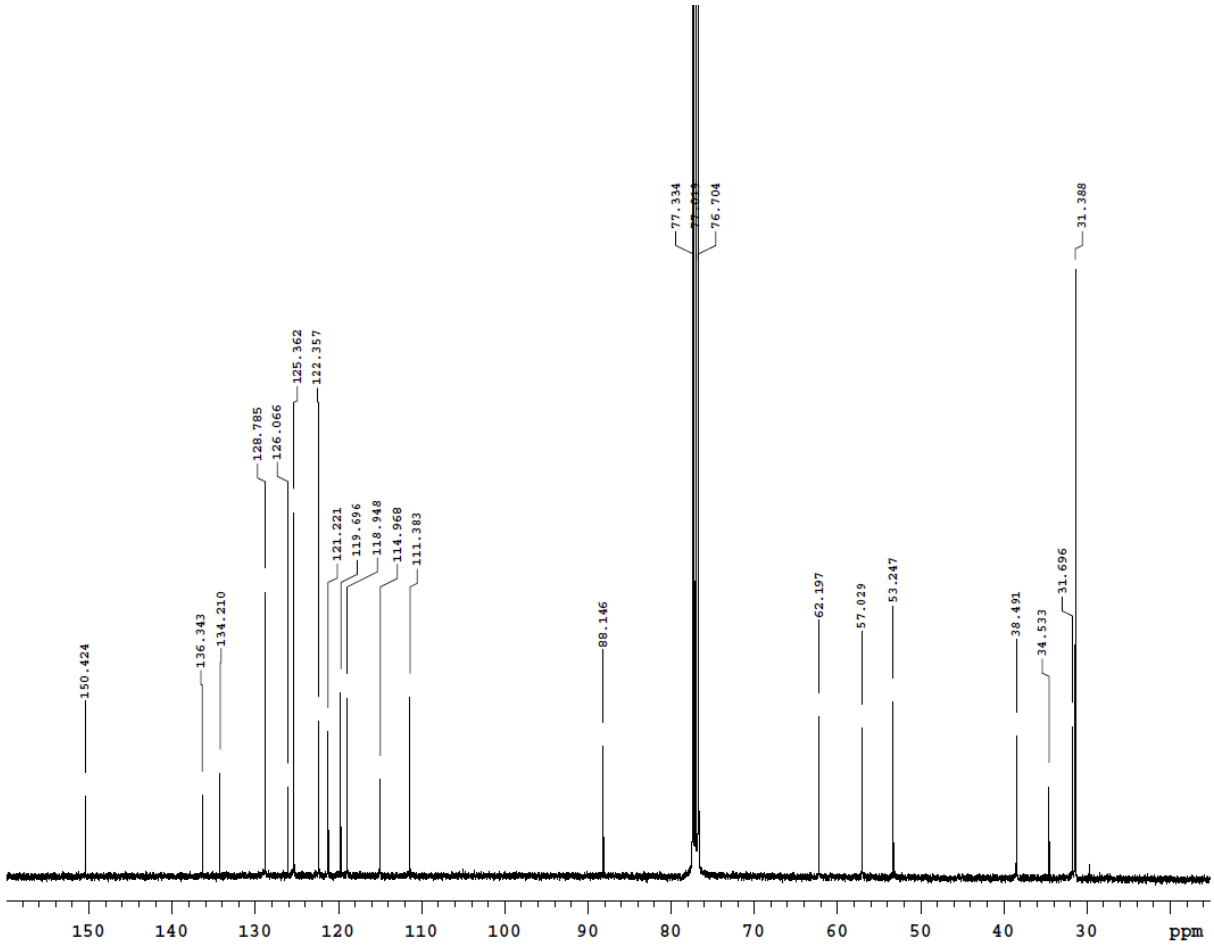
150.424
136.343
134.210
128.785
126.066
125.362
122.357
121.221
119.696
118.948
114.968
111.383
88.146
77.334
76.704
62.197
57.029
53.247
38.491
34.533
31.696
31.388
150
140
130
120
110
100
90
80
70
60
50
40
30
ppm

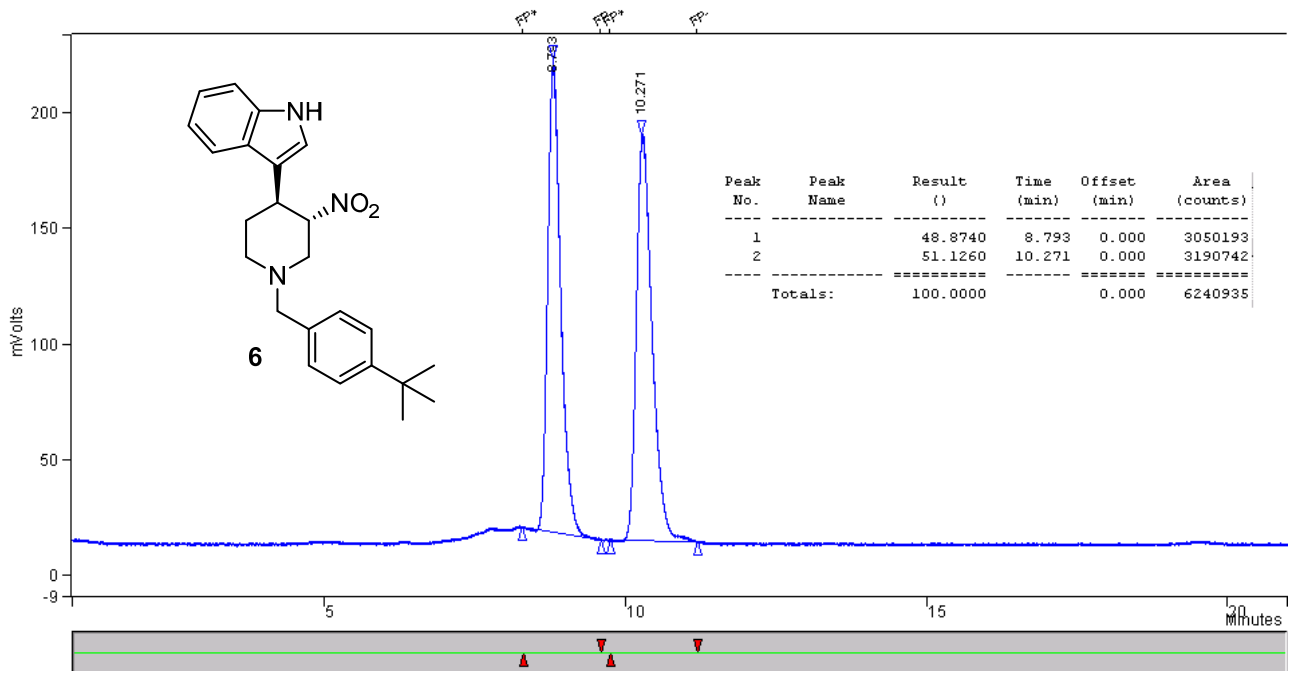


| Peak No. | Peak Name | Result () | Time (min) | Offset (min) | Area (counts) |
|---|---|---|---|---|---|
| 1 | | 48.8740 | 8.793 | 0.000 | 3050193 |
| 2 | | 51.1260 | 10.271 | 0.000 | 3190742 |
| | Totals: | 100.0000 | | 0.000 | 6240935 |

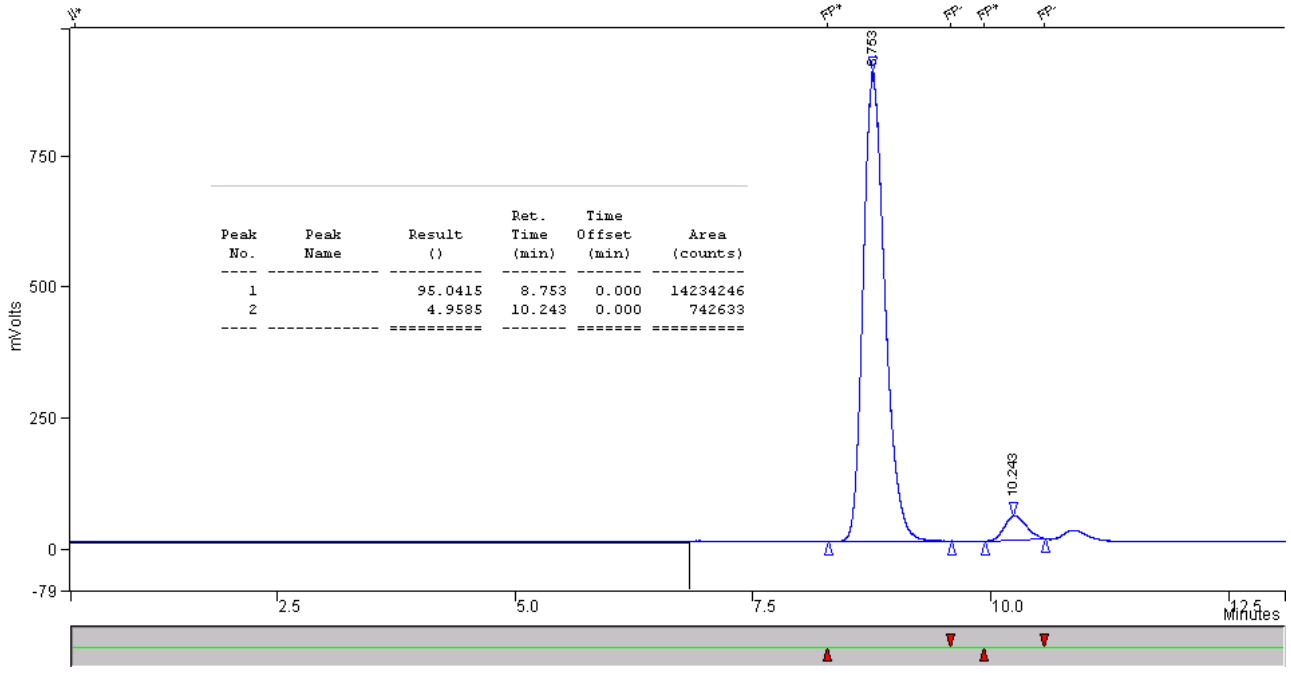


| Peak No. | Peak Name | Result () | Ret. Time (min) | Time Offset (min) | Area (counts) |
|---|---|---|---|---|---|
| 1 | | 95.0415 | 8.753 | 0.000 | 14234246 |
| 2 | | 4.9585 | 10.243 | 0.000 | 742633 |

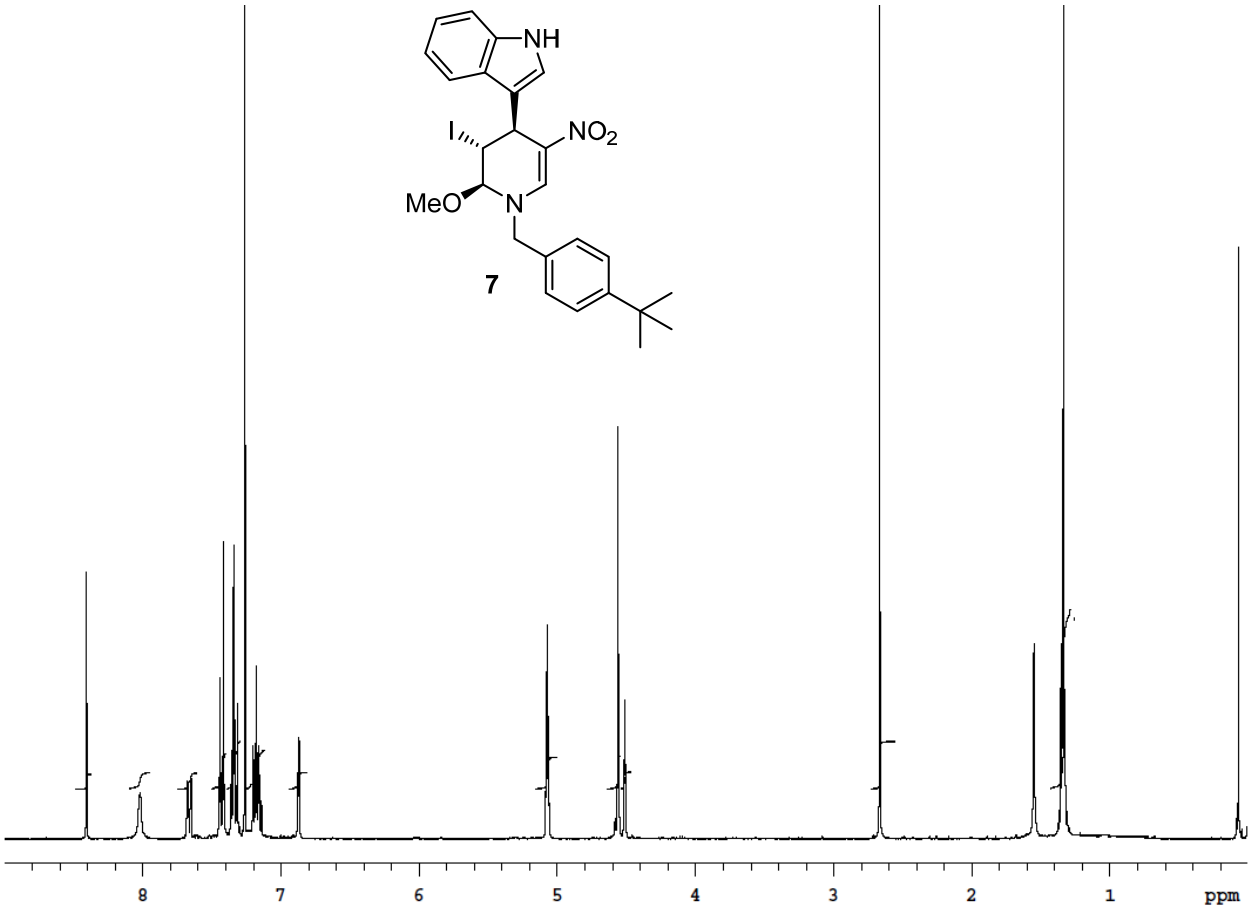
NH
I
NO2
MeO
N
7
8
7
6
5
4
3
2
1
ppm

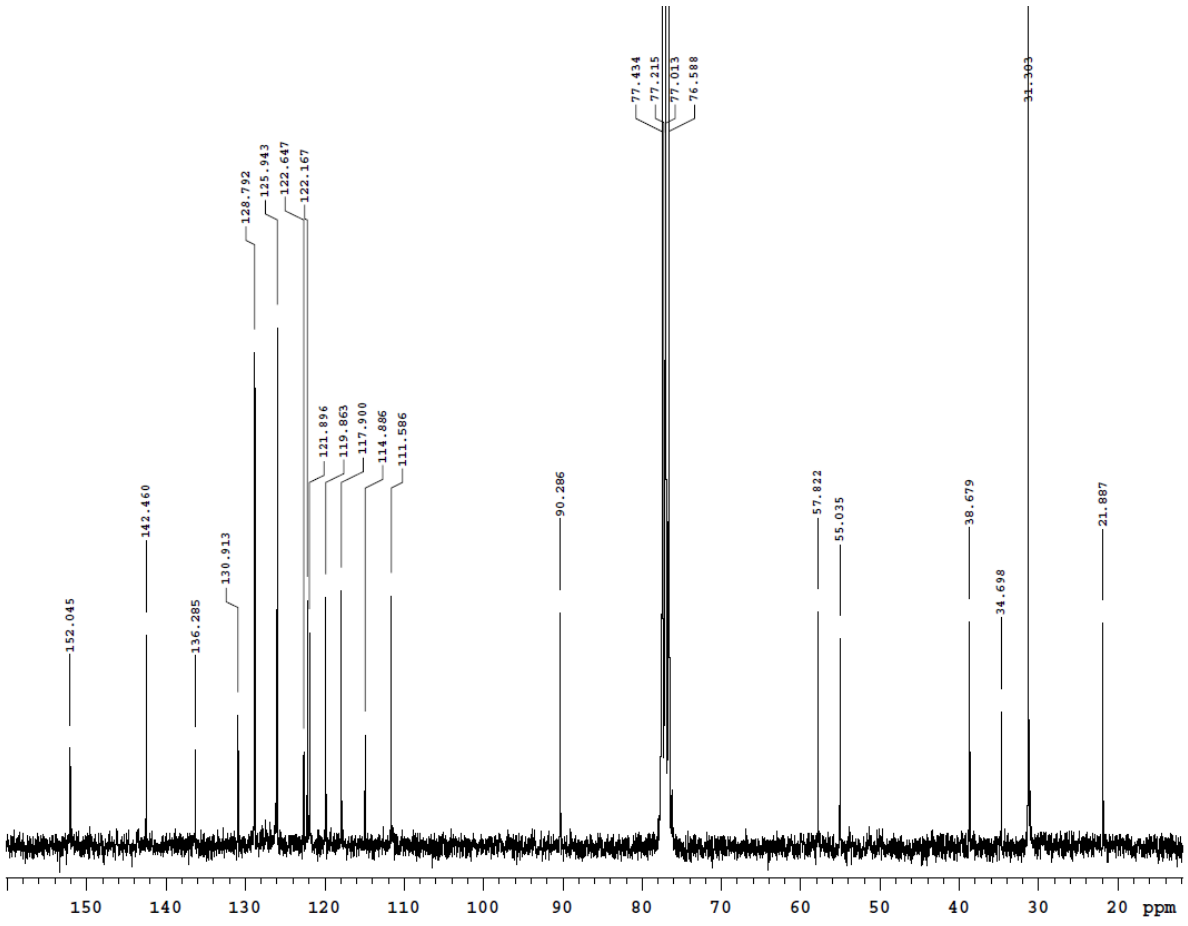
152.045
142.460
136.285
130.913
128.792
125.943
122.647
122.167
121.896
119.863
117.900
114.886
111.586
90.286
77.434
77.215
77.013
76.588
57.822
55.035
38.679
34.698
31.303
21.887
150
140
130
120
110
100
90
80
70
60
50
40
30
20
ppm

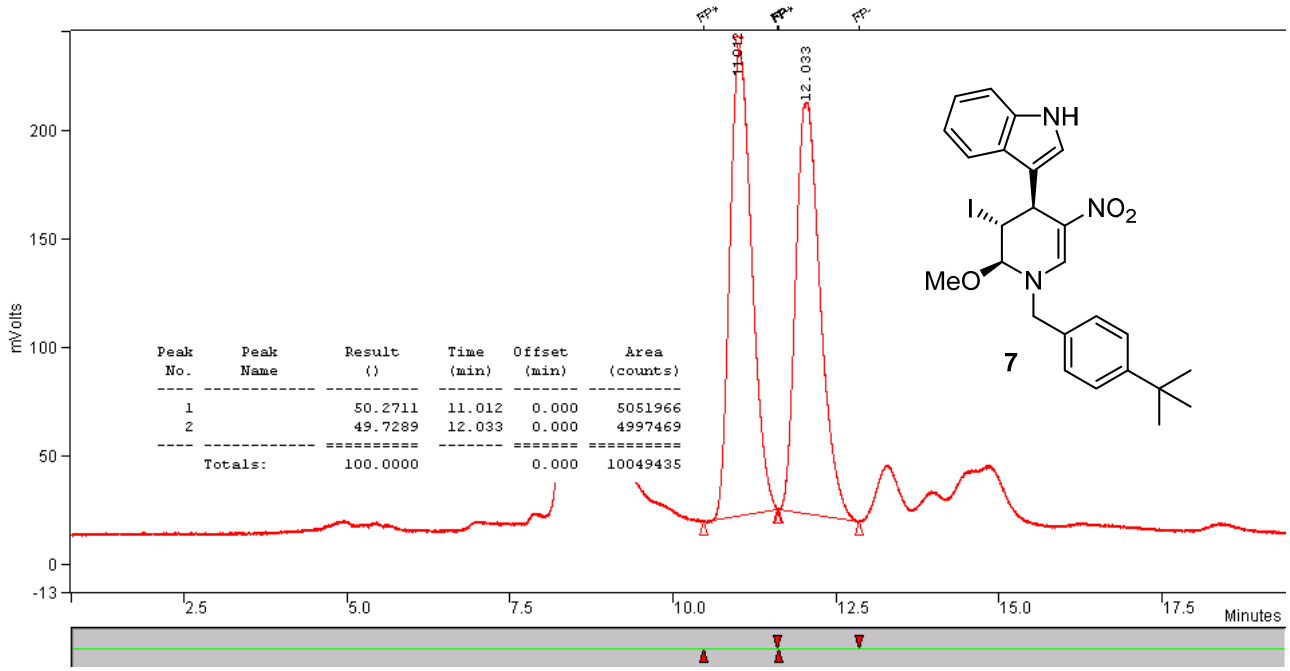


| Peak No. | Peak Name | Result () | Time (min) | Offset (min) | Area (counts) |
|---|---|---|---|---|---|
| 1 | | 50.2711 | 11.012 | 0.000 | 5051966 |
| 2 | | 49.7289 | 12.033 | 0.000 | 4997469 |
| Totals: | | 100.0000 | | 0.000 | 10049435 |

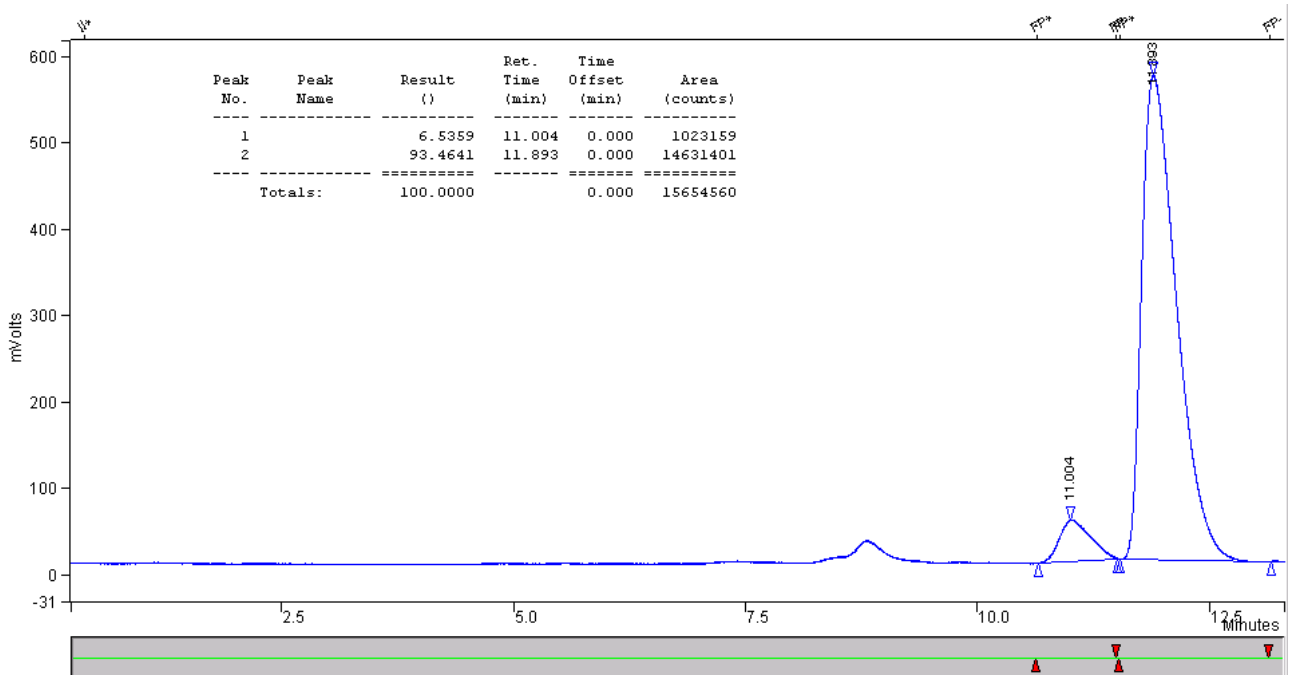


| Peak No. | Peak Name | Result () | Ret. Time (min) | Time Offset (min) | Area (counts) |
|---|---|---|---|---|---|
| 1 | | 6.5359 | 11.004 | 0.000 | 1023159 |
| 2 | | 93.4641 | 11.893 | 0.000 | 14631401 |
| Totals: | | 100.0000 | | 0.000 | 15654560 |

## Copies of the HRMS(ESI) spectra